TECHNICAL UNIVERSITY OF CRETE

School of Chemical and Environmental Engineering

Atmospheric Environment & Climate Change Lab

Ph.D. DISSERTATION

Future Climate Change Impact on Wildfire Danger over the Mediterranean: the case of Greece

Anastasios Rovithakis

Supervisor: Professor Apostolos Voulgarakis

Chania, July 2024

ΠΟΛΥΤΕΧΝΕΙΟ ΚΡΗΤΗΣ

Σχολή Χημικών Μηχανικών και Μηχανικών Περιβάλλοντος

Εργαστήριο Ατμοσφαιρικού Περιβάλλοντος και Κλιματικής Αλλαγής

ΔΙΔΑΚΤΟΡΙΚΗ ΔΙΑΤΡΙΒΗ

Μελλοντικές Επιπτώσεις Κλιματικής Αλλαγής στον Κίνδυνο Πυρκαγιάς στη Μεσόγειο: Η Περίπτωση της Ελλάδας

Αναστάσιος Ροβιθάκης

Επιβλέπων: Καθηγητής Απόστολος Βουλγαράκης

Χανιά, Ιούλιος 2024

"Don't be pushed around by the fears in your mind. Be led by the dreams in your heart."

Roy T. Bennett

Examining Committee

1. Professor Apostolos Voulgarakis – Supervisor
   School of Chemical and Environmental Engineering
   Technical University of Crete, Greece

2. Professor Mihalis Lazaridis
   School of Chemical and Environmental Engineering
   Technical University of Crete, Greece

3. Professor Dionysia Kolokotsa
   School of Chemical and Environmental Engineering
   Technical University of Crete, Greece

4. Associate Professor Aristeidis Koutroulis
   School of Chemical and Environmental Engineering
   Technical University of Crete, Greece

5. Professor Maria Kanakidou
   Department of Chemistry,
   University of Crete, Greece

6. Research Director Christos Giannakopoulos
   National Observatory of Athens

7. Professor Prodromos Zanis
   Department of Meteorology and Climatology, School of Geology
   Aristotle University of Thessaloniki

Acknowledgements

All research projects leading to this PhD Thesis had been carried out at the Laboratory of Atmospheric Environment and Climate Change, at the School of Chemical and Environmental Engineering, Technical University of Crete, under the supervision of Professor Apostolos Voulgarakis.

The PhD supervisor can either make you or break you. Of course it takes organization, devotion of countless study hours and perseverance from the PhD candidate but all that is definitely more manageable when having a supervisor that is down to earth, finds time for you, supports you and guides you both scientifically and in everyday life. For all those reasons I cannot thank Professor Apostolos Voulgarakis enough for being so kind and helpful to me.

This research would not have been possible without the enormous help from Dr Emmanouil Grilakis. He taught me all the fundamentals I know about programming but most importantly how to have a programming mind set. Of course, I have got to thank Konstantinos Seiradakis for setting up all the technological equipment I used for my research and for enduring my impatience when the equipment didn't work. Additionally, I want to thank Dr Matt Kasoar, Dr Chantelle Burton and Katie Blackford for their help and assistance.

I would also like to thank Prof. Dionysia Kolokotsa and Prof. Mihalis Lazaridis, as well as all the members of the PhD committee, for their guidance and feedback.

Most importantly I want to thank my family my parents George and Dina and my sister Maria. Even though they are far away, they supported me continuously throughout my stay in Chania. Finally, I would like to thank Tania for her never-ending support and understanding but mainly for tolerating me all these years. Without their encouragement this work would never have been possible.

SPECIAL ACKNOWLEDGEMENTS

My research has been financially supported by the following programs/Institutes:

The Leverhulme Centre for Wildfires, Environment, and Society through the Leverhulme Trust, grant number RC-2018-023.

The AXA Research Fund and the Hellenic Foundation for Research and Innovation.

The project/program "National Network on Climate Change and its Impacts – Climpact I & II" financed by the Public Investment Program of Greece.

Abstract

This thesis studies the anticipated impact of climate change on wildfire danger in Greece, using meteorological variables and both atmospheric and land modelling techniques. The combined insights from this thesis underline the multifaceted challenges posed by climate change and wildfires in Mediterranean regions, and particularly in Greece. The projected increase in fire danger due to climate change necessitates robust fire management strategies and adaptive policies. Integrating advanced atmospheric and land modeling simulations, such as with WRF-Chem and JULES-INFERNO, can provide valuable predictions and guide effective interventions. As climate conditions continue to evolve, continuous monitoring and adaptive management will be essential to mitigate the adverse impacts of wildfires on ecosystems, human health, and economies.

The first paper “Future climate change impact on wildfire danger over the Mediterranean: the case of Greece” focuses on three Representative Concentration Pathways (RCPs): RCP2.6 (optimistic), RCP4.5 (moderate), and RCP8.5 (pessimistic) to study their effect on future fire danger. Findings indicate a significant increase in fire danger across Greece, particularly in high-risk areas such as Crete, the Aegean Islands, the Attica region, and parts of the Peloponnese. Projections show that, under the RCP8.5 scenario, these regions could experience up to 40 additional days of critical fire danger by the late 21st century compared to the late 20th century. The study highlights the importance of localized FWI thresholds due to varying climatic conditions across regions. The extension of the fire season is also anticipated, with some areas experiencing an increase of up to one month under the worst-case scenario. This could lead to higher frequencies of wildfires and associated health impacts from particulate emissions.

The second study "Wildfire Aerosols and Their Impact on Weather: A Case Study of the August 2021 Fires in Greece Using the WRF-Chem Model" investigates the impact of aerosols emitted from the August 2021 catastrophic wildfires in Greece on local weather patterns using the Weather Research and Forecasting model coupled with Chemistry (WRF-Chem). The study focuses on how wildfire aerosols affect temperature amongst other atmospheric variables. The results demonstrate that wildfire aerosols significantly modify atmospheric conditions, leading to decreased solar radiation reaching the surface, which in turn reduces surface temperatures. Moreover, the study finds that aerosols in the smoke plume can absorb solar radiation leading to the creation of rising air movement as well as a remote atmospheric circulation feedback away from the plume where pressure increases to counteract the lower pressure above the smoke plume, resulting in higher surface temperatures. The study underscores the importance of integrating aerosol data into weather forecasting models to improve the

accuracy of weather predictions during wildfire events and enhance emergency response strategies.

Connecting the first two studies, the third one titled “Automatic smoke plume detection using satellites” investigates the detection and analysis of aerosols released by wildfires in Greece using satellite products such as thermal anomalies and aerosol optical depth (AOD), in addition to the Canadian Fire Weather Index (FWI) that is produced from the widely used MERRA reanalysis weather data. This dataset was used as it provides long-term continues high temporal and spatial resolution essential for regional climate studies. It also incorporates obseravations from satellites and ground stations resulting in a reliable dataset that uses a consistent methodology essential for capturing climate data trends. The research attempts to separate fire-related aerosols and establish a relationship between AOD levels and wildfire activity by utilizing a variety of filtering techniques. The findings show that a dependable technique for tracking wildfire emissions is to combine thermal anomaly detection with AOD filtering based on the 99^{th} percentile of readings. The results highlight how integrating satellite data might enhance air quality monitoring and wildfire identification, especially in areas where fires occur often.

The forth research titled "Estimating future burnt area changes over Greece using the JULES-INFERNO model" explores the role of changing climate conditions as well as the evolution of different types of vegetation cover to examine future burnt area trends over Greece using the Joint UK Land Environment Simulator (JULES) combined with the INteractive Fire and Emission algoRithm for Natural envirOnments (INFERNO) wildfire scheme. The study highlights that when keeping a static vegetation cover, burnt area is projected to increase everywhere in Greece in response to dryer climatological conditions. When the vegetation is allowed to change dynamicaly, however, the overall burning is overall smaller, with the main agricultural areas of the country actually experiencing a reduction in burned area. With the potential for up to 1000 additional big burnt area incidents in a future period of 20 years (2080-2090) when compared with the period (2030-2040) across Greece, high emission scenarios greatly raised the probability of wildfires, with eastern continental Greece being especially susceptible. Future predictions using static vegetation resulted in an average increase of 0.8 km^2 in burnt area over Greece. On the other hand, because burnt areas were less likely to burn again, dynamic vegetation simulations projected a lesser increase of 0.3 km^2, showcasing that vegetation dynamics have a substantial impact on the future of wildfire activity.

Περίληψη

Αυτή η διατριβή μελετά τον αναμενόμενο αντίκτυπο της κλιματικής αλλαγής στον κίνδυνο πυρκαγιάς στην Ελλάδα, χρησιμοποιώντας μετεωρολογικούς δείκτες και τεχνικές μοντελοποίησης της ατμόσφαιρας και της γης. Τα αποτελέσματα από αυτήν τη διατριβή υπογραμμίζουν τις πολυδιάστατες προκλήσεις που θέτουν η κλιματική αλλαγή και οι πυρκαγιές στις μεσογειακές περιοχές και ιδιαίτερα στην Ελλάδα. Η προβλεπόμενη αύξηση του κινδύνου πυρκαγιάς λόγω της κλιματικής αλλαγής απαιτεί ισχυρές στρατηγικές διαχείρισης πυρκαγιών και προσαρμοστικές πολιτικές. Η ενσωμάτωση μοντελοποίησης της ατμόσφαιρας και της γης, όπως με τα μοντέλα WRF-Chem και JULES-INFERNO, μπορεί να παρέχει πολύτιμες προβλέψεις και να καθοδηγεί αποτελεσματικές παρεμβάσεις. Καθώς οι κλιματικές συνθήκες συνεχίζουν να εξελίσσονται, η συνεχής παρακολούθηση και προσαρμοστική διαχείριση θα είναι απαραίτητες για τον μετριασμό των αρνητικών επιπτώσεων των πυρκαγιών στα οικοσυστήματα, την ανθρώπινη υγεία και την οικονομία.

Η πρώτη εργασία "Future climate change impact on wildfire danger over the Mediterranean: the case of Greece" επικεντρώνεται σε τρία Σενάρια Αντιπροσωπευτικής Συγκέντρωσης (RCPs): RCP2.6 (αισιόδοξο), RCP4.5 (μέτριο) και RCP8.5 (απαισιόδοξο) για τη μελέτη της επίδρασής τους στον μελλοντικό κίνδυνο πυρκαγιών. Τα ευρήματα δείχνουν σημαντική αύξηση του κινδύνου πυρκαγιάς σε όλη την Ελλάδα, ιδιαίτερα σε περιοχές υψηλού κινδύνου όπως η Κρήτη, τα νησιά του Αιγαίου, η περιοχή της Αττικής και τμήματα της Πελοποννήσου. Οι προβλέψεις δείχνουν ότι, σύμφωνα με το σενάριο RCP8.5, αυτές οι περιοχές είναι πιθανό να υποστούν έως και 40 επιπλέον ημέρες κρίσιμου κινδύνου πυρκαγιάς έως τα τέλη του 21ου αιώνα σε σύγκριση με τα τέλη του 20ού αιώνα. Η μελέτη τονίζει τη σημασία των τοπικών ορίων επικινδυνότητας του Δείκτη Καιρικών Συνθηκών Πυρκαγιάς (FWI) λόγω των διαφορετικών κλιματικών συνθηκών ανά περιοχή. Αναμένεται επίσης η επέκταση της περιόδου πυρκαγιάς, με ορισμένες περιοχές να υποστούν αύξηση έως και 40 ημερών στο χειρότερο σενάριο. Αυτό θα μπορούσε να οδηγήσει σε υψηλότερη συχνότητα πυρκαγιών καθώς και σε επιπτώσεις στην υγεία από εκπομπές σωματιδίων.

Η δεύτερη μελέτη "Wildfire Aerosols and Their Impact on Weather: A Case Study of the August 2021 Fires in Greece Using the WRF-Chem Model" διερευνά τον αντίκτυπο των αερολυμάτων που εκλύθηκαν από τις καταστροφικές πυρκαγιές του Αυγούστου 2021 στην Ελλάδα στα τοπικά καιρικά φαινόμενα, χρησιμοποιώντας το μοντέλο Έρευνας και Πρόγνωσης Καιρού με Χημεία (WRF-Chem). Η μελέτη επικεντρώνεται στο πώς τα αερολύματα των πυρκαγιών επηρεάζουν τη θερμοκρασία, μεταξύ άλλων ατμοσφαιρικών μεταβλητών. Τα αποτελέσματα δείχνουν ότι αυτά τα αερολύματα τροποποιούν σημαντικά τις ατμοσφαιρικές συνθήκες, οδηγώντας σε μείωση της ηλιακής ακτινοβολίας που φτάνει στην επιφάνεια, η οποία με τη σειρά της μειώνει τις

επιφανειακές θερμοκρασίες. Επιπλέον, η μελέτη διαπιστώνει ότι τα αερολύματα στον καπνό μπορούν να απορροφούν ηλιακή ακτινοβολία, οδηγώντας στη δημιουργία ανοδικής κίνησης του αέρα καθώς και σε απομακρυσμένη ανατροφοδότηση ατμοσφαιρικής κυκλοφορίας μακριά από τον καπνό, όπου η πίεση αυξάνεται για να αντισταθμίσει τη χαμηλότερη πίεση πάνω από την περιοχή με τον καπνό, με αποτέλεσμα την αύξηση των επιφανειακών θερμοκρασιών σε αυτές τις περιοχές. Η μελέτη υπογραμμίζει τη σημασία της ενσωμάτωσης δεδομένων αερολυμάτων στα μοντέλα πρόγνωσης καιρού για τη βελτίωση της ακρίβειας των προβλέψεων καιρού κατά τη διάρκεια γεγονότων πυρκαγιάς και την ενίσχυση των στρατηγικών απόκρισης εκτάκτου ανάγκης.

Συνδέοντας τις δύο πρώτες μελέτες, η τρίτη η οποία έχει τίτλο “Automatic smoke plume detection using satellites” διερευνά την ανίχνευση και ανάλυση αερολυμάτων που εκλύονται από πυρκαγιές στην Ελλάδα χρησιμοποιώντας δορυφορικά προϊόντα όπως θερμικές ανωμαλίες και οπτικό βάθος αερολύματος (AOD), σε συνδυασμό με τον Καναδικό Δείκτη Καιρού Πυρκαγιάς (FWI) που παράχθηκε από τα ευρέως χρησιμοποιημένα καιρικά δεδομένα MERRA reanalysis. Αυτά τα δεδομένα χρησιμοποιήθηκαν καθώς παρέχουν μακροπρόθεσμη συνεχή υψηλή χρονική και χωρική ανάλυση απαραίτητη για τις περιφερειακές κλιματικές μελέτες. Ενσωματώνουν επίσης παρατηρήσεις από δορυφόρους και επίγειους σταθμούς δημιουργώντας ένα αξιόπιστο σύνολο δεδομένων που χρησιμοποιεί μια συνεπή μεθοδολογία απαραίτητη για την καταγραφή των τάσεων των κλιματικών δεδομένων. Η έρευνα επιχειρεί να διαχωρίσει και να επιλέξει τα αερολύματα που σχετίζονται με τη φωτιά και να δημιουργήσει μια σχέση μεταξύ των επιπέδων AOD και των δασικών πυρκαγιών χρησιμοποιώντας μια ποικιλία τεχνικών φιλτραρίσματος. Τα ευρήματα δείχνουν ότι μια αξιόπιστη τεχνική για την παρακολούθηση των εκπομπών δασικών πυρκαγιών είναι ο συνδυασμός της ανίχνευσης θερμικών ανωμαλιών με το φιλτράρισμα AOD με βάση το 99^{o} εκατοστημόριο των μετρήσεων. Τα αποτελέσματα υπογραμμίζουν πώς η ενσωμάτωση δορυφορικών δεδομένων μπορεί να βελτιώσει την παρακολούθηση της ποιότητας του αέρα και τον εντοπισμό των δασικών πυρκαγιών, ειδικά σε περιοχές όπου εμφανίζονται συχνά πυρκαγιές.

Η τέταρτη έρευνα "Estimating future burnt area changes over Greece using the JULES-INFERNO model" εξετάζει τον ρόλο των κλιματικών συνθηκών καθώς και την εξέλιξη των διαφορετικών τύπων βλάστησης για την εκτίμηση των μελλοντικών τάσεων καμένης έκτασης στην Ελλάδα, χρησιμοποιώντας τον Προσομοιωτή Περιβάλλοντος Γης του Ηνωμένου Βασιλείου (JULES). Η μελέτη εξάγει το συμπέρασμα ότι, με στατική κάλυψη βλάστησης, η καμένη έκταση προβλέπεται να αυξηθεί παντού στην Ελλάδα λόγω τις ύπαρξης πιο ξηρών κλιματολογικών συνθηκών στο μέλλον. Ωστόσο, όταν η βλάστηση ορίζεται να αλλάζει δυναμικά, η συνολική καμένη έκταση είναι σχετικά μικρότερη, με τις κύριες αγροτικές περιοχές της χώρας να παρουσιάζουν ακόμα και μείωση στην καμένη έκταση. Τα σενάρια υψηλών εκπομπών δείχνουν σημαντική

αύξηση της πιθανότητας πυρκαγιών, με εκτίμηση για έως και 1000 επιπλέον μεγάλα περιστατικά πυρκαγιών σε μια μελλοντική περίοδο 20 ετών (2030-2040) and (2080-2090) σε όλη την Ελλάδα, με την ανατολική ηπειρωτική Ελλάδα να είναι ιδιαίτερα ευαίσθητη περιοχή, τονίζοντας την επείγουσα ανάγκη μετριασμού της κλιματικής αλλαγής. Οι μελλοντικές προβλέψεις με στατικές προσομοιώσεις βλάστησης οδήγησαν σε μέση αύξηση 0,8 km^2 στις καμένες εκτάσεις. Ενώ οι δυναμικές προσομοιώσεις βλάστησης προέβλεψαν αύξηση κατά 0,3 km^2, καθώς σε αυτές οι καμένες περιοχές είναι λιγότερο πιθανό να καούν ξανά, δείχνοντας το σημαντικό αντίκτυπο της εξέλιξης της βλάστησης στον προσδιορισμό των μελλοντικών καμένων εκτάσεων.

Publications

Publications in scientific journals

Directly related to the PhD thesis field

1. Rovithakis, Anastasios, Manolis G. Grillakis, Konstantinos D. Seiradakis, Christos Giannakopoulos, Anna Karali, Robert Field, Mihalis Lazaridis, and Apostolos Voulgarakis. "Future climate change impact on wildfire danger over the Mediterranean: the case of Greece." Environmental Research Letters 17, no. 4 (2022): 045022. https://doi.org/10.1088/1748-9326/ac5f94

2. Rovithakis, A.; Voulgarakis, A. Modeling the Air Pollution and Weather Feedback from Wildfire Emissions with WRF–Chem over Greece. Environ. Sci. Proc. 2023, 26, 201. https://doi.org/10.3390/environsciproc2023026201

3. Rovithakis, Anastasios and Voulgarakis, Apostolos, An Investigation of Fire Emissions Impacts on Weather Over Greece Using WRF-Chem. Available at http://dx.doi.org/10.2139/ssrn.4576640

4. The entirety of the results and analysis found on the following chapter “Wildfire aerosols and their impact on weather: a case study of the August 2021 fires in Greece using the WRF-Chem model” has been submitted to Atmospheric Science Letters and has passed the major revision process

5. The following chapter “Estimating future burnt area changes over Greece using the JULES-INFERNO model” is in preparation for submission

6. The following chapter “Automatic smoke plume detection using satellites” is in preparation for submission

Indirectly related to the PhD thesis field

1. Grillakis, Manolis, Apostolos Voulgarakis, Anastasios Rovithakis, Konstantinos D. Seiradakis, Aristeidis Koutroulis, Robert D. Field, Matthew Kasoar, Athanasios Papadopoulos, and Mihalis Lazaridis. "Climate drivers of global wildfire burned area." Environmental Research Letters 17, no. 4 (2022): 045021. https://doi.org/10.1088/1748-9326/ac5fa1

2. Haleema Misal, Elsa Varela, Apostolos Voulgarakis, Anastasios Rovithakis, Manolis Grillakis, Yiannis Kountouris. " Assessing public preferences for a

wildfire mitigation policy in Crete, Greece" Forest Policy and Economics 153 (2023): 102976. https://doi.org/10.1016/j.forpol.2023.102976

International scientific conferences

1. Rovithakis, A., Voulgarakis, A., Grillakis, M., Giannakopoulos, C., and Karali, A.: Future Climate Change Impact on Wildfire Danger over the Mediterranean: the case of Greece, EGU General Assembly 2021, online, 19–30 Apr 2021, EGU21-11198, https://doi.org/10.5194/egusphere-egu21-11198, 2021.

2. Rovithakis, A., Voulgarakis, A., Grillakis, M., Giannakopoulos, C., and Karali, A.: Future Climate Change Impact on Wildfire Danger over the Mediterranean: the case of Greece, 15th International Conference on Meteorology Climatology and Atmospheric Physics – COMECAP2021, Online, Ioannina, Greece, 26 – 29 September, 2021.

3. Rovithakis, A., Voulgarakis, A., Grillakis, M., Giannakopoulos, C., and Karali, A.: Future Climate Change Impact on Wildfire Danger over the Mediterranean: the case of Greece, Fire in the Earth System Abstracts, Vol. 1 FES-Climate-fire links-69, Valencia, Spain, 3-7 November, 2021.

4. Rovithakis, A., Voulgarakis, A., Grillakis, M., Lazaridis, M., Chatoutsidou, E.: Fire Weather Index's Predictive Power of Aerosol Pollution over Greece, International Association of Wildland Fire - IAW, Pasadena, USA, 23-27 May, 2022.

5. Rovithakis, A., Voulgarakis, A., Grillakis, M., Lazaridis, M., Chatoutsidou, E.: Fire Weather Index's Predictive Power of Aerosol Pollution over Greece, International Aerosol Conference – IAC2022, Athens, Greece, 4-9 September, 2022.

6. Rovithakis, A., Voulgarakis.: Studying air pollution and weather feedbacks from wildfires over Greece using WRF-Chem", EGU General Assembly 2023, Vienna, Austria, 24-28 April, 2023.

7. Rovithakis, A., Voulgarakis.: Feedbacks on weather via fire-generated aerosols over Greece, Fire in the Earth System: Humans and Nature – fes2023, Granada, Spain, 4-8 July, 2023.

8. Rovithakis, A., Voulgarakis.: Modelling the air pollution and weather feedbacks from wild-fire emissions with WRF-Chem over Greece, Conference on Meteorology, Climatology and Atmospheric Physics –COMECAP 2023, Athens, Greece, 25-29 September, 2023.

9. Rovithakis, A., Voulgarakis.: Examining the Impact of Fire Emissions on Weather via air pollution over Greece using WRF-Chem, International Fire Ecology and Management Congress, Monterey, California, 4-8 December, 2023.

Table of Contents

Examining Committee vii

Acknowledgements i

Abstract iii

Περίληψη v

Publications viii

Table of Contents i

List of Figures iii

1 Introduction 1

1.1 Understanding Wildfires 1

1.2 Preventing Wildfires 8

1.3 Detecting Wildfires 9

1.4 The Climate-Wildfire-Air Quality System 10

1.5 Modelling the System: Integrating Models Across Disciplines 14

1.6 Research Topics Contribution and Novelty of PhD Thesis 19

2. Future climate change impact on wildfire danger over the Mediterranean: the case of Greece 21

2.1 Introduction 22

2.2. Data and Methodology 24

2.2.1 Study area characteristics 24

2.2.2 FWI description and thresholds 25

2.2.3 Climate data used for predictions 26

2.2.4 Signal to noise ratio 27

2.2.5 Fire season length 27

2.3. Results and discussion 27

2.3.1 Determining areas of increased fire danger 28

2.3.2 Fire season length and seasonal variability change 32

2.4. Conclusions 36

3. Wildfire aerosols and their impact on weather: a case study of the August 2021 fires in Greece using the WRF-Chem model 39

3.1 Introduction 40

3.2 Data and Methodology 42

3.2.1 WRF-Chem model setup 42
3.2.2 Climate data used for comparison 43
3.2.3 Selection of fire smoke plume affected areas 44
3.2.4 Error improvement 44
3.3 Results 44
3.3.1 Model performance and the role of fire emissions 44
3.3.2 Physical mechanisms 49
3.4 Conclusions 53
4. Automatic smoke plume detection using satellites 55
4.1. Introduction 55
4.2. Data and Methodology 57
4.2.1 MODIS Aerosol and Thermal Anomalies products 57
4.2.2 Detection and isolation of fire emitted aerosols 57
4.2.3 Selection of the fire plume affected areas 58
4.3. Results and discussion 59
4.3.1 Determining the optimal smoke plume selection methodology 59
4.3.2 AOD correlations with weather variables 62
4.4 Conclusions 65
5. Estimating future burnt area changes over Greece using the JULES-INFERNO model 66
5.1 Introduction 67
5.2 Data and JULES model setup 68
5.3 Results 70
5.3.1 Model performance 70
5.3.2 Future changes and climatic drivers 75
5.3.3 Frequency of High Burnt Area events and Connection of Burnt Area and FWI 79
5.3.4 The role of static vs dynamic vegetation on Burnt Area 82
5.4 Conclusions 88
6. Conclusions 90
7. Future Research 92
Bibliography 94

List of Figures

Figure 1.1. The different impacts of wildfires on the atmosphere, land and ocean (D. S. Ward et al. 2012)..

Figure 1.2. The air quality component is represented by black, the climate component by blue, and the wildfire component by red in the conceptual space-time diagram of the climate-wildfire-air quality system. Additionally, this graphic shows the impacts (single-pointed arrows) and feedback loops (double-pointed arrows) of the climate-wildfire-air quality system at various scales. (Stavros, Mckenzie, and Larkin 2014).

Figure 1.3. The figure illustrates the mean radiative forcing throughout an 80-year fire cycle in Alaska's interior boreal forest. The percentage of the total net radiative force from each component is shown by the numbers. Negative numbers indicate decreased forcing, whereas positive numbers indicate increased forcing, which results in a positive feedback on climate change. The feedback loop is closed by the dashed line, which represents the change in the climatic driving of fire regimes. (Stavros, Mckenzie, and Larkin 2014).

Figure 1.4. The main components of the INteractive Fire and Emission Algorithm for Natural Environments (INFERNO) (Mangeon et al. 2016).

Figure 1.5. Structure of the Canadian Forest Fire Weather Index System FWI (B. Stocks et al. 1989)

Figure 2.1. Panel (a) represents the annual ensemble mean total number of days (NOD) with FWI>30 for the reference period (1970-2000). Panel (b) is the (NOD)>30 for the fire season only of the same ensemble mean and time period as panel (a). Panels (c, d, e, f, g, h) showcase the difference in the annual ensemble mean (NOD) with FWI>30 for every RCP scenario separately between the future periods and the reference period. The left column corresponds to the difference for the near future period [(2021-2050) – (1971-2000)] and the right column to the difference for the distant future [(2069-2098) – (1971-2000)].

Figure 2.2. Panel (a) is a comparison of spatially averaged yearly FWI fire season values of all RCP scenarios and time periods against the EFFIS fire danger classes shown on the right-hand side of the y axis of panel (a). Panel (b) shows the average fire season FWI values from all models together with the extreme FWI>150 as depicted by the cross hatched regions, whereas maps (c, d, e, f, g, h) representing the 30-year ensemble average FWI change based on the average of all 3 different GCM simulations during the fire season months (May-September) between the two future time periods from the reference period, for all RCP scenarios. Hatched regions depict the values that are higher than the 90th percentile of the SN ratio for the corresponding time period.

Figure 2.3. All model average fire season length change between the future periods (for all future scenarios) and the reference. Subplots (a, b, c, d, e, and f) represent the 30-year average difference whereas subplot (g) represent the entire Greek domain averaged fire season length change for every RCP scenario and time period.

Figure 2.4. Seasonal variability change between near future and reference period in sub-figure (a) and distant future and reference period in sub-figure (b) for each of the three climate models for the entire Greek domain, under all the tested RCP scenarios.

Figure 3.1. Panel (a): Study area in blue colour corresponding to the non-affected areas and the entire simulation domain in grey colour. Orange stripes inside the blue study area represent the wildfire smoke plume affected areas that were selected based on the methodology explained in subsection 3.2.3 in the South-eastern part of Greece. Comparison of WRF-Chem AOD output to MODIS observations. Panel (b1) shows a MODIS AOD snapshot for 8/8/2021 8:40 AM. Panel (b2) is a snapshot for the same day at 9:00 AM from WRF-Chem ensemble mean output. Panel (c) shows comparison for all days, spatially averaged for the fire smoke affected areas in the Greek domain, for MODIS and for the two WRF-Chem simulations (averaged over all 10 ensemble members). The bars on top of the boxes represent the total spread of all 10 ensemble members for each of the 2 WRF-Chem simulations whereas the boxes indicate the spread of the middle 50% of the 10 ensemble members. Panel (d) shows the error improvement between the two WRF-Chem simulations (w/ minus w/o fire) when compared with the MODIS observations.

Figure 3.2. Time evolution of the spatially averaged Black Carbon emissions over the fire smoke affected areas in the Greek domain during the first 10 days of August.

Figure 3.3. Comparison of WRF-Chem surface temperature output to ERA5 reanalysis and to ground station data. Panels (a) and (b) show the correlation between ERA5 and WRF-Chem 2m temperature, for the two simulations. Stippled regions are those with no significant difference between observed and simulated data as defined by the p-values < 0.05 (i.e. good agreement with observations). Panel (c) shows the difference between the two correlations in panel (a) and (b). Hatching indicates areas with differences that are not significant, using standard error propagation of the results from panels (a) and (b). Panel (d) shows the comparison of WRF-Chem simulations (averaged over all 10 ensemble members) with ERA5 data, spatially averaged for the wildfire smoke affected areas and for all days. The bars on top of the boxes represent the total spread of all 10 ensemble members for each of the 2 WRF-Chem simulations, whereas the boxes indicate the spread of the middle 50% of the 10 ensemble members. Panel (e) shows the error improvement in temperature of the two WRF-Chem simulations relative to ERA5.

Figure 3.4. Ensemble mean differences in the longwave and shortwave radiation budget over the fire smoke affected areas in the Greek domain, between the WRF-Chem simulations with and without fire emissions:

Figure 3.5. Ensemble mean differences in temperature, aerosol abundances and associated meteorological variables, between the WRF-Chem simulations with and without fire emissions: Panel (a): surface temperature difference at 14:00 (^{o}C). Panel (b): AOD difference at 14:00. Panel (c): net downward shortwave radiation difference at the surface (W/m^{2}). Panel (d): surface water vapour difference (kg/kg). Panel (e): total cloud fraction difference expressed as areas with less cloud coverage during fire simulations (-0.1 - 0) and higher cloud coverage (0 - 0.1). Panel (f): difference in geopotential height and in the wind vector at 850 hPa. Panel (g): vertical wind speed changes at 850 hPa. Blue areas experience rising air and red areas sinking air.

Figure 3.6. Temperature regression against AOD in the simulation including fire emissions and in observations. We find positive tendencies for areas in other parts of the country and negative tendencies for areas collocated with the smoke plume.

Figure 4.1 Isolation and selection of smoke plume affected areas based on the 99th percentile of the AOD values seen inside the red circles that are in close proximity to the thermal anomalies data representing wildfire centers marked with the green circles.

Figure 4.2. Correlation between the different stages of fire related AOD isolation with the corresponding FWI time steps. Subplot (a) is the original correlation between AOD (from MODIS) and FWI. Subplot (b) is the same correlation as subplot (a) after selecting only the days with potential fire hotspots using the Thermal Anomalies product. Subplot (c) is the same correlation as subplot (b) after further removing the days with AOD < 99th percentile of the entire domain of interest AOD values.

Figure 4.3. Correlations between different types of aerosol optical depth products with the reanalysis FWI. Subplot (a) is the FWI correlation with the original AOD (from OMI). Subplot (b) is the correlation between the AOD (from MODIS) and FWI filtered using the Thermal Anomalies product. Subplot (c) is the correlation between AOD and FWI filtered with the 95th percentile of the AI values whereas subplot (d) is the same concept correlation as subplot (c) using the 95th percentile of the AAOD instead of the AOD. Subplots (e and f) are scatterplots of two representative areas with high R values in Peloponnese.

Figure 4.4. Correlations between AOD (from MODIS) and relative humidity in subplot (a), precipitation in subplot (b), wind speed in subplot (c) and temperature in subplot (d) filtered using the Thermal Anomalies product.

Figure 4.5. Average regressions between AOD from the areas affected by fire plumes directly and the corresponding FWI in subplot (a), wind speed in subplot (b), relative humidity in subplot (c) and temperature in subplot (d). Red dots represent the consecutive days with the 2007 catastrophic wildfires.

Figure 5.1. Panels (a) and (b) show the correlation between GFED5 and JULES-INFERNO Burnt Area, for the simulation with static vegetation cover and the one with dynamically changing, respectively. Panel (c) shows the difference between the two correlations in panel (b) - (a). Panel (d) shows comparison for all years for the domain-wide spatial average, between the GFED observations and the simulated Burnt Areas with static and dynamically changing vegetation cover.

Figure 5.2. Spatial distribution of the mean burned area (BA) in Greece from 2004 to 2019. Each pair of panels compares the modelled BA (left) with the Global Fire Emissions Database (GFED) observed BA (right). Panels (a1, a2) Annual mean BA (b1, b2) Winter mean BA (c1, c2) Spring mean BA (d1, d2) Summer mean BA (e1, e2) Autumn mean BA (f1, f2) May mean BA (g1, g2) June mean BA (h1, h2) July mean BA (i1, i2) August mean BA (j1, j2) September mean BA.

Figure 5.3. Comparison of climatological condition differences for the 3 RCP scenarios between near future and reference panels (a1-l1). Burnt Area differences 1st row. Temperature differences 2nd row. Relative humidity differences 3rd row. Precipitation differences 4th row. Soil moisture differences 5th row.

Figure 5.4. Comparison of climatological condition differences for the 3 RCP scenarios between distant future and reference panels (a2-l2). Burnt Area differences 1st row. Temperature differences 2nd row. Relative humidity differences 3rd row. Precipitation differences 4th row. Soil moisture differences 5th row.

Figure 5.5 Distribution of Burnt Area size change under Different SSP Scenarios for future Periods (2030-2040 and 2080-2090) compared to the historical period (1980-1990).

Figure 5.6. Frequency of high Burned Area (BA) Events greater than the 99th percentile of the historical period in Greece under Different SSP Scenarios. Panels a, b, and c show the spatial distribution of the frequency of high BA events for the periods 2030-2040 and 2080-2090 under SSP126, SSP370, and SSP585 scenarios, respectively. Panels (d) and (e) display the temporal distribution of the frequency of high BA events per month aggregated for all of Greece for the periods 2030-2040 and 2080-2090 respectively under the same SSP scenarios.

Figure 5.7. Boxplots showing the evolution of Burnt Area for the 3 RCP scenarios panel (a), compared to the FWI for the same time periods as calculated from our previous study (Rovithakis et al. 2022) panel (b).

Figure 5.8. Spatial correlations between burned area (BA) and various weather variables during fire season months across Greece. Panels show comparisons between static (left column) and dynamic vegetation (right column) conditions in the JULES-INFERNO model. Panel a and b show the correlation between temperature and Burnt Area. Panel c and d show the correlation between wind speed and Burnt Area. Panel e and f show the correlation between relative humidity and Burnt Area. Panel g and h show the correlation between precipitation and Burnt Area.

Figure 5.9. Burnt Area differences between distant future and near future from the simulation with static vegetation for the 3 RCP scenarios panels (a-c). Burnt Area differences between distant future and near future from the simulation with dynamic vegetation for the 3 RCP scenarios panels (d-f). Panels (g-i) show Burnt Area differences between the simulation with static and dynamic changing vegetation. We observe two areas (NG and SG) within the domain with the highest and lowest differences respectively in panel (i).

Figure 5.10. To explain the highest and lowest differences respectively in Figure 4 panel (i) for the areas NG and SG, panels (j-o) show comparisons of Carbon Mass in Vegetation for the years 2015-2100 and for the three RCP scenarios spatially averaged for NG (top row) and for SG (bottom row).

1 Introduction

1.1 Understanding Wildfires

What are wildfires?

In the domain of non-urban areas, various terms are utilized internationally to depict vegetation fires. In the United States, the expression "wildland fire" covers any non-structure blaze in the wilderness. Australia uses the term "bushfire" for any vegetation blaze, while the more general term "wildfire" includes unplanned vegetation fires, such as grass, forest, and scrub fires. In their yearly report on fires in European countries, the European Commission Joint Research Centre Institute for Environment and Sustainability uses the term "forest fire," and in Canada, the Canadian Interagency Forest Fire Centre defines them as "forest fire" and "wildfire" (Bento-Gonçalves et al. 2012). Wildland fires are a pervasive and frequent issue, affecting overall more than 30% of the global land surface during the period 2000-2006 based on MODIS active fire data (Chuvieco, Giglio, and Justice 2008).

Wildfires an integral part of nature

Fires hold a unique place among natural disasters because humans both start and manage them, while also battling them. This "command and control" approach often fails to recognize the ecological importance of fire for biodiversity and ecosystem services. Without viewing fire as a natural process and planning accordingly, its impacts on social and ecological systems will persist (Holling and Meffe 1996).

In recent times, wildfires have increasingly affected human lives, cultural heritage, homes, infrastructure, air quality and carbon storage. These outcomes stem from a variety of causes and have complex effects (Fernandes 2013). The frequency and size of fires vary widely among ecosystems, and human activities have further altered fire regimes through practices such as timber harvesting and fire suppression. While many wildfire policies focus on reducing fuel, few address the underlying issue of community planning and location (Driscoll et al. 2010).

As climate change is projected to increase fire activity, a new approach is needed. Considering fire problems within the context of coupled socio-ecological systems (SESs), can help us better understand the interaction between humans and their environments. By synthesizing knowledge about fire's ecological role and human life in fire-prone areas, we can identify vulnerabilities, trade-offs, and adaptation policies, across diverse landscapes (Moritz et al. 2012).

The Earth's forests and vegetation play a crucial role as a substantial fuel source, with fires consuming extensive amounts of biomass across diverse ecosystems, from tundra to savannah and from boreal to tropical forests. Many ecosystems are fire dependent. Fires are typically categorized based on their propagation height as ground, surface, or crown fires (Buscarino et al. 2015).

Causes and Impacts of Wildfires

While some fires are natural in specific climates, the majority of wildfires result from human activity, with only a minor portion attributed to environmental factors (FAO, 2001). Human actions have evidently altered fire patterns over time, particularly due to recent population growth, economic influences, and land use practices (Pausas and Keeley 2009). Specific fire behaviours can now be seen as driven by human activities (Archibald et al., 2013). Furthermore, climate change is expected to change the distribution of wildfires, a process influenced by environmental and spatial conditions (Krawchuk et al. 2009).

Fires have a considerable impact on soil and air quality (Stavros, Mckenzie, and Larkin 2014). They can affect soil structure and temperature, influencing soil productivity and making it more susceptible to runoff and erosion (Buxton et al. 2011). Soil heating can also change soil chemical and biological properties, impacting nutrient cycling, and water retention. When organic matter burns, nutrients are released, but they can also be lost through leaching and runoff (Tsibart et al. 2015).

Wildfires and prescribed fires can have short and long-term air quality impacts, typically seen as negative for environmental quality (Hyslop 2009). Wildfires can also cause significant damage to infrastructure which can be exacerbated by post-fire floods (Neary et al. 2012).

The connection between climate, wildfires, and air quality is of great social concern, as the emissions from wildfires can directly impact human health (Langmann et al. 2009). The emissions from wildfires as seen in Figure 1.1 can be quite harmful, consisting of substances such as carbon monoxide (CO) and fine particulate matter ($PM_{2.5}$), along with secondary pollutants such as tropospheric ozone (O_3) (Pfister, Wiedinmyer, and Emmons 2008). These pollutants can seriously affect human health, with CO able to change pollution levels over a wide area, especially tropospheric O_3 level, as it is an O_3 precursor (ref). Additionally, wildfires can affect surface O_3 levels, sometimes even above accepted health guidelines, in nearby and distant areas (D. E. Ward and Hardy

1991). Elevated surface tropospheric O_3 levels can lead to respiratory problems such as irritation, reduced lung function, and worsened asthma symptoms. Fine particulate matter, e.g. particles with diameters of less than 2.5 µm ($PM_{2.5}$) are also emitted from wildfires, and are a concern due to their ability to penetrate deep into the lungs, causing health issues or even mortality. Furthermore, particulate matter (PM) emitted from wildfires is more harmful than an equivalent concentration from other sources. Other pollutants like mercury, which can accumulate and be released into the air during combustion, can also pose health risks (Bowman and Johnston 2005). Research has shown that exposure to wildfire smoke correlates with increased hospital visits for respiratory conditions such as asthma. While air pollutants can have multiple sources, the amount emitted from wildfires can be substantial, especially during periods of extensive biomass burning (Langmann et al. 2009).

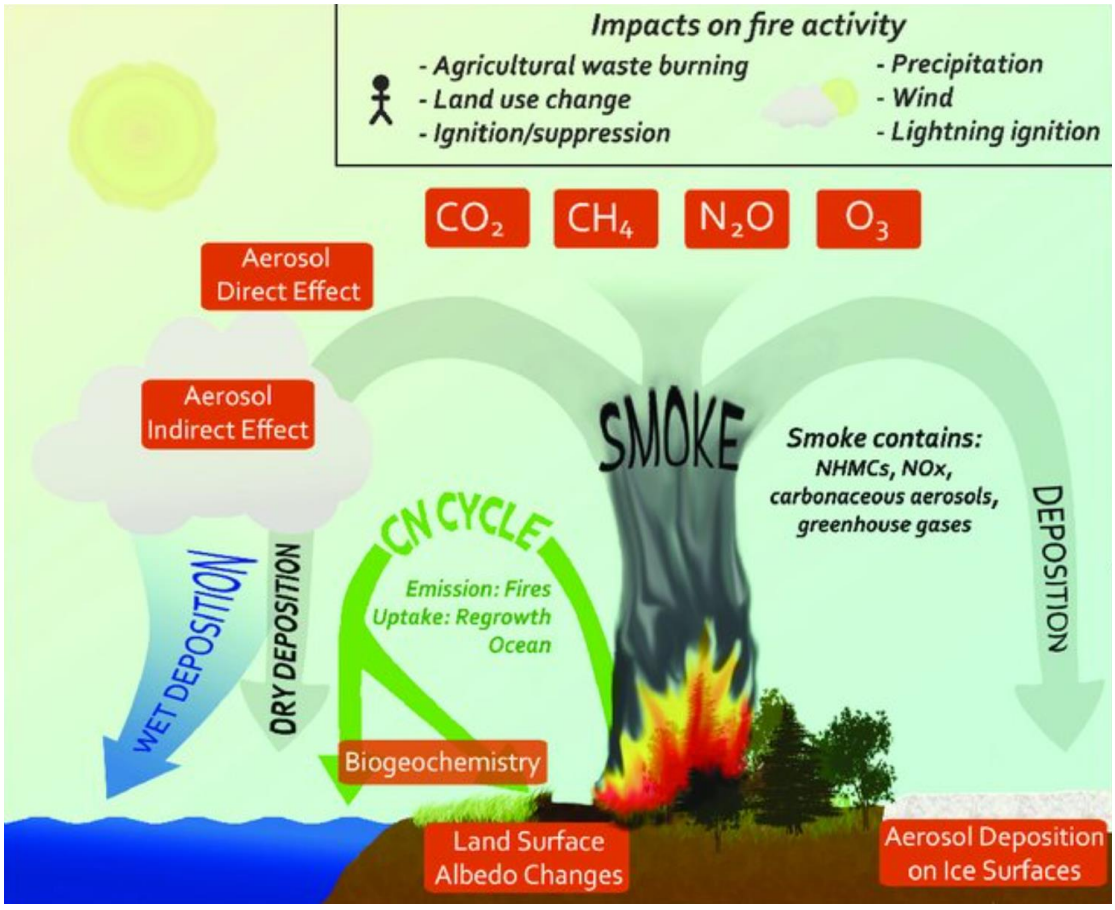

Figure 1.1. The different impacts of wildfires on the atmosphere, land and ocean (D. S. Ward et al. 2012).

The composition of the atmosphere and climate are greatly influenced by two essential components of wildfire emissions: organic carbon (OC) and black carbon (BC). BC is a particulate matter that warms the atmosphere by absorbing sunlight and resulting from incomplete combustion of carbonaceous materials. OC is made up of a range of organic substances that have the ability to scatter sunlight and chill the atmosphere (Bond et al. 2013). Both BC and OC have a substantial negative influence on health, increasing

the risk of cardiovascular and respiratory conditions (Bowman and Johnston 2005). Understanding these carbonaceous aerosols' emissions from wildfires is crucial because of the intricate interactions between them and their roles in climate forcing (Bond et al. 2013).

Fire and ecosystems

The role of fire in ecosystems varies based on human alteration compared to natural or historical conditions. In semi-wilderness areas such as the western US and Australia, preserving or restoring specific fire patterns is crucial for maintaining habitats and ecosystem functions, emphasizing the link between fire characteristics and ecological impacts. Conversely, in regions such as the Mediterranean basin with significant human influence, defining what is "natural" is challenging. Fire have always been a part of the Mediterranean ecosystems making the local vegetation well adapted as many types of trees need fire to resproute (Riva et al. 2016;Pausas and Keeley 2009). Some ecosystems are primarily influenced by climate factors such as drought frequency, while others are shaped by local elements such as terrain and fuel availability (Moritz et al. 2014).

Resilience and climate change

Fire patterns in naturally fire-prone ecosystems are primarily dictated by broader climate trends. Local factors such as ignition rates and fuel accumulation play a greater role in less intense fires. However, this simplification requires management strategies to address the ensuing complexity (Schoennagel, Veblen, and Romme 2004).

Climate change introduces additional hurdles, as it may create unprecedented environmental conditions. While the goal is to maintain fire regimes that reduce biodiversity loss, uncertainty surrounding future climates and environmental processes complicates adaptation efforts. A suggested approach is to bolster ecosystem resilience through diversifying vegetation and stand structures. Varied topography also plays a role, creating microclimates that can serve as refuges and impact fire behaviour in mountainous terrain (Krawchuk and Moritz 2011).

Climate change is expected to have a major impact on fire patterns, potentially overshadowing the direct effects of global warming on species distribution and productivity.

Fire patterns are influenced by climate change, changes in natural ignition rates, the spread of non-native plants affecting fuels, the distribution changes of native plants and fuels, and changes in human populations affecting land use, fragmentation, and the frequency of human-caused ignitions (Tsibart et al. 2015).

In ecosystems with a limited history of fire, encouraging burning under different circumstances can foster diversity and limit fuel build up (Millar, Stephenson, and Stephens 2007).

Socioecological systems and fire

Sustainable resolution of environmental issues hinges on understanding the intricate connections between humans and ecosystems (Chapin et al. 2008). While there's extensive research on the impact of climate change on boreal forests and rural indigenous communities, comprehending the densely populated Wildland-Urban Interface (WUI), where most wildfire fatalities and property losses occur, remains a challenge (Chapin et al. 2006). Given the complexity of wildfires across ecosystems and human interactions with them, a coupled socio-ecological systems (SES) approach is vital. By redefining the issue to mitigate climate-induced risks in fire-prone areas, an integrated SES perspective can be forged (Moritz et al. 2012). This perspective recognizes the role of geographic context in shaping wildfire impacts across the SES. The features of the WUI largely determine how fires are handled and their consequences for communities (Paveglio et al. 2009).

Sustainable coexistence with wildfires necessitates cooperative efforts among governments and at-risk communities. This entails integrating building, planning, fuel management, and fire suppression capacities at various scales. Sustainable coexistence should enable environmentally fitting fire regimes to function close to or far from the WUI, reducing hazards to people, property, and resources., and enhancing ecosystem services. This strategy should reduce firefighting costs and diminish risks for firefighters (Chapin et al. 2006).

In the natural world, wildfires can be seen as a significant and sometimes necessary disruption to the environment (Littell et al. 2010). They often act as a catalyst for changes in plant life, particularly in areas where the climate is shifting. This process, known as vegetation succession, is crucial for the evolution of plant species. In some cases, wildfires are even used as a means of maintaining and restoring ecosystems, especially when it comes to managing the gaps left by fire for new growth. This not only impacts the structure, composition, and age of plant life but also affects the overall disturbance pattern of an area. Rejuvenating the landscape following a fire is crucial because it contributes to key ecosystem services including nitrogen cycling and carbon sequestration and directly affects biodiversity, soil fertility, and wood resources (G. D. Peterson 2002). Nevertheless, the advantages of wildfires may be outweighed by their effects on air quality, especially when the emissions from the flames have an adverse effect on the ecosystems nearby. This may lead to reduced forest growth, a rise in tree death rate, increased disease susceptibility, and the extinction of vulnerable species, while also leading to the invasion of non-native species.

To address these challenges, we need to take a holistic approach that considers climate, wildfires, and air quality as interrelated elements of a larger system (Littell et al. 2010). By doing so, we can better understand how to meet air-quality standards and develop strategies for managing and mitigating the effects of wildfires. This includes both direct and indirect management strategies (Van Der Werf et al. 2006). Direct strategies may

involve controlled burning during specific seasons and conditions, mechanical thinning of fuel to reduce emissions, and fire suppression when necessary to protect health. Indirect strategies, on the other hand, may involve limiting emissions from other sources, such as pollution from anthropogenic activities, to reduce the overall impact on air quality (Hyslop 2009).

There are also other, less obvious ways in which human activity can influence the system. For example, land management practices can impact the frequency and intensity of fires, while urban development can create barriers to fire spread (Bytnerowicz et al. 2010). These factors should also be considered when developing management strategies (Hurteau, Koch, and Hungate 2008). Furthermore, understanding how human activity can influence the climate-wildfire-air quality system can help us develop better models for predicting and managing these events (Jaffe et al. 2008). By studying this system, we can also gain valuable insights into the larger carbon cycle and how it interacts with the climate system. This, in turn, can help us develop more accurate models for predicting climate change and its impacts on air quality (Stavros, Mckenzie, and Larkin 2014)

Achieving sustainable coexistence with wildfire

The intricacies of coupled wildfire socio-ecological systems (SESs) result in different thresholds for action during different stages of wildfires. Societal pressures often influence the extent to which scientific discoveries guide adaptive responses (Moritz et al. 2014).

Context-specific and place-based techniques are necessary to address the many SES challenges related to wildfires. This is because different institutional and social contexts impact people's abilities to reduce risk, and some fire regimes are inherently manageable (Moritz et al. 2014).

The long-term evolution of WUI and its influence on transboundary hazards are significantly influenced by governments. As a result, it is crucial to give land-use development more consideration (Holling and Meffe 1996). Important measures for regulating the coupling in a wildfire SES include land-use regulations, such as building laws linked to fire safety or construction limitations in regions that are prone to wildfires (Buxton et al. 2011).

Effective risk mitigation inside projects and long-term control of fire regimes across landscapes depend on addressing hazard at the WUI. While compromises and trade-offs are unavoidable in order to balance conflicting demands, focusing risk mitigation management efforts on the WUI reduces the likelihood of unfavourable effects on environmental assets in those areas. Assessing these trade-offs requires improved maps of ecosystem services, fire dangers, and the consequences of climate change (Moritz et al. 2014).

Improved planning, management, and policies in all areas of the linked wildfire SES issue are supported by a wealth of research. Finding solutions that consider fire's advantages and disadvantages for human and ecological systems requires acknowledging fire as a natural and inescapable danger (Moritz et al. 2014).

Wildland-Urban interface

The Wildland-Urban Interface (WUI) is a crucial zone where human development meets fire-prone landscapes, crucial for understanding and managing wildfire risks as urbanization encroaches on previously undeveloped areas. The WUI is expanding globally, intensifying wildfire socio-ecological systems (SESs) (Moritz et al. 2014).

In the western US, the WUI grew significantly since 1970, especially in fire-prone, privately-owned areas. Although much remains undeveloped, fire risk increases with population growth. Similar patterns are seen in Mediterranean Europe and Australia (Moritz et al. 2014).

Global studies are needed to understand human settlements in fire-prone zones, as population density affects fire vulnerability. Some regions are more fire-prone irrespective of forest cover. In the Mediterranean basin, high-density areas often see extensive fires despite low forest cover (Bar-Massada, Radeloff, and Stewart 2014).

Recognizing diverse fire-prone environments and resident vegetation is vital for effective fuel treatments and resource allocation (Paveglio et al. 2009). Communities vary in their mitigation capabilities, influenced by social and institutional factors (Calkin et al. 2014).

Mediterranean basin

The Mediterranean landscape is characterized by a mix of shrublands, oak, and pine forests, along with pastures, cultivated areas, and abandoned agricultural fields. The historical use of fire has significantly shaped this landscape for rangeland. On the other hand, the dynamics of fire and vegetation have changed in recent years. Due to overuse of land and decreased plant cover, the southern and eastern areas are experiencing desertification and a loss of ecosystem services. Meanwhile, the northern region experiences increased fire hazards and losses due to socioeconomic factors, with dense shrublands and woodlands supporting high-intensity "crown" fires driven by climate change (Pausas and Fernández-Muñoz 2012).

European Union countries have forest policies addressing wildfires, but there is no consensus on fire and ecosystem management. Despite investments in firefighting capabilities and preparedness, devastating fires have still occurred in several Mediterranean countries due to extreme fire-weather conditions. A new framework is being proposed to promote traditional fire practices and adapt to different territorial contexts. Prescribed burning, primarily managed at the local level, is on the rise across Europe to moderate fuel loads and the risk of high-intensity fires. However, regional,

and national wildfire policies still focus on temporary suppression actions, raising concerns about the environmental impacts of current fire patterns. Human-cantered fire exclusion remains the dominant approach across most Mediterranean landscapes (Moritz et al. 2014).

1.2 Preventing Wildfires

Various strategies and methods are being implemented to mitigate the impact of wildfires. For example, the construction of ZIFs (Forest Intervention zones) can incorporate prescribed fire, a common technique for controlling fuel loads in rangelands and forests (Carreiras et al. 2014). The ZIF approach, aims to improve forest management by addressing current constraints, improving fire protection, ensuring coordinated interventions, and promoting sustainability (Martins and Borges 2007). Forest owners and producers developing the Forest Management Plan are responsible for implementing it. Funding is from a shared fund and public sources. Active landowner participation is crucial for ZIF's success, requiring multiple information sessions for recruitment (Valente et al. 2013).

Grazing activities in forest and rangeland areas are sometimes encouraged. In mountainous regions, goats, are employed to manage underlying vegetation and minimize wildfire risk. The promotion of grazing can foster landscape and economic diversity, creating conditions conducive to increased human population (Carreiras et al. 2014).

Fire suppression infrastructure consists of equipment and systems deployed across landscapes to assist in fire control. This includes lookout towers, initial intervention brigades, and a road network for fast response. The infrastructure also features water tanks and firebreaks (Carreiras et al. 2014).

Prescribed fire, a controversial technique, was first used to lower fire risk by reducing organic matter and increasing landscape diversity. However, in recent decades, it has been reintroduced as a tool for forest and shrubland management. It involves the controlled burning of rangeland and undergrowth during winter under specific environmental conditions to create a low-temperature burn. This technique helps prevent soil and ecosystem degradation and is executed against the wind (Carreiras et al. 2014).

Road and firebreak locations are optimized to reduce fire advancement by creating fuel discontinuities (Valente et al., 2013). Various techniques can be used, and land planning is essential for coordinated management. These plans identify and prioritize fire risks and encourage discontinuities to hinder fire progression. (Martins and Borges 2007).

1.3 Detecting Wildfires

The evolution of utilizing aerial vehicles in forest fire management, dates to the 1920s when aircraft were initially used to extinguish fires by dropping water. This method however, had limited success, leading to a shift towards using aircraft for fire detection. Post-World War II, in the late 1960s, aircraft usage for fire suppression, involving airplanes and helicopters, resurfaced. However, this approach was costly and risky due to the need for pilots to fly near fires, resulting in an increase in firefighting-related aircraft incidents (Zohdi 2021).

Recent technological advancements in unmanned aerial vehicles UAVs have opened new possibilities for employing aircraft in forest firefighting. Various UAV models have been developed for early wildfire detection, such as the sophisticated drone by Krüll et al. (2012) and a project initiated by the Balkan-Med area for monitoring and forecasting forest fires (De et al. 2019). Initial configurations involve a network of ground cameras for continuous surveillance, but challenges such as camera placement and false positives arise. To address these, a standby multi-rotor UAV inspects signals from ground cameras, resolving issues and optimizing drone flight time. Comprehensive setups involve employing both fixed-wing and rotary-wing UAVs for close monitoring of challenging terrains. High-endurance fixed-wing UAVs, equipped with infrared cameras, offer long-term surveillance, and transmit signals with GPS coordinates to a control station upon detecting temperature increases. When these signals are received, two smaller rotary-wing drones are deployed to observe the region closely and confirm the signal's veracity. Future research involves utilizing surveillance data to explore artificial intelligence for enhanced forest fire monitoring using UAVs (De et al. 2019).

Wireless sensor-network techniques, as suggested by Alkhatib (2014), are suitable for providing rapid signals in the event of a forest fire outbreak. These sensor networks have gained global attention for detecting and sensing forest fires, raising alarms, tripping off during power surges, communicating distress messages, and differentiating between real and false fire smoke (Okokpujie et al. 2019). They can track atmospheric parameters, such as carbon oxides, nitrogen oxides, pressure, relative humidity, and temperature, offering an inexpensive, self-organizing, and self-healing solution for wireless networking. The combined use of web cameras and wireless sensor networks is effective in hybrid wood fire detection. Additionally, use of GPS and fire-sensors devices is more effective than traditional methods in detecting forest fires (Hartung et al. 2006). High-tech sensor and camera devices have been employed for early wildfire detection, capable of tracking smoke, fire thermal levels, and laser rays backscattered from wildfire smoke (Alkhatib 2014). These devices operate on various algorithms, providing signals on smoke and fire levels. The forest fire finder can differentiate between organic smoke from forest fires and industrial smoke up to 15 km away,

utilizing the principle of sunlight-absorbed chemical constituents (French, Goovaerts, and Kasischke 2004).

Researchers have adopted spacecraft-based techniques, utilizing cutting-edge high-resolution radiometers and common resolution imaging spectro-radiometers for timely information and feedback on wildfire occurrences. However, these methods suffer from limitations in accuracy, feedback, and early detection (Fernandez, Erena, and Pecci 2012).

1.4 The Climate-Wildfire-Air Quality System

Global warming, primarily caused by increased greenhouse gases (GHGs) in the atmosphere, leads to more frequent and larger wildfires each year. These fires, in turn, induce various climate changes, such as altering vegetation patterns, changing the reflectivity of surfaces within the fire area, and increasing GHG and aerosol emissions. Through modifications to temperature and precipitation patterns, these changes also affect the environment and ultimately increase the number of indirect fire ignitions. Figure 1.2 illustrates this cyclical process, which creates a feedback loop that keeps escalating the connections between air quality, wildfires, and climate (Price and Rind 1994).

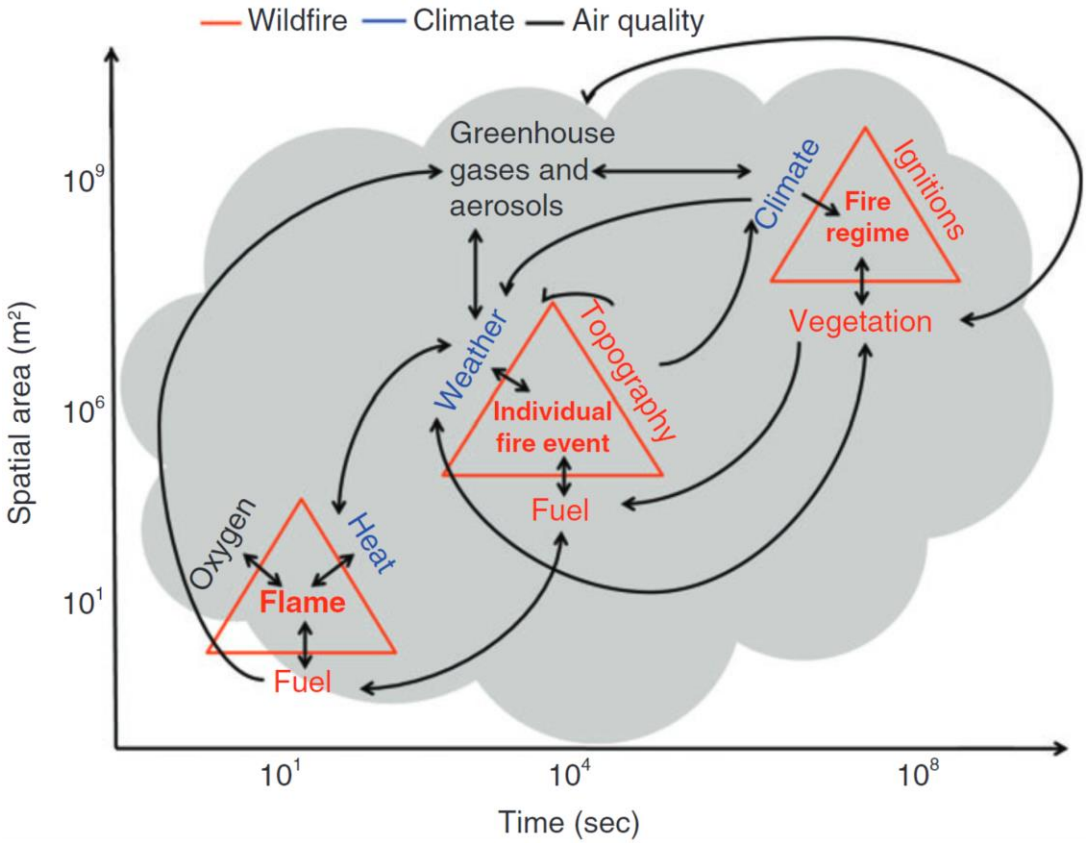

Figure 1.2. The air quality component is represented by black, the climate component by blue, and the wildfire component by red in the conceptual space-time diagram of the climate-wildfire-air quality system. Additionally, this graphic shows the impacts (single-pointed arrows) and feedback loops (double-pointed arrows) of the climate-wildfire-air quality system at various scales (Stavros, Mckenzie, and Larkin 2014).

Wildfire component

Feedback loops occur on a variety of sizes, from tiny and intermediate ones, such as the relationship between specific fire occurrences and fuels, to larger ones, such as the relationship between vegetation types and fire regimes. Disturbance regimes can affect the kind of vegetation that regenerates, even though climate is a major factor in the biological niches of many tree species (W. D. Peterson and Peterson 2001). Certain vegetation species, such as some chaparral plants, depend on fire for regeneration, making them flammable and contributing to fire-dependent communities (Kasischke, Christensen, and Stocks 1995).

Climate component

The climate element of the climate-wildfire-air quality system encompasses two processes that operate across varying temporal and spatial scales.

Firstly, climate influences weather through several feedback mechanisms within the climate system. For instance, as the climate warms, the positions of jet streams change, leading to shifts in the transport of air masses, thus influencing storm trajectories and regional meteorological factors as wind, temperature, and precipitation trends.

Secondly, there is a feedback loop that connects the heat produced by combustion to the weather. While the heat generated by flames affects local weather at intermediate dimensions, weather conditions frequently supply the initial heat needed for combustion at finer geographical and temporal scales. The weather in the area of burning is statistically significantly affected by large flames that release more than 100 Wm^{-2}. The kind and structure of fuel loads are the primary determinants of plume ascent, vertical mixing, and emissions distribution due to the non-uniform heat created by the fire (Stavros, Mckenzie, and Larkin 2014).

Climate, wildfires, and air quality interactions

As Figure 1.2 illustrates, the interaction of air quality, wildfire, and climate stresses the need of looking at these factors as an integrated system. The diagram's arrows show how they interact. Heat, oxygen, and fuel are all part of an internal feedback loop. Three subcategories of interactions are part of the loop: wildfire and air quality, climate and air quality, and wildfire and climate. The subcategory of climate and air quality includes the feedback loops between air quality, climate, and weather as well as wildfire and climate. The last section, wildfire and climate, covers the effects of topography on climate and weather, whereas the feedback loop between weather and specific fire

events, covers the influence of climate on fire regimes, and the feedback loop between vegetation and weather (Stavros, Mckenzie, and Larkin 2014).

The three components namely air quality, wildfire, and climate systems are intimately connected through fine-scale internal feedback loops involving fuel, heat, and oxygen. These feedback loops are managed by the combustion process, which entails preheating, the distillation and burning of volatiles, the distillation and combustion of residual charcoal, and cooling. Fuels hold onto heat throughout the preheating process, and this heat is enhanced as moisture evaporates. This escalation moves the ignition process on to the next stage. More heat is produced when the flame grows larger due to the fuel's own fuel. This causes the surrounding fuel to dry up, increasing its flammability and facilitating combustion. If there is sufficient oxygen, fuel, and heat to keep a flame going, this process will continue. (Stavros, Mckenzie, and Larkin 2014).

Wildfire and air quality

The kind of emissions generated are influenced by the fuel's composition, structure, and moisture content. These factors ultimately affect air quality. Fuel moisture has an impact on combustion's water vapour production and flammability. The kind, structure, and chemical makeup of the burnt fuels, as well as the thoroughness and effectiveness of the combustion process, all influence the composition of the emissions. For instance, incomplete combustion in wildfires generates carbonaceous materials such as coarse particulate matter and charcoal, affecting surface albedo and radiative forcing as seen in Figure 1.3. Aerosols, which influence radiative forcing by absorbing and scattering solar radiation, also contribute to cloud formation and can alter the albedo of snow and ice upon deposition (Swann et al. 2010).

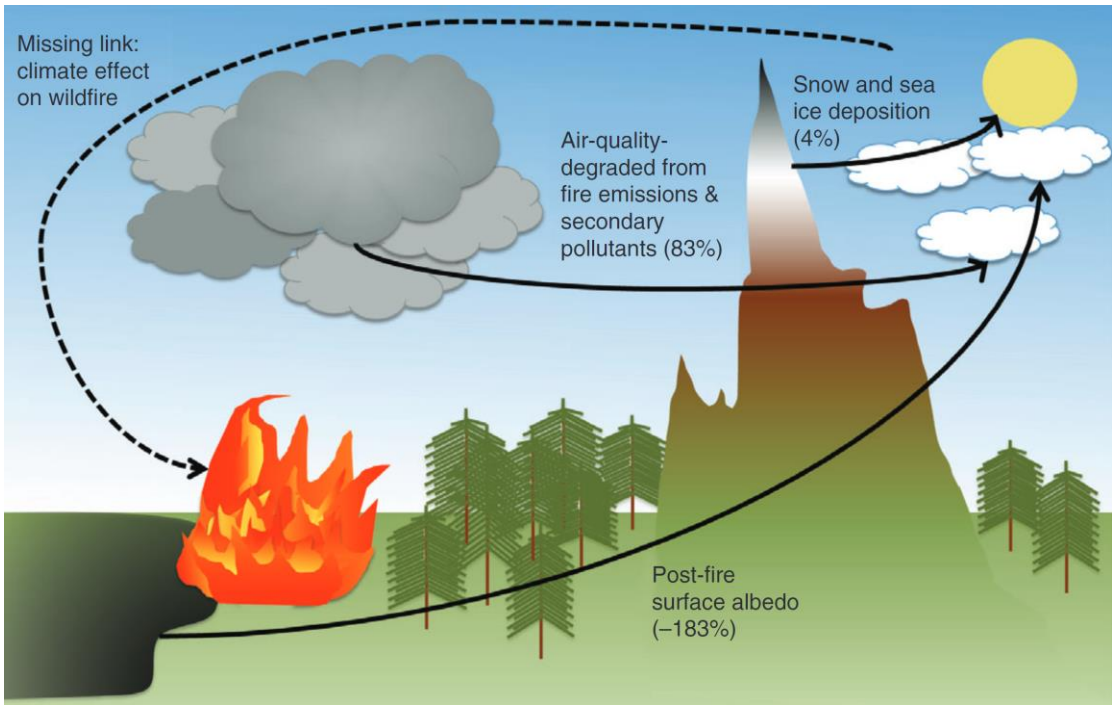

Figure 1.3. The figure illustrates the mean radiative forcing throughout an 80-year fire cycle in a boreal forest. The percentage of the total net radiative force from each component is shown by the numbers. Negative numbers indicate decreased forcing, whereas positive numbers indicate increased forcing, which results in a positive feedback on climate change. The feedback loop is closed by the dashed line, which represents the change in the climatic driving of fire regimes (Stavros, Mckenzie, and Larkin 2014).

There is a reciprocal link between vegetation and air quality. Some plant species' production can be impacted by bad air quality, and air quality can be influenced by plant productivity. Exposure to tropospheric ozone (O_3), a secondary pollutant formed by the reaction of nitrogen oxides (NOx) and volatile organic compounds (VOCs), especially at high quantities, may cause certain plant species to produce less. On the other hand, carbon dioxide (CO_2) is a necessary component of photosynthesis, but vegetation also produces volatile organic compounds (VOCs) (D. E. Ward and Hardy 1991).

Climate and air quality

A feedback loop exists between weather and air quality, where moisture from fuels during a fire, energy generated by the fire, and ambient weather all determine how high emissions are injected into the atmosphere, which in turn affects how they travel and diffuse. While wet deposition eliminates the aerosols and improves air quality, dry weather lengthens their lifespan and increases their travel distance. (Liu, 2005).

By serving as nuclei for cloud condensation or by absorbing light and affecting precipitation, wildfire aerosols can have an impact on cloud formation. Temperature-dependent water vapour also affects the amount of moisture that can precipitate. Aerosols have the ability to absorb and scatter solar radiation, which can alter radiative forcing and available light. This can then have an impact on photochemical processes involving CO, methane (CH_4), VOCs, and NOx, leading to the formation of tropospheric ozone (Langmann et al. 2009).

Due to variations in the characteristics of aerosol species, as well as their source and injection height, the effect of aerosol emissions on the climate system is poorly quantified and might result in either net warming or cooling. The distribution of aerosols and greenhouse gases (GHGs) in space and time can be changed by climate change, which can have an impact on air quality. For example, transported emissions from wildfires during periods of high wildfire activity in Canada can raise background pollutant levels in the United States, especially tropospheric O_3. Aerosol movement and deposition can also alter snow surface albedo and sea ice, which affects radiative forcing and its effects on climate as seen in Figure 1.3 (Littell et al. 2010).

Wildfire and climate

Both directly and indirectly, the climate affects the fire regime. Climate directly impacts flammability, fuel availability, duration of the fire season, and ignitions (M. Grillakis et

al. 2022). With a warming climate, it is anticipated that these factors would increase yearly burnt area and lightning-ignited fires (Kitzberger et al. 2012). The most significant predictors of area burned in places such as the south-western United States, Chile, and the Mediterranean ecosystems of the Iberian Peninsula are factors related to the climate of the year prior, which affects fuel availability and connectivity across landscapes (Littell et al. 2010).

A feedback loop exists between weather and fire behaviour at both fine and intermediate scales. In the short term, weather affects wildfire behaviour by influencing fine-fuel moisture, fire line intensity, and spread rate. Conversely, fire behaviour affects weather due to changes in air temperature, wind, and relative humidity. For instance, when a fire breaks out in a basin and hot air rises, the air column's relative humidity gradient shifts, influencing convective winds and vertical mixing, both of which have an additional effect on the behaviour of the fire (Langmann et al. 2009).

The weather and plants have a complicated interaction. The amount of water that transpires and evaporates in an area is influenced by the vegetative surface cover. It also affects local wind circulation. The local climate therefore influences the vegetation's composition, production, and mortality (Holz et al. 2012).

Landforms have an impact on fire-climate dynamics globally because they determine the weather at intermediate geographical scales and climate at wide regions. Different fire regimes are seen in continental climates due to orographic restrictions on broad-scale air circulation over land, as opposed to coastal climates. At intermediate length scales, topography modifies the length of time that certain elements are under shadow, impacting heat, moisture, and convective winds that are produced by air moving between warm and cool temperatures. Rainfall amounts can be influenced by the geography of the area, and temperature variations can have an impact on relative humidity. Finally, individual intermediate-scale fire occurrences have an impact on climate through alterations in surface albedo, which subsequently affects radiative forcing and temperature (Pielke et al. 1999).

1.5 Modelling the System: Integrating Models Across Disciplines

Climate, wildfires, and air quality are frequently studied on specific scales but tend to overlook the intricate interactions among system components (Pfister, Wiedinmyer, and Emmons 2008). This is addressed via a process-oriented approach, which finds the many scales at which important processes in the climate, wildfire, and air quality system interact. There are five phases in this process: the formulation of a research topic, the identification of relevant system elements, the determination of interaction scales in space and time, the development or application of models at these scales, and

the integration of models into a system framework. Understanding how climate change affects wildfires, air quality, and climate change itself serves as an example of this strategy. Climate, fire regime, aerosols, and greenhouse gases (GHGs) are the system's main constituents (Wegesser, Pinkerton, and Last 2009).

Modelling the climate-wildfire-air quality system is necessary to comprehend and measure future wildland fires and air quality deterioration. Models are simplified depictions of reality that assist in drawing conclusions about the system. This multifaceted system can be modelled through three crucial steps: (1) identifying its constituents, (2) evaluating available data and tools, and (3) acknowledging the assumptions and simplifications that could result in errors or uncertainties.

A concise overview of the available models is provided, as well as how they can be combined to establish a framework for studying the system (Holz et al. 2012). The uncertainties associated with each component are also recognized (McKenzie et al. 2014).

The global climate is depicted by global climate models (GCMs), which include various feedback loops and processes at an economically feasible resolution. Nonetheless, GCMs lack the detail needed for accurate wildfire modelling. Therefore, it is essential to model regional climates. Two primary methods are utilized: the static approach, which statistically downscales GCMs using gradient modelling, and the dynamic approach, which utilizes regional climate models (RCMs) for dynamic regional climate simulations, incorporating boundary conditions from GCMs (Stavros, Mckenzie, and Larkin 2014).

At a regional level, climate influences vegetation directly and indirectly via disturbance regimes, which alters the spatial distribution of vegetation (B. J. Stocks 1993). Two dynamic climate-smart vegetation models exist: Dynamic global vegetation models or DGVMs and Landscape fire succession models or LFSMs. DGVMs use plant functional types (PFTs) and a fire module to simulate the relationships between vegetation, fire, and climate (McKenzie et al. 2014). On the other hand, LFSMs create complex patterns in the landscape that affect smoke, fire spread, and the succession of flora after a fire. LFSMs are not as well adapted for the regional or sub-continental simulations required to explore the climate-wildfire-air quality system as they are for testing DGVMs due to their computational complexity (Barrett et al. 2011).

Similar to yearly area burnt, fire regime data are produced using statistical or deterministic modelling and are used to define average circumstances. An important area of uncertainty in the climate, wildfire, and air quality system's fire modelling is our comprehension of heat transmission at tiny temporal scales and its effects on fuel conditions, weather, and emissions dispersal (Bessie and Johnson 1995). Fuel does not normally cause fire behaviour in severe weather, although heat from fires can pre-dry fuels ahead of the flame front, making them more flammable and accelerating the

spread of fires. It could be essential to include this feedback in models at large geographical dimensions. Integrating fine-scale fuel and vegetation variability with larger-scale fire-spread dynamics may enhance forecasts of the fire regime across vast scales, while further research is needed to confirm this (Littell et al. 2010).

Often, the differences in fuel types are not well reflected by Regional Climate Models (RCMs) and Dynamic Global Vegetation Models (DGVMs) due to their coarse geographical resolution. Preliminary maps of fuel and vegetation are often created using a Geographic Information System (GIS) layer, utilizing ground estimations, satellite data, and empirical or quasi-empirical models (Ruefenacht et al. 2008). These methods are not without uncertainty, however, particularly when it comes to how they will affect the uneven heat output that can have an impact on plume rise, vertical mixing, and emissions distribution (Andreae and Merlet 2001a).

First-order fire effects models (FOFEMs) are used to evaluate fuel consumption and subsequent emissions. There are two types of FOFEMs: one that uses process-based heat-transfer equations, and the other that is based on empirical models derived from field and lab consumption measurements (Andreae and Merlet 2001a). Based on these approximations, emissions are computed, accounting for variables such as the kind and quantity of biomass utilized, the percentage of chemical species in the fuel, and the burning phase. Variations in the frequency of fires or the emissions variables associated with various vegetation types give rise to uncertainties that might impact emission estimations and consumption rates. Distinct chemical reactions that take place over various time periods are also present during different phases of combustion. For example, flaming combustion is short-lived, while smouldering can persist for days or weeks, leading to potential bias in emission factor estimates. Although flaming and smouldering are often assumed to be separate phases, in reality, they often occur simultaneously. This assumption justifies the use of a smouldering fraction to differentiate emission factors for different combustion phases (Andreae and Merlet 2001a).

Smoke Transport (ST) models simulate the movement and evolution of pollutants and secondary aerosols in the atmosphere. These models use computational fluid dynamics (CFD) to follow the flow of gases and particles in plumes. The two main types of ST models are Eulerian and Lagrangian models. Whereas Eulerian models track the flow of air volumes carrying a certain quantity of pollution past a defined place, Lagrangian models track the movement of the smoke plume throughout space and time. Lagrangian models, often called puff-dispersion or plume models, are easier to use and appropriate for rapid evaluations of air quality. Although they need a lot of computing power, more intricate puff or particle dispersion models are employed to forecast surface smoke concentrations with more accuracy. Since Eulerian models incorporate chemistry transport models (CTMs), which are sub models of atmospheric chemistry, they more accurately represent actual atmospheric conditions (Stein et al. 2009).

Nevertheless, modelling smoke dispersion at narrow spatial resolutions has some uncertainty since models could either dilute the source to fit the grid or assume a single source. Furthermore, uncertainty arises from variations in the smoke's composition and emission concentration, which depend on the smoke plume's release height. The quantity of heat emitted by the fire, wind speed, and atmospheric stability all affect the injection height or plume rise. Plume profiles can be assessed using a variety of methods, including explicit numerical simulations based on fundamental atmospheric dynamics, buoyancy flux conversion factors, and instantaneous homogeneous mixing assumptions. For more precise plume modelling results, it is imperative to link fine-scale fire behaviour and canopy sub models with intermediate-scale processes. Nevertheless, a trade-off exists between generalizing assumptions across an intermediate size and computationally costly modelling of fine-scale dynamics over broad regions, which adds uncertainty to ST modelling (Jeong, Park, and Youn 2008).

Global fire modelling has made great progress in our knowledge of the dynamics of fires and how they affect climate systems. Global simulations of fire behaviour and its interactions with climate have been achieved through the development of models such as INFERNO (INteractive Fire and Emission Algorithm for Natural Environments) which is also used in this thesis.INFERNO simulates the ignition, spread, and suppression of fires by integrating a number of variables, including plant type, fuel load, and meteorological conditions as seen in Figure 1.4 (Mangeon et al. 2016). Also part of the larger effort includes programs like the Fire Model Intercomparison Project (FireMIP), which compares fire models to better anticipate fire behaviour and repercussions.

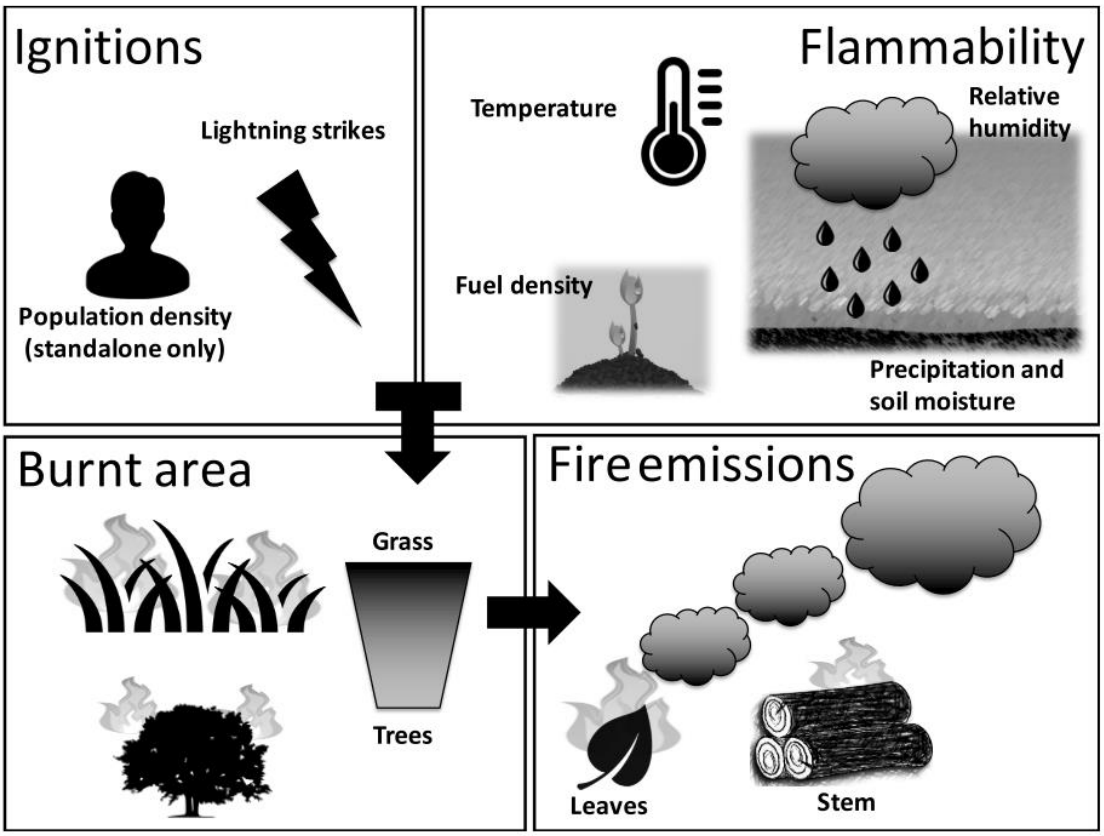

Figure 1.4. The main components of the INteractive Fire and Emission Algorithm for Natural Environments (INFERNO) (Mangeon et al. 2016).

Representing the possibility of potential wildfire events occurring several fire weather indices have been developed. One of the indices used worldwide to evaluate the risk of wildfire is the Fire Weather Index (FWI), which is a component of the Canadian Forest Fire Weather Index System (Van Wagner 1987). The McArthur Forest Fire Danger Index (FFDI) used in Australia (Dowdy et al. 2009), and the National Fire Danger Rating System (NFDRS) used in the United States are other noteworthy fire weather indices (Y. Liu, Goodrick, and Heilman 2014). Based on local circumstances, each of these indices estimates the risk of fire using a variety of factors and techniques.

Because of the FWI system's comprehensiveness and flexibility to different forest kinds and climates, it is widely utilized. It combines several weather-based indicators such as 12:00 local time surface temperature, relative humidity, wind speed and 24-hour precipitation to calculate the Fire Weather Index itself, the Buildup Index (BUI), the initial spread index (ISI), the Duff Moisture Code (DMC), the Fine Fuel Moisture Code (FFMC) and the Drought Code (DC) as seen in Figure 1.5. Surface litter and other fine fuels' moisture content is measured using the FFMC. Whereas the DC analyses the moisture content of deep, solid organic layers, the DMC evaluates the moisture content of the forest floor's loosely compacted, decaying organic layer. The wind speed and FFMC are used to calculate the ISI, which represents the rate of fire spread. To indicate the entire amount of fuel accessible for combustion, the BUI combines the DMC and DC. Lastly, the ISI and BUI are combined by calculate the FWI providing a general

measure of fire intensity (B. Stocks et al. 1989).

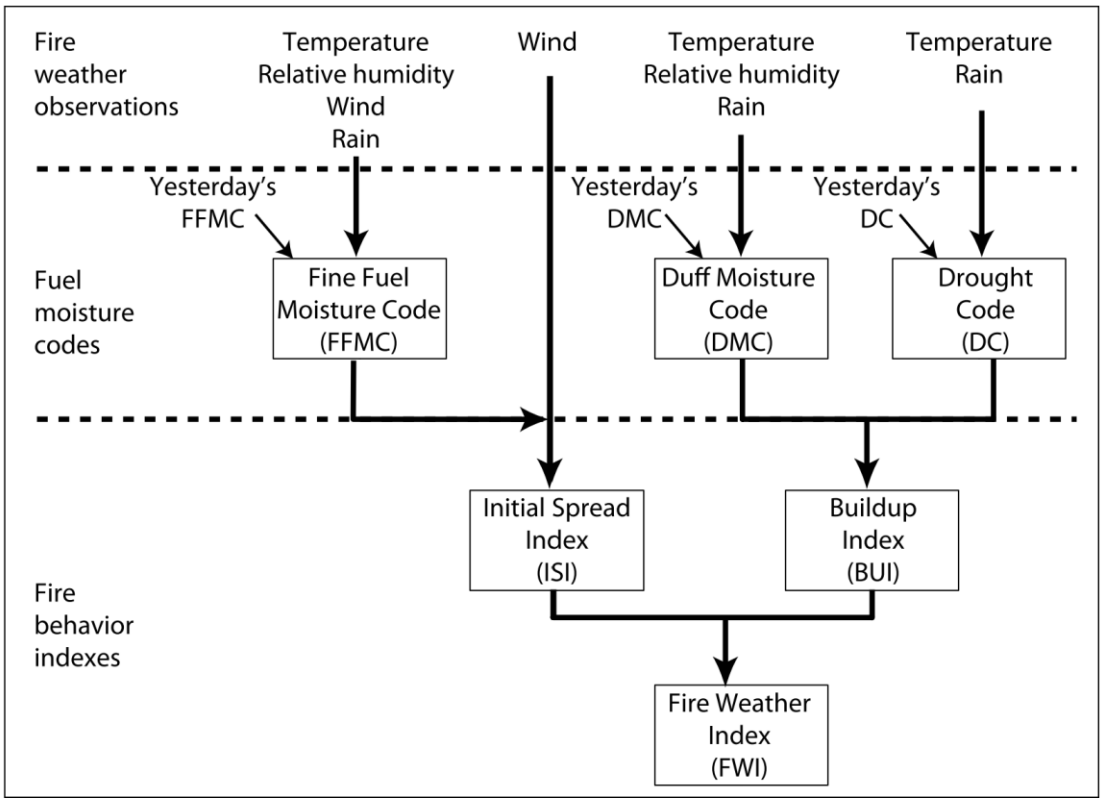

Figure 1.5. Structure of the Canadian Forest Fire Weather Index System FWI (B. Stocks et al. 1989)

1.6 Research Topics Contribution and Novelty of PhD Thesis

This thesis makes three significant contributions to understanding and managing the complex interactions between wildfires, climate change, and air pollution, particularly within Greece and the broader Mediterranean region.

1. Projections on the Impact of Climate Change

The current thesis discusses how climate change may affect the risk of wildfires throughout the Mediterranean in the future with a focus on Greece. Helping to influence the region's future wildfire management and policy decisions by utilizing the changes in fire weather forecasts, which emphasize places that may see increased fire hazard as a result of changes in weather variables driven by climate change.

2. Interdisciplinary Integration of Models

Another important contribution is the integration of land surface and atmospheric models to investigate the wildfire linkages with land cover change, air pollution, and climate. The thesis delves at the processes that exist between weather patterns and wildfire emissions. It determines the effects of wildfire-produced aerosols on

atmospheric conditions, by changing weather patterns and impacting fire behavior even more. Moreover, by comparing static and dynamic vegetation scenarios under various emission paths, future burned area changes in Greece were estimated. The simulation with dynamic vegetation shows a reduced rise in burnt areas overall, pointing to possible moderating effects of vegetation changes, whereas the one with static vegetation predict a general increase in burnt areas owing to drier climatic conditions. By using both types of simulations, future wildfire hazards and the ways in which land cover changes influence those risks may be better understood.

3. Novel Methodologies for Smoke Plume Detection

This thesis makes a technological contribution by creating an automated smoke plume detection system using satellite data. A new approach is presented for the identification and isolation of fire-emitted aerosols by utilizing several types of MODIS satellite products. This development makes it easier to respond to wildfire incidents quickly and efficiently in addition to improving the accuracy of tracking the effects of wildfires on air pollution.

Overall, this PhD thesis fills important knowledge gaps in the dynamics of wildfires, the effects of climate change, and the interactions between wildfires, meteorology and air pollution. These discoveries have practical applications for enhancing wildfire planning and response tactics in a changing environment, in addition to their academic significance.

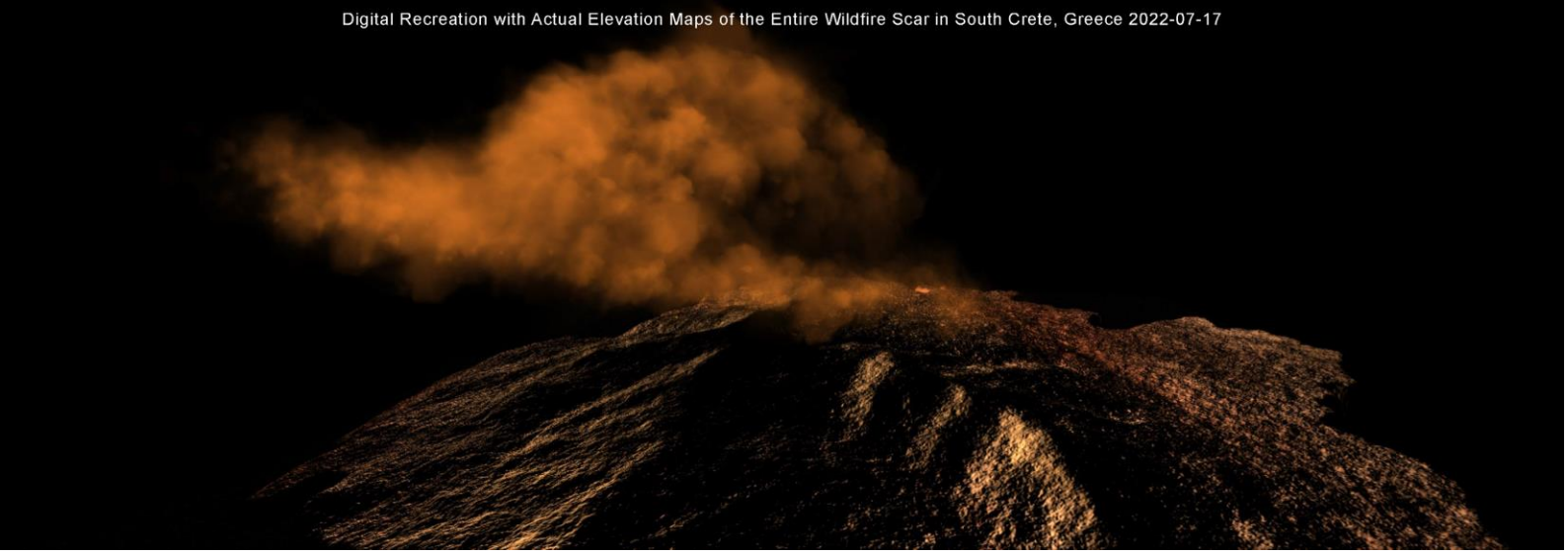

2. Future climate change impact on wildfire danger over the Mediterranean: the case of Greece

This chapter is based on the following publication:

Rovithakis, Anastasios, Manolis G. Grillakis, Konstantinos D. Seiradakis, Christos Giannakopoulos, Anna Karali, Robert Field, Mihalis Lazaridis, and Apostolos Voulgarakis. "Future climate change impact on wildfire danger over the Mediterranean: the case of Greece." Environmental Research Letters 17, no. 4 (2022): 045022. https://doi.org/10.1088/1748-9326/ac5f94

Abstract

Recent studies have shown that temperature and precipitation in the Mediterranean are expected to change, contributing to longer and more intense summer droughts that even extend out of season. In connection to this, the frequency of forest fire occurrence and intensity will likely increase. In the present study, the changes in future fire danger conditions are assessed for the different regions of Greece using the Canadian Fire Weather Index (FWI). Gridded future climate output as estimated from three regional climate models from the Coordinated Regional Downscaling Experiment (CORDEX) are utilized. We use three Representative Concentration Pathways (RCPs) consisting of an optimistic emissions scenario where emissions peak and decline beyond 2020 (RCP2.6), a middle-of-the-road scenario (RCP4.5) and a pessimistic scenario, in terms of mitigation where emissions continue to rise throughout the century (RCP8.5). Based on established critical fire FWI threshold values for Greece, the future change in days with critical fire danger were calculated for different areas of the Greek domain. The results show that fire danger is expected to progressively increase in the future especially in the high-end climate change scenario, with southern and eastern regions of Greece expected to have up to 40 additional days of high fire danger relative to the late 20th century, on average. Crete, the Aegean Islands, the Attica region, as well as parts of Peloponnese are predicted to experience a stronger increase in fire danger.

2.1 Introduction

Extreme wildfire events can have devastating consequences for ecosystems (Andela et al. 2018), the atmospheric environment (Voulgarakis and Field 2015), human health (Chuvieco et al. 2018) and the economy (Nielsen-Pincus, Moseley, and Gebert 2014). Fire can be both a natural and an anthropogenic disturbance process prevalent across most land surfaces with regular ignitions from humans particularly in agricultural areas where it is often used as a tool (Abatzoglou et al. 2018). In southern Greece, a wildfire in August 2007 resulted in a loss of 84 human lives more than 3000 destroyed houses and 270,000 ha of burnt area. The second deadliest wildfire event ever in the country (102 casualties) has been the recent wildfire in eastern Attica (July 2018), which burned an area of ~1250 ha (Lagouvardos et al. 2019).

Mediterranean ecosystems are considered fire-prone, with severe associated economic and environmental damages every year (Turco et al. 2018). Although Mediterranean vegetation is able to cope with fire, land use changes in the area burned and the consequent changes in fire recurrence can have consequences at landscape level. Thus, understanding changes in fire regime and their relation to climate is a key factor for predicting the future of Mediterranean ecosystems (Pausas 2004).

Drought events of unforeseen spatial extent and duration, are projected to occur up to twice per decade in the future, regardless of the degree of mitigation for Europe (M. G. Grillakis 2019). Such climate-driven changes are expected to increase the risk of fire occurrence (Carvalho et al. 2011; Dupuy et al. 2020), reduce the time intervals between fire events (Pausas 2004) and lengthen the duration of the fire season (Goss et al. 2020). Current trends in the Mediterranean climate and more specifically in Greece, indicate an increase in summer droughts due to global warming (Tramblay et al. 2020). Studies have consistently reported that climate change is expected to increase summer temperatures especially in the southern parts of Europe by the end of the 21st century. Projections regarding the southeastern Mediterranean region for the end of the century have shown an increase of 1.7^{o}C - 2.5^{o}C for the moderate climate change scenario (RCP4.5) and 3.5^{o}C - 5^{o}C for the higher-end scenario (RCP 8.5) (Zittis et al. 2019).

The FWI index is solely based on meteorological parameters, disregarding geomorphic characteristics and vegetation types as well as related characteristics that may affect fire spread such as land use fragmentation and topography. To this end, the FWI is usually used along with related thresholds that have been found to work well for specific regions and vegetation types (Dimitrakopoulos, Bemmerzouk, and Mitsopoulos 2011; De Groot et al. 2007; Karali et al. 2014). The FWI was developed for the eastern pine forests of Canada but has been used for several areas globally like for the Mediterranean region (Carvalho et al. 2011) (Bedia et al. 2014) Ruffault et al. (2020)

focused on the frequency of current and future climate conditions associated with wildfires, finding that heat-induced fire-weather is projected to increase by 14% by the end of the century (2071–2100) under the RCP4.5 and by 30% under the RCP8.5 for the Mediterranean. These results are fairly similar with our calculated fire weather increase by 17% and by 26% respectively for the Greek domain. Novo and Lorenzo (2020) utilized the FWI along with additional forest fire occurrence indicators to study how forest management can be optimized in Spain in order to prevent the impacts of wildfires. Moreover Bedia et al. (2014); Amatulli, Camia, and San-Miguel-Ayanz (2013) estimated the future fire danger using the FWI for several countries bordering the Mediterranean and found out that there is a strong correlation of the index with burnt area for the Mediterranean region, whereas that correlation is weaker when individual countries were examined. Giannaros, Kotroni, and Lagouvardos (2021) used the number of days with FWI>30 as an index for the assessment of fire weather extremes in the Euro-Mediterranean. Focusing on Greece Karali et al. (2014) have correlated the number of fires with the FWI in order to determine the fire-related, region-specific thresholds for the FWI. They established three critical fire danger threshold values for the main areas of Greece based on daily mean meteorological data; these are FWI = 15, FWI = 30 and FWI = 45 increasing from the northwest to the southeast. These macroscale differences in the FWI thresholds were calculated by correlating the number of fires and the FWI for the different regions.

During the 2018 Attica fires, the extreme fire growth on July 23 was associated with a sharp increase in FWI driven by hot (35 ^{o}C) and dry (RH=29%) conditions and no precipitation during the previous two weeks (Field 2020). Giannakopoulos et al. (2011) calculated different meteorological indices related to fire danger based on a single regional climate model. However, there has not been a study in Greece using the FWI from different regional climate models to reduce the influence of potential model biases to estimate fire prone areas, correlation with input weather variables and fire season length changes.

The present study aims to estimate future fire danger for the Greek domain using the FWI index using climate output from EURO-CORDEX regional climate model (RCM) simulations, as it was projected for 3 future emissions scenarios namely the RCP2.6, RCP4.5 and RCP8.5. The regional climate model outputs have a high resolution of 0.11 degrees since the GCM's can only model processes in coarse grid-cells which are unsuitable for local level case studies (Navarro-Racines et al. 2020; Jacob et al. 2020). Especially for mountainous terrains like that of Greece increasing the model's resolution has benefits in simulating temperature, precipitation, and wind extremes over Europe (Iles et al. 2020; Torma, Giorgi, and Coppola 2015). On the other hand downscaling from GCM to RCM leads to sources of uncertainty which in this study is accounted for by using the results from an ensemble of RCMs (Chokkavarapu and Mandla 2019). Results are analyzed and compared for three time periods (1971-2000,

2021-2050, 2069-2098) and for several key Greek regions, using metrics like the number of days with FWI>30 as well as by calculating the FWI changes between the aforementioned time periods. The fire season length is another useful metric quantifying the persistence of fire weather, so we determine how much this metric is predicted to change in the future. Based on the three models that were utilized in this study, temperature is expected to increase by up to 2.5°C in the near future (2021-2050) and up to 5°C in the distant future (2069-2098) for the RCP8.5 scenario. It is shown that the three scenarios considered exhibit a similar warming pattern in the near future, while temperature trajectories vary considerably beyond the 2050s.

This is the first study that assesses the impact of climate change on a fire danger index over Greece using the output from multiple climate models. We present our data and methods in Section 2.2, our results in Section 2.3, and our main conclusions in Section 2.4.

2.2. Data and Methodology

2.2.1 Study area characteristics

The area studied is Greece and its sub-regions located in southeastern Europe between 34° and 42° northern latitude and 19° and 28° eastern longitude, covering an area of approximately 132,000 km^2 and occupying the southernmost part of the Balkan Peninsula.

Climatologically, Greece mainly belongs to the Mediterranean climatic type. It is characterized by mild winters during which precipitation peaks, relatively warm and dry summers and a long sunshine duration almost throughout the year. It varies from continental Mediterranean in the country's north (Csa), according to the Köppen climate classification) to subtropical Mediterranean in the far south (Csb) (Kottek et al. 2006).

Moreover, the annual cycle can be divided climatologically into a cold and rainy period (October–March) as well as a warm and dry period (April–September), while October and April can be characterized as transition months (Karali et al., 2014).

Situated in the eastern Mediterranean basin, Greece is also an area highly responsive to climate change particularly with respect to temperature rise, precipitation decrease and fire danger increase. Temperature has been documented to increase since the mid-1970s (Tramblay et al. 2020;Giannakopoulos et al. 2011), while fire statistics indicate a significant increase in both the number of wildfires and the burnt area (Dimitrakopoulos, Bemmerzouk, and Mitsopoulos 2011). According to the official records of the Greek Fire Service, the dominant vegetation types affected by wildfires

are phryganic ecosystems, Pinus halepensis and Pinus brutia forests, Quercus coccifera shrublands, and grasslands, which collectively cover about 39% of the total surface of Greece (Dimitrakopoulos 2002).

2.2.2 FWI description and thresholds

There are many fire weather indices other than the FWI with the most notable ones being the National Fire Danger Rating System in US (NFDRS) (Bradshaw et al. 1984), the Forest Fire Danger Index (FFDI) (Noble, Gill, and Bary 1980) and a much simpler fire weather index (F index) developed by Sharples et al. (2009) and used for Mediterranean climates by Satir et al. (2016). Dowdy et al. (2009) have made comparisons between the FWI and FFDI and the main conclusion is that these indexes are very similar in terms of their fire weather predicting capability. Fire weather indices are widely used to estimate current fire danger such as in the European Forest Fire Information System (EFFIS), the Canadian Wildland Fire Information System (CWFIS) and the Australian FDI forecast system.

The FWI System is composed of three fuel moisture codes and three fire behavior indexes and uses 12:00 local time surface temperature, relative humidity, wind speed and 24-hour precipitation as input. The Fine Fuel Moisture Code (FFMC) is a numeric rating of the moisture content of litter and other cured fine fuels and is considered as an indicator of the relative ease of ignition and flammability of fine fuels (B. Stocks et al. 1989). The Duff Moisture Code (DMC) is a numeric rating of the moisture content of loosely compacted organic (duff) layers of moderate depth. The Drought Code (DC) is a numeric rating of the moisture content of deep compact organic layers. When it comes to the two intermediate fire behavior indexes (steps), the Initial Spread Index (ISI) is a numeric rating of the expected rate of fire spread. The Buildup Index (BUI) is a numeric rating of the total amount of fuel available for combustion. The Fire Weather Index (FWI), combines ISI and BUI to represent the intensity of a spreading fire as energy output rate per unit length of fire front (Van Wagner 1987).

Here, a threshold of FWI = 30 has been used for determining the critical fire danger regions, following the research of Papagiannaki et al. (2020) and Karali et al. (2014), as a representative value for the entire Greek domain. Furthermore, the number of days with FWI>30 was also estimated as an index quantifying the increase in fire weather severity in the future periods when compared to the reference one.

2.2.3 Climate data used for predictions

Readily available projection data for FWI from the Copernicus Climate Change Service (C3S) (Giannakopoulos and Karali, 2019) were downloaded to determine the wildfire danger over the Greek domain. This data derives from meteorological variables every three hours of which the three hourly data at 12UTC was used as proxy for the noon value which is needed for the FWI calculation. Simulations from three versions of the RCA4 regional climate model were used, driven by three different global GCMs which were part of the EURO-CORDEX initiative (Jacob et al. 2013). The RCA4 is stated by Kjellström et al. (2016) that is useful with regards to helping in the creation of fundamental climate information. Three GCMs were used the HadGEM2-ES (UK Met Office, UK), EC-EARTH (ICHEC, Ireland) and MPI-ESM-LR (MPI, Germany) since only those three had the variables of interest and were available for all RCP8.5, RCP4.5 and RCP2.6, to more accurately compare results from these scenarios. These models are some of the most established ones able to accurately represent the climate (Jacob et al. 2020). Iles et al. (2020) studied how well EURO-CORDEX models captured reality by comparing several meteorological parameters with gridded data based on observations (E-OBS). They found that these models tend to overestimate temperature, precipitation and wind speed extremes for the period 1985-2011. Also atmospheric humidity is found to positively correlate well with temperature for these EURO-CORDEX models (Knist et al. 2016). When it comes to the EC-EARTH GCM, it is found to represent the main patterns of climate variability well, though with colder surface temperatures (Hazeleger et al. 2012). Based on other studies all three models underestimate rainfall and thus represent a slightly dryer and hotter version of the actual climate. (Ayugi et al. 2020; Bartok et al. 2021). Le Pichon et al. (2015) used high-resolution ground-based observations and determined that the MPI-ESM-LR and EC-EARTH have a good agreement with wind and temperature. The RCM's (and therefore the calculated FWI's) resolution is 0.11 degrees which is a novelty since it makes it possible to study the domain of interest in detail. In order to assess the impact of climate change on wildfire danger, an optimistic, a mid-range and a pessimistic RCP were used (Moss et al. 2010; O'Neill et al. 2014). The RCP2.6 is an optimistic emission scenario where emissions peak and decline beyond 2020. RCP4.5 is a mid-range climate change scenario that describes a stabilization in the radiative forcings after 2100 (Wise et al. 2009). RCP8.5 is a high-end climate change scenario with radiative forcing increasing steadily until 2100 and beyond (Riahi et al. 2011). Comparisons are made using a recent reference period (1971-2000) and two future time periods i.e. the period 2021-2050 (mid-century) and 2069-2098 (late century).

2.2.4 Signal to noise ratio

The signal to noise ratio (SN) was also calculated as it represents the strength of the change signal compared to natural variability (noise), and the signal stands out against the noise when and where this ratio is large (Julien et al. 2018). The SN was calculated individually for each grid cell and for the entire sequence of daily FWI values within the three 30-year time periods as seen in Equation (2):

$$SN = \left| \frac{\Delta}{\sigma} \right| \tag{2}$$

where SN is the signal to noise ratio of a specific variable, Δ is the difference between the 30-year average FWI value of the future minus the reference periods, and σ is the standard deviation of the FWI over the reference period. Specifically, the SN was calculated using the aforementioned way for each of the three regional climate model simulations and then averaged to represent the ensemble mean. This same process was followed for each of the three RCP scenarios individually and for the entire sequence of daily values within three 30-year time periods. In Section 2.3.1, the FWI and the values that are higher than the 90th percentile of the SN ratio has been calculated since this percentile has been established by other papers to be a threshold representative of extreme values (Kirchmeier-Young et al. 2017; Wang et al. 2015).

2.2.5 Fire season length

This metric is defined by Jolly et al. (2015) and Abatzoglou, Williams, and Barbero (2019) as the number of days each year when fire danger is above half its value range, for each year in each grid cell. The change in fire season length was calculated for all RCP scenarios by calculating the difference between the future periods and the reference and by averaging the results from all individual climate models temporally as seen in Figure 2.3 and subplots (a, b, c, d, e, and f) for the entire Greek domain. Wildfire season can become longer based on conditions that allow fires to start and to burn, e.g. extended drought, tree mortality from pine beetles and invasive species such as cheat grass that allow fire to ignite easily and spread rapidly. (M. Flannigan et al. 2013).

2.3. Results and discussion

2.3.1 Determining areas of increased fire danger

Based on the aforementioned FWI thresholds determined in Karali et al (2014) and according to the Greek climatological conditions, locations where the FWI index is greater than 30 are considered prone to fire occurrence. Initially the number of days with FWI>30 for the reference period (1971-2000), both annually and for the fire season (May-September) were calculated (Figure 2.1, panels (a) and (b) respectively). The higher values occur in the lower elevation areas. High fire danger areas are also predominantly found along the eastern Greek coastline due to the presence of the pindus mountain range acting as a precipitation barrier for the eastern coastline (Tsiros et al. 2020). The higher number of days with FWI>30 for the reference period is occurring for the coastal parts of Macedonia and Thrace, Thesssaly, Attica region, Peloponnese and Crete.

The change in the number of days with FWI>30 was calculated based on the average of all three global climate models, for the near (2021-2050) and distant (2069-2098) future Figure 2.1 panels (c, d, e, f, g, h). First the number of days with FWI>30 was calculated for each RCM individually based on daily FWI values and then these results were averaged to find the multi-model mean. There is a negative correlation between the aforementioned areas in Figure 2.1, panels (a) and (b) with the areas that experience the greatest change in number of days with FWI>30 Figure 2.1, panels (c, d, e, f, g, h) due to saturation effects at high end climate change. The majority of those fire prone areas exhibiting the greatest change are located at the country's central and southern parts according to the spatial patterns that highlight hotspots of danger in Figure 2.1 panels (c, d, e, f, g, h). The left panels (c, e, g), which depict the change in the number of days with FWI>30 between the near future and reference periods for all RCP scenarios show a 2-week increase in the potential fire danger days. The left panels also exhibit less spatial heterogeneity than the right panels. Changes for the distant future right panels (d, f, h) are found to be more drastic, especially for the RCP8.5 having the highest number of days with FWI>30, with some areas in central and southern Greece featuring 14-20 additional fire danger days for the near future and 40-50 additional fire danger days for the distant future. The RCP2.6 scenario shows a peak in the radiative forcing of around 3 W/m^2 mid-century resulting in up to 14 fire danger days and a decline afterwards to 2.6 W/m^2 (van Vuuren et al. 2011). This decline translates into fairly similar distant future FWI values as those for the near future resulting in the same fire danger days. Finally, the RCP4.5 predicts up to 20 FWI>30 days for the distant future.

To summarize, from Figure 2.1, the Greek areas predicted to experience the greatest increases in fire danger in the future, based solely on climatic conditions are Crete, the Aegean Islands, the Attica region, parts of central Peloponnese and central Greece as well as parts of Thrace.

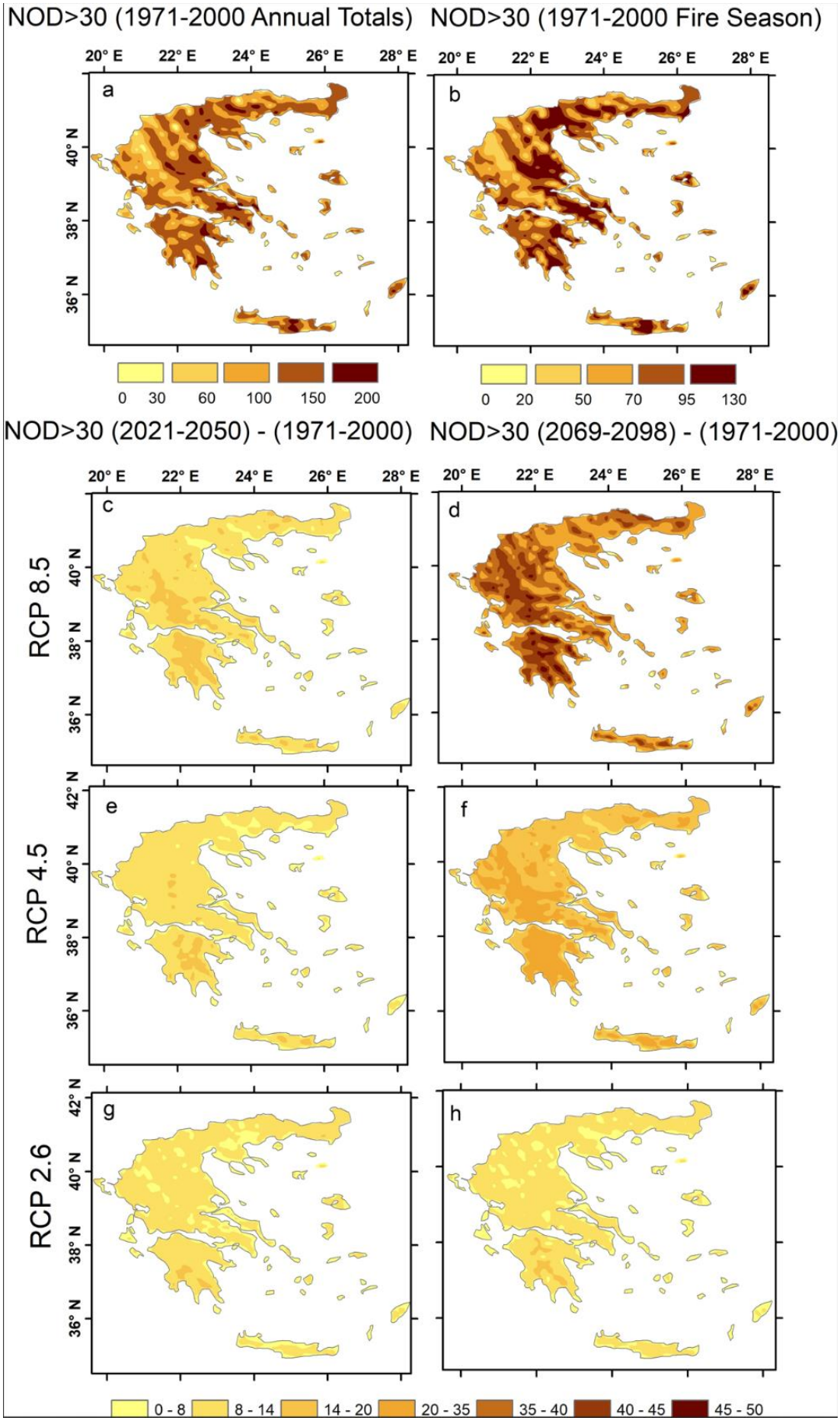
NOD>30 (1971-2000 Annual Totals)
NOD>30 (1971-2000 Fire Season)
20° E
22° E
24° E
26° E
28° E
a
b
40° N
38° N
36° N
0 30 60 100 150 200
0 20 50 70 95 130
NOD>30 (2021-2050) - (1971-2000)
NOD>30 (2069-2098) - (1971-2000)
RCP 8.5
RCP 4.5
RCP 2.6
c
d
e
f
g
h
42° N
0 - 8
8 - 14
14 - 20
20 - 35
35 - 40
40 - 45
45 - 50

Figure 2.1. Panel (a) represents the annual ensemble mean total number of days (NOD) with FWI>30 for the reference period (1970-2000). Panel (b) is the (NOD)>30 for the fire season only of the same ensemble mean and time period as panel (a). Panels (c, d, e, f, g, h) showcase the difference in the annual ensemble mean (NOD) with FWI>30 for every RCP scenario separately between the future periods and the reference period. The left column corresponds to the difference for the near future period [(2021-2050) – (1971-2000)] and the right column to the difference for the distant future [(2069-2098) – (1971-2000)].

In addition to threshold exceedances, the multi-model mean FWI values were also calculated based on the fire season months (May-September) of the Reference time period from all individual regional climate models based on daily FWI values. Overlaid on top of Figure 2.2(b) shown by the hatched areas is the extreme FWI>150 corresponding to the 90th percentile of the maximum FWI values from the reference period. Moreover, the changes in average FWI during the fire season months Figure 2.2 (c, d, e, f, g, h) and the corresponding signal to noise ratio (SN) of their changes were also calculated. The values that are higher than the 90th percentile of the SN ratio for the corresponding time period are shown as hatched areas on the Figure 2.2 (c, d, e, f, g, h) with black lines. Using this definition, changes in the parts of Thrace and northern Greece are subject to more noise, despite showing strong future changes. Based on all RCP scenarios, the higher SN is occurring mainly in Central and Southern parts of Greece and so these areas are considered to have less noise than Northern Greece since the signal between these 3 main regions is very comparable.

Figure 2.2 (a) was made by calculating the spatial average yearly FWI values from all models for the fire season and that was done for each of the three 30-year time periods and for every RCP scenario separately. Since these are country wide averages an increase of one EFFIS fire danger class is a drastic change. That way the potential severity in fire danger is better understood. It can be seen that the three RCP scenarios in the near future have a slightly higher mean FWI compared to the reference period, whilst being in the same class, nonetheless. RCP4.5 in the distant future is in the same fire danger class but has slightly higher FWI than the near future and reference period. RCP2.6 is almost identical in the distant future to what it is for the near future. Finally, RCP8.5 in the distant future showcase the greatest differences compared to the reference period as it is increasing by one class (from ‘very high’ to ‘extreme’).

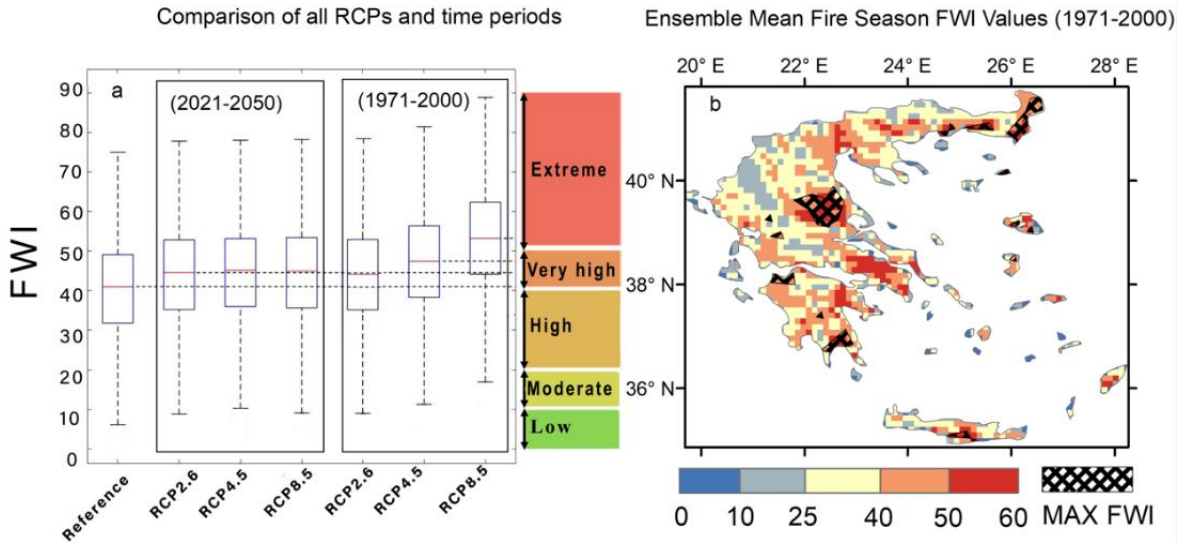

Figure 2.2. Panel (a) is a comparison of spatially averaged yearly FWI fire season values of all RCP scenarios and time periods against the EFFIS fire danger classes shown on the right-hand side of the y axis of panel (a). Panel (b) shows the average fire season FWI values from all models together with the extreme FWI>150 from the period (1971-2000) as depicted by the cross hatched regions

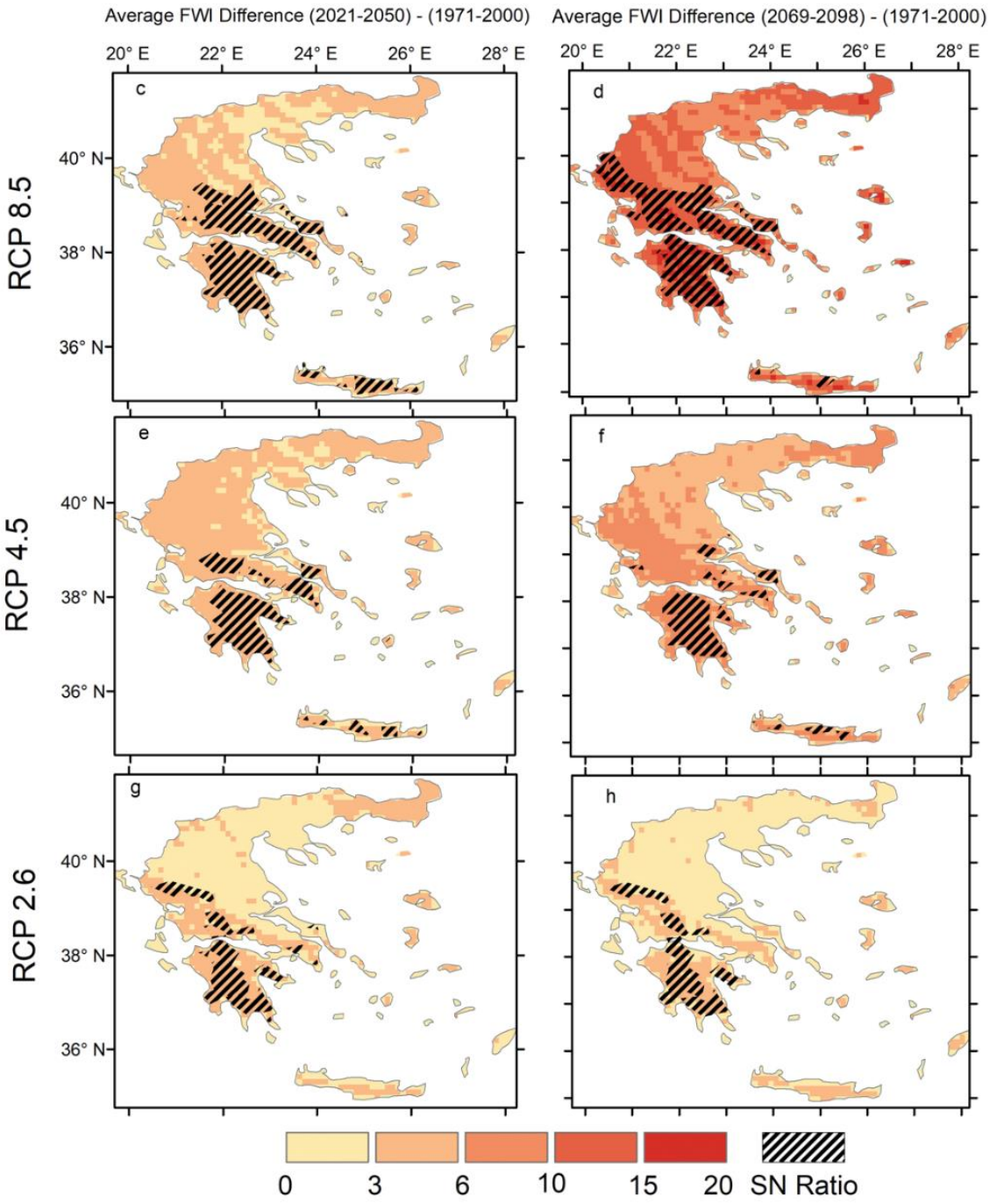

, Figure 2.2. Maps (c, d, e, f, g, h) representing the 30-year ensemble average FWI change based on the average of all 3 different RCM-GCM simulations during the fire season months (May-September) between the two future time periods from the reference period, for all RCP scenarios. Hatched regions depict the values that are higher than the 90th percentile of the SN ratio for the corresponding time period.

2.3.2 Fire season length and seasonal variability change

So far for the creation of the previous figures the typical fire season (May-September) was used. However, to determine how the fire season has been affected during the

three studied time periods the change in fire season length is calculated. Regarding the maps under the RCP8.5 scenario some areas in the distant future are exhibiting an increase in the fire season length of up to 40 days whereas the RCP4.5 scenario is predicting an increase of up to 33 days. The RCP2.6 predicts an increase of up to 19 days. Considering the entire Greek domain by observing the bar graph of Figure 2.3 panel (g) representing the country wide fire season length change, RCP8.5 is predicting an average increase of up to 13 days in the distant future compared to the reference, whereas the RCP4.5 an average increase of up to 7 days. The RCP2.6 however does not predict any increase in fire season as its emissions peak and decline beyond 2020 resulting in 3 days in the distant future, which is less than the near future estimate (4 days)

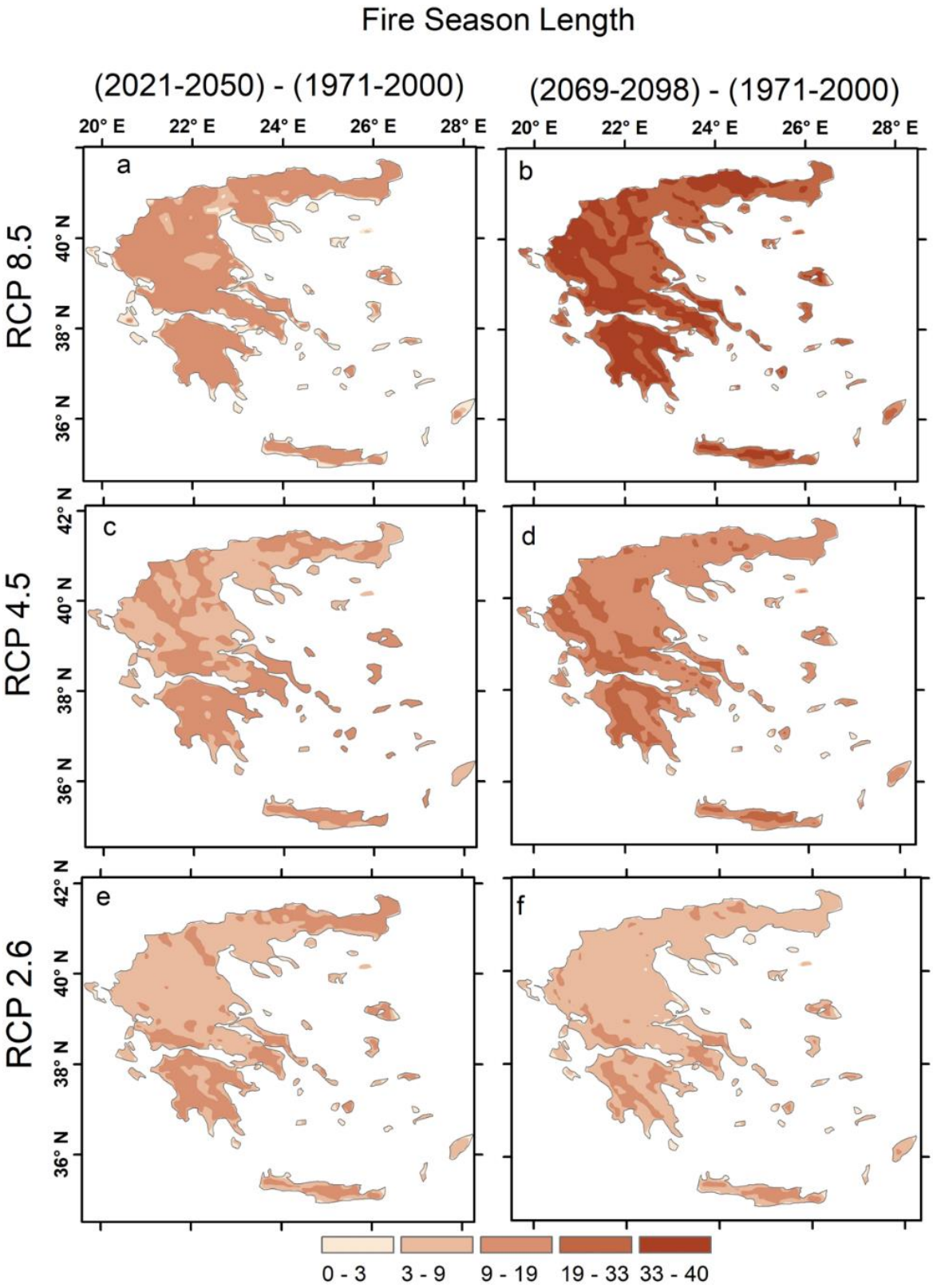

Figure 2.3. All model average fire season length change between the future periods (for all future scenarios) and the reference. Subplots (a, b, c, d, e, and f) represent the 30-year average difference

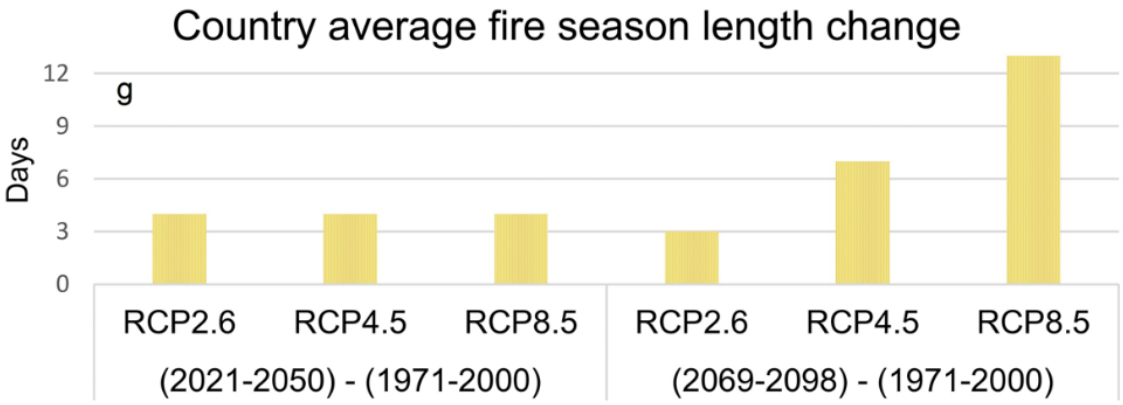

Figure 2.3. Subplot (g) represent the entire Greek domain averaged fire season length change for every RCP scenario and time period.

As a final step of the analysis, the change in seasonal variability between the two future periods and the reference was examined for all RCP scenarios for the entire domain of Greece. Figure 2.4 shows the multi-year monthly mean FWI. For the majority of the models the summer months are exhibiting the highest change; however, for many models there is a secondary spike for the month of September. That can be verified by another paper from Dimitrakopoulos, Bemmerzouk, and Mitsopoulos (2011) where they found the majority of fires to occur during the month of September for the Eastern Mediterranean environment as they explain that no rain has occurred since late spring, creating a prolonged drought period. The strongest increase for the distant future under the RCP8.5 scenario in Figure 2.4b is found for the MPI-ESM-LR model during the month of June and estimated to be 7 units. On the other hand for the near future Figure 2.4a even though the HadGEM2-ES model shows the strongest increase in a single month (July), the MPI-ESM-LR model shows the overall strongest average FWI change and overall it is the model with the consistently strongest increase between all RCP scenarios and time periods.

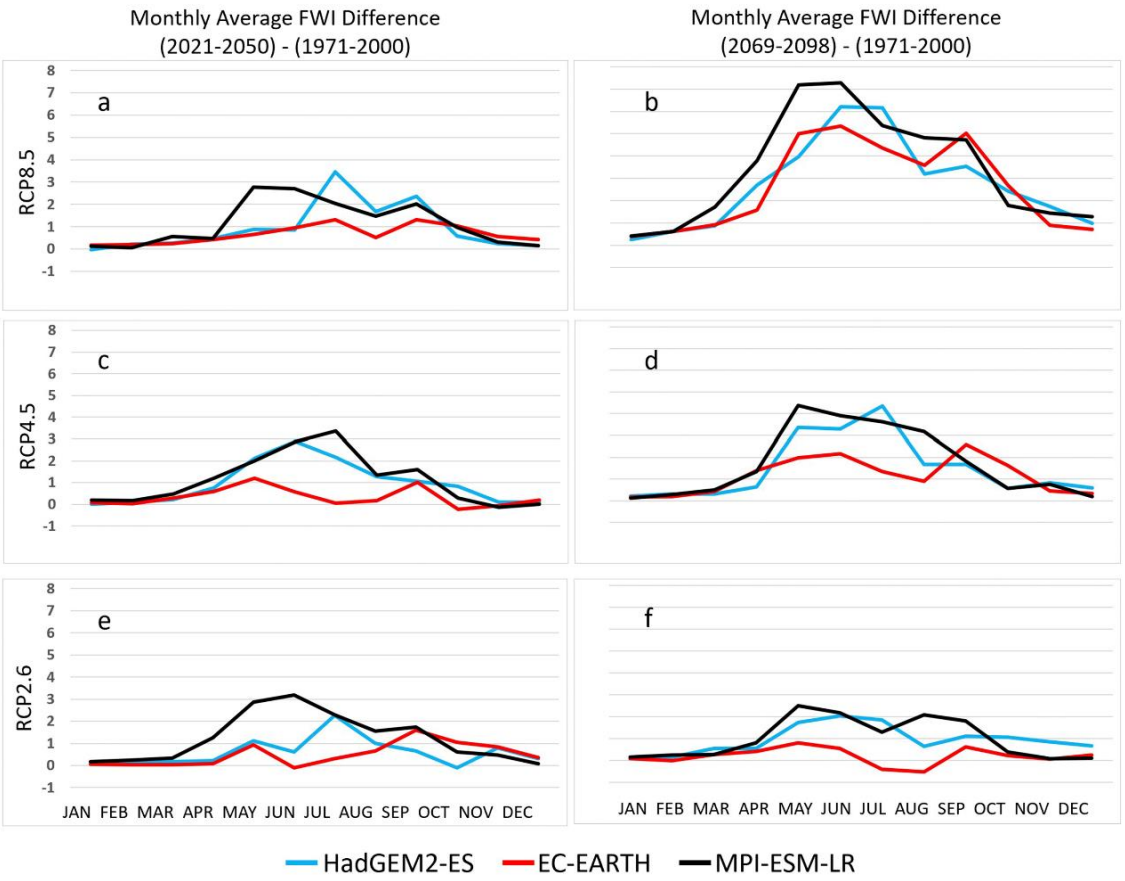

Figure 2.4. Seasonal variability change between near future and reference period in sub-figure (a) and distant future and reference period in sub-figure (b) for each of the three climate models for the entire Greek domain, under all the tested RCP scenarios.

2.4. Conclusions

The present study evaluated the FWI index as calculated from the output of three different regional climate model simulations. We analyse results for three time periods (1971-2000, 2021-2050, 2069-2098), and for three climate change scenarios, i.e. RCP2.6, RCP4.5 and RCP8.5. The following Greek areas are deemed to have the highest fire danger in the reference period (recent past): Crete, the Aegean Islands, the Attica region, and parts of Peloponnese. These fire prone areas seem to link closely with the areas in Greece with the highest burnt area as found by Papagiannaki et al. (2020). Regarding the future, the results showcase a general trend of increasing FWI index, indicating increased wildfire danger for Greece in response to global warming.

The threshold FWI>30 has been established for the Greek climate as it represents potential fire danger. Even though this threshold is found to be representable of the entire Greek domain other more precise thresholds have been found ranging from northwest to southeast Greece which might result in over or under estimates depending on the area (Karali et al. 2014). On a broader sense, these FWI thresholds

are custom for every country and dependent on the country's climatological conditions. For example in Canada where this index was created an FWI value above 30 is considered extreme (Kirchmeier-Young et al. 2017) while for a Mediterranean type climate extreme FWI values start above 150 as seen in Figure 2.2. That is why the country specific calibration of the index is particularly important. Based on the threshold of FWI>30, it was calculated that in the distant future, there is the possibility of 40-50 additional fire danger days when compared to the reference period under the RCP8.5 scenario. This number is also in line with the fire danger days found in (Karali et al. 2014).

In the distant future, it is also predicted for the Greek domain to experience an increase of one fire danger class under the RCP8.5 scenario. The length of the fire season for some areas under the RCP8.5 scenario is predicted to increase in the distant future up to 40 days and up to 13 days when considering the entire Greek domain. Looking at the fire season length in a global context, most of the Northern hemisphere is predicted to experience an increase in the future of up to 20 additional days with some Mediterranean (e.g. Greece) and central European Countries as well as eastern and southern US states experiencing an increase of more than 20 days. (M. Flannigan et al. 2013; Wotton and Flannigan 1993). Increase in the fire season length leads to potentially higher number of fires and thus increase in human respiratory symptoms due to hazardous fire emitted particles (Lazaridis et al. 2008). Finally, after calculating the seasonal variability for all available climate models a trend towards increasing FWI average monthly values was found for the month of September.

This study is subject to certain limitations. First, the results are estimated under the assumption of a stationary land cover which makes the threshold employed (FWI=30) valid for the present, but potentially not valid in the distant future under a changed climate. Furthermore, it must be noted here that the FWI estimation provided by Copernicus is based on climate model output that is uncorrected for biases, which may influence our results as well. Nevertheless, our results show clear indications of increased fire danger over Greece in the future due to the ongoing climate change that takes place and is expected to further unfold.

Data availability statement

The data that support the findings of this study are openly available at the following URL/DOI:

https://cds.climate.copernicus.eu/cdsapp#!/dataset/sis-tourism-fire-danger-dicators?tab=overview

Acknowledgements

This project is supported by the project/program "National Network on Climate Change and its Impacts - Climpact" financed by the Public Investment Program of Greece and based on the results from FWI simulations provided by Copernicus Climate Change Service. Also, this research was partially funded by the Leverhulme Centre for Wildfires, Environment, and Society through the Leverhulme Trust, grant number RC-2018-023.

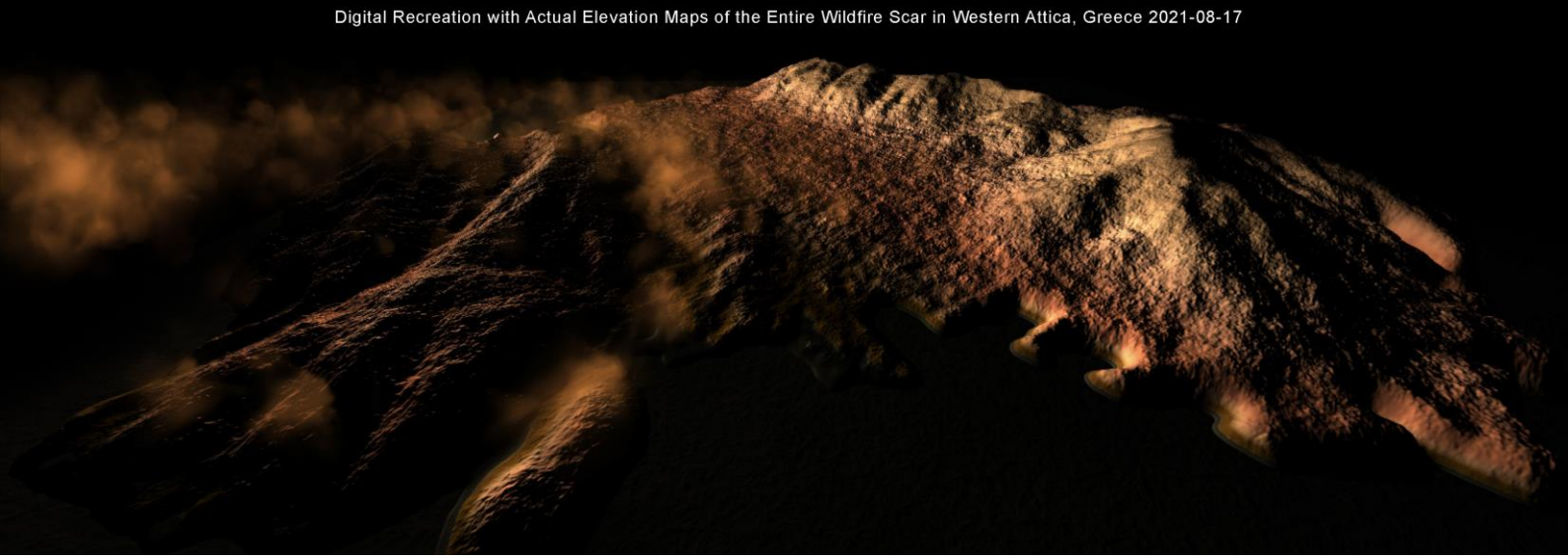

3. Wildfire aerosols and their impact on weather: a case study of the August 2021 fires in Greece using the WRF-Chem model

This chapter is based on the following publications:

Rovithakis, A.; Voulgarakis, A. Modeling the Air Pollution and Weather Feedback from Wildfire Emissions with WRF–Chem over Greece. Environ. Sci. Proc. 2023, 26, 201. https://doi.org/10.3390/environsciproc2023026201

Rovithakis, Anastasios and Voulgarakis, Apostolos, An Investigation of Fire Emissions Impacts on Weather Over Greece Using Wrf-Chem. http://dx.doi.org/10.2139/ssrn.4576640

Abstract.

Wildfires are significant contributors to atmospheric gases and aerosols, impacting air quality and composition. This pollution from fires also affects radiative forcing, influencing short-term weather patterns and climate dynamics. Our research employs the Weather Research and Forecasting model coupled with Chemistry (WRF-Chem) to investigate the repercussions of wildfires on aerosol abundances and associated immediate weather responses. We examine the summer season of 2021, a period marked by severe wildfire events in the country during a heatwave period. We conducted sensitivity experiments including and excluding wildfire emissions to measure their effects on aerosol optical depth (AOD), radiative forcing, and weather features such as temperature, humidity, clouds, and atmospheric circulation. Our findings demonstrate that the radiative impacts of wildfires negatively influence the local temperature over the fire smoke plume affected areas. Conversely, neighbouring areas of continental Greece experience increases in temperature due to remote effects of wildfire emissions, caused by meteorological feedbacks that reduce atmospheric

humidity. Crucially, including fire emissions significantly improves the simulated surface temperatures predicted by the model over the Greek domain. Our work demonstrates that wildfire-generated aerosols can significantly impact weather conditions, and highlights the importance of including both local radiative effects and remote feedbacks for achieving more accurate weather prediction.

3.1 Introduction

Fire is a natural, recurring episodic event in almost all ecosystems (Bistinas et al. 2014). However, wildfire events of unprecedented size and intensity are increasing in several world regions and are expected to increase in frequency (Rovithakis et al. 2022; Le et al. 2017), leading to significant ecological and socio-economic impacts (Tedim et al. 2018). These wildfires often exceed suppression capacities, leading to significant damages and frequently resulting in fatalities among civilians and firefighters. A significant, recent example for the Mediterranean region is the catastrophic wildfires which occurred in early August 2021 in Greece. They arise in several Greek regions mainly Attica and Peloponnese on August 3rd and 4th 2021 and continued for several days. These five wildfires collectively burnt nearly 94,000 ha, accounting for more than 70% of the 2021 total burnt area, exceeding the country's 2008–2021 annual average burnt area by three times. They exhibited severe fire dynamics, marked by unpredictable fire progression, extensive ember transport, and the formation of pyrocumulonimbus clouds (Giannaros et al. 2022). Compared to observational records for the period 2010-2019, the first two winter months of 2021 were wetter than average, whereas the rest of the months leading to the 2021 fire season were dryer than average (Giannaros et al. 2022). In addition, temperatures especially for the wildfire-affected areas were warmer than average. So overall the 2021 weather conditions initially created fuel abundance which then efficiently dried (Giannaros et al. 2022). During the main catastrophic wildfire events the prevailing weather conditions were extreme with temperatures higher than 38 ^{o}C, relative humidity between 10-15%, gusts of wind up to 48 km/h and extremely hazy atmosphere (Maura 2021)

Fire aerosols can have strong impacts on the regional and global atmospheric environment, climate, and ecosystems (Voulgarakis and Field 2015; Sokolik et al. 2019). They pose risk in human life, including cardiopulmonary conditions, acute and chronic respiratory infections, and lung cancer (Cohen et al. 2005; Jethva and Torres 2019).

The major chemical components of fire aerosols are diverse and can vary depending on the type of vegetation burning and combustion conditions, amongst other factors. Organic carbon (OC) and black carbon (BC) are the key aerosol components emitted during biomass burning and are primary carbonaceous aerosols resulting from

incomplete combustion of organic material (Andreae and Merlet 2001b). Secondary aerosols are formed in the atmosphere through the oxidation of gas-phase precursors emitted during wildfires, leading to the production of sulphate ($SO4^{-2}$), nitrate (NO^{-3}), and secondary organic aerosols (SOA). Other emissions from wildfires include Polycyclic Aromatic Hydrocarbons (PAHs) that are formed during incomplete combustion (Simoneit 2002), and inorganic gases such as nitrogen oxides (NO_x), sulphur dioxide (SO_2), carbon monoxide (CO), ammonia (NH_3), and metals (Yokelson et al. 2009). Also, trace Gases such as carbon dioxide (CO_2), methane (CH_4), ozone (O_3), and volatile organic compounds (VOCs) are emitted or produced in the atmosphere during wildfires (Akagi et al. 2011).

Aerosols have the ability to affect the Earth's climate by affecting solar radiation (Voulgarakis and Field 2015; Papadimas et al. 2012). The effects of aerosols can be classified into direct and indirect. Direct effects encompass the scattering of incoming sunlight, leading to a reduction in shortwave radiation reaching the ground, as well as the absorption of solar radiation by black carbon and other light-absorbing aerosol particles, changing surface temperature, relative humidity and impacting cloud formation. Indirect effects involve aerosol particles serving as cloud condensation nuclei, impacting cloud thermodynamic properties, and as a result, cloud cover, lifetime and precipitation (Silveira et al. 2021). Wildfire-emitted particles are estimated to have a negative global radiative forcing and to reduce global surface temperature by 0.13 K due to direct (scattering) and indirect effects (M. G. Tosca, D. J. Diner, M.J.Garay 2014; Tosca, Randerson, and Zender 2013; Jiang et al. 2020).

The Mediterranean basin is in the crossroad of many different aerosol sources, such as fine European originated anthropogenic aerosols, North African and Middle Eastern desert dust, and Mediterranean maritime aerosols (Kalivitis et al. 2007). Even though wildfire is a common disturbance in the Mediterranean ecosystem and many plant species have adapted to it, in recent years the number of wildfires has increased drastically, producing more aerosols in the atmosphere, affecting air quality and radiation balance (Vilén and Fernandes, 2011; Kaskaoutis *et al.*, 2011). The aerosols emitted during the intense 2007 wildfires in Greece were estimated to have had significant health impacts, while also leading to decreased incident solar radiation on the ground and lower surface temperatures close to the forest-fire locations (Kaskaoutis et al. 2011; Amiridis et al. 2009; Diapouli et al. 2017).

Since wildfire impact radiative forcing locally and regionally, it is natural to hypothesise that they are also expected to influence the evolution of weather phenomena. For the US, Zhang *et al.* (2022) found that wildfires increase the severity of storms and weather hazards downstream, using modelling along with observations. However, studies of how wildfire emissions can impact the weather have been limited. In this study, we use the WRF-Chem v4.4.2 to model the impacts of the devastating Greek wildfires that occurred from August 4th to August 8th, 2021, on weather, via affecting aerosol

abundances. This research is the first to assess the significance of wildfire emissions in an ensemble of weather simulations over the Greek domain, and one of the first studies to do so for any region around the globe.

3.2 Data and Methodology

3.2.1 WRF-Chem model setup

WRF-Chem is a numerical weather and atmospheric simulation model that is coupled with atmospheric chemistry (Grell et al. 2005). It can calculate the emission of pollutants, the chemical reactions that they undergo, and their transport in the atmosphere and transformation at multiple spatial scales (Tuladhar, Manandhar, and Shrestha 2021). It has been widely used for simulating air pollutionimpacts from wildfires in different parts of the globe, such as North America (D. Chen et al. 2014), Mediterranean region of Europe (Rizza et al. 2018), Africa (J. Wang et al. 2018), and the Middle East (Ukhov et al. 2020). Here, the domain covers the Eastern Mediterranean region centred over the city of Athens including North Africa, Italy, the majority of the Balkan countries and most of Turkey as seen in Figure 2.3.1a with 100 × 90 points, with a resolution of 0.25^{o} and 34 vertical levels up to 50 hPa. The simulations cover 14 days, starting on July 29th, 00:00 UTC, in order to spin up aerosol fields before the main aforementioned period of the fire events. Boundary and initial conditions were provided from NCAR/NCEP Final Analysis (FNL from GFS) (ds083.3), with a 0.25^{o} resolution. An idealized vertical profile for each chemical species is provided to initialise the model simulation. Anthropogenic emissions were provided by the 0.1^{o} Emission Database for Global Atmospheric Research (EDGAR). Biogenic emissions with 1 km resolution were included in the simulation using the Model of Emissions of Gases and Aerosols from Nature (MEGAN). These emissions can react in the atmosphere to form secondary pollutants, such as ozone and organic aerosols, which can be detrimental for air pollutionand climate. Daily 1 km resolution biomass burning emissions were used from the Fire Inventory NCAR (FINN) and were zeroed in a counter-factual experiment to study the wildfire effects on air pollution.

The RADM2 (second generation Regional Acid Deposition Model) gas-phase chemistry mechanism with the MADE/SORGAM (Modal Aerosol Dynamics for Europe / Secondary Organic Aerosol Model) aerosol scheme was used. RADM2 is a mechanism that includes about 40 gas-phase reactions and MADE/SORGAM is a comprehensive size-resolved primary and secondary aerosol scheme designed to simulate their life cycle from emission to transport, chemical transformation and removal considering sulphate, organic, and black carbon aerosols and their interactions with chemical and physical

processes in the atmosphere. This combination of gas-phase chemistry and aerosol scheme is often used for regional air pollutionsimulations (Adams 2001).

The Morrison and Gettelman (2008) aerosol microphysics scheme was used which focuses on the role of aerosols in cloud formation and precipitation and is based on the two-moment bulk microphysics scheme. Six species of water are included: vapour, cloud droplets, cloud ice, rain, snow, and graupel/hail. Predicting both number concentration and mixing ratio, known as two-moments prediction, enables a more robust treatment of particle size distributions. These distributions play a pivotal role in calculating microphysical process rates and the evolution of clouds and precipitation.

The model's horizontal resolution of 0.25 degree provides the simulations with the necessary spatial detail for such a study (Forkel et al. 2015; Michael et al. 2022). Greece was the centre of a simulation domain covering the Eastern Mediterranean basin, which was deemed an adequate domain size to resolve the atmospheric systems' movements in the internal Greek domain of interest (Lagouvardos et al. 2019; Guion et al. 2022).

To account for weather's random nature, the initial conditions for the variables of temperature and wind speed were perturbed using a stochastic random field native to WRF-Chem's initialization routine with 10 different seeds (Yu et al. 2017; Peng et al. 2017; Baker 2021). Thus, an ensemble of 10 simulations was created for both the model experiments (with and without wildfire emissions).

3.2.2 Climate data used for comparison

Two observational datasets were used for evaluation of modelled results. Hourly gridded 0.25^{o} ERA5 reanalysis surface temperature data used for modelled temperature evaluation. Reanalysis combines model data with observations from across the world into a globally complete and consistent dataset. ERA5 reanalysis surface temperature (Hersbach et al. 2020) in combination with ground temperature observations from the NOANN network's automatic weather stations of the National Observatory of Athens was an additional step to assure the model's evaluation when it comes to the core weather variable of interest, i.e. temperature. Velikou et al. (2022) found that in comparison to observational data, ERA5 mean monthly temperature biases are small and do not exceed ±0.3 °C. Both these datasets inherently account for the impact of emissions from real fire events, as they rely on real-world observational data (Vitolo et al. 2020).

When it comes to aerosols evaluation, the MCD19A2 Version 6 data product was used from the Moderate Resolution Imaging Spectroradiometer (MODIS) on-board the Terra and Aqua satellites, which is widely used for aerosol monitoring purposes (Grgurić et al. 2014), combined with the Multi-Angle Implementation of Atmospheric Correction

(MAIAC) Land Aerosol Optical Depth (AOD) gridded Level 2 product produced daily at a 1 kilometre (km) pixel resolution. Chew et al. (2016) found acceptable correlations between MODIS and ground stations' AOD from AERONET. The AOD indicates the extent to which particles in the air (aerosols) prevent light from traveling through the atmosphere due to scattering and absorption of incoming solar radiation.

3.2.3 Selection of fire smoke plume affected areas

To draw definitive conclusions on wildfire effects, only regions within Greece influenced by the smoke plume were analysed. These areas were identified based on average AOD values exceeding the 90th percentile, derived from all 10 simulations that included wildfire emissions. This approach allowed for a distinct separation of wildfire-affected areas and facilitated a more precise comparison with the unaffected ones, and thus is used for the figures below.

3.2.4 Error improvement

The error improvement graphs seen in Figure 3.1 and Figure 3.3 were made following Equations (1) and (2), respectively. This was a way to track the improvement of simulated AOD and temperature when including the fire emissions as opposed to when ignoring them.

$$AOD\ Error\ improvement\ \% = \left|\frac{Observation - Simulation\ no\ fire\ emision}{Observation}\right| * 100 - \left|\frac{Observation - Simulation\ fire\ emission}{Observation}\right| * 100 \quad (1)$$

$$\Delta T = |Observation - Simulation\ no\ fire\ emision| - |Observation - Simulation\ fire\ emission| \quad (2)$$

3.3 Results

3.3.1 Model performance and the role of fire emissions

We first examined the performance of our WRF-Chem simulations in terms of simulating aerosol abundances, as indicated by AOD, and whether the model skill in predicting AOD is impacted when including wildfire emissions in the simulation. For aerosols, MODIS AOD data were used to compare against. A limiting aspect is that MODIS data are scarce for the area and the days of interest. In cases where MODIS had somewhat consistent data such as for 8/8/2021, the simulated AOD distribution in the wildfire-affected area of southern Greece (Figure 3.1 b2) agrees fairly well with that found in the observational data (Figure 3.1 b1). We additionally created a fire smoke

plume mask based on the simulated AOD values that are greater than the 90th percentile (explained in Subsection 3.2.3). Then the MODIS as well as the WRF-Chem values from both simulations were averaged for the areas affected by smoke and plotted in Figure 3.1c.

It is clear that when fire emissions are activated in the model, the latter is able to simulate the AOD with far greater accuracy, as also indicated by the error improvement bar graph in Figure 3.1d. During the early part of the simulated period (August 1st to 3rd) there were constantly fire emissions in the input data representing a number of smaller wildfires that actually occurred in that time period. Emissions then increased sharply between August 4th to 8th, as this is when the major Greek catastrophic wildfires that are studied here occurred. The fact that there are AOD differences between the two simulations in Figure 3.1c even before the 4th of August is explained by the smaller fires that were occurring then as seen by the presence of Black Carbon emissions in Figure 3.2. All days show an error improvement of 20% or more, with some (i.e. August 5th and 8th) showing an improvement of 80% or higher. The error improvement is on average highest between the 4th and 8th of August, which corresponds to the more intense fire activity days.

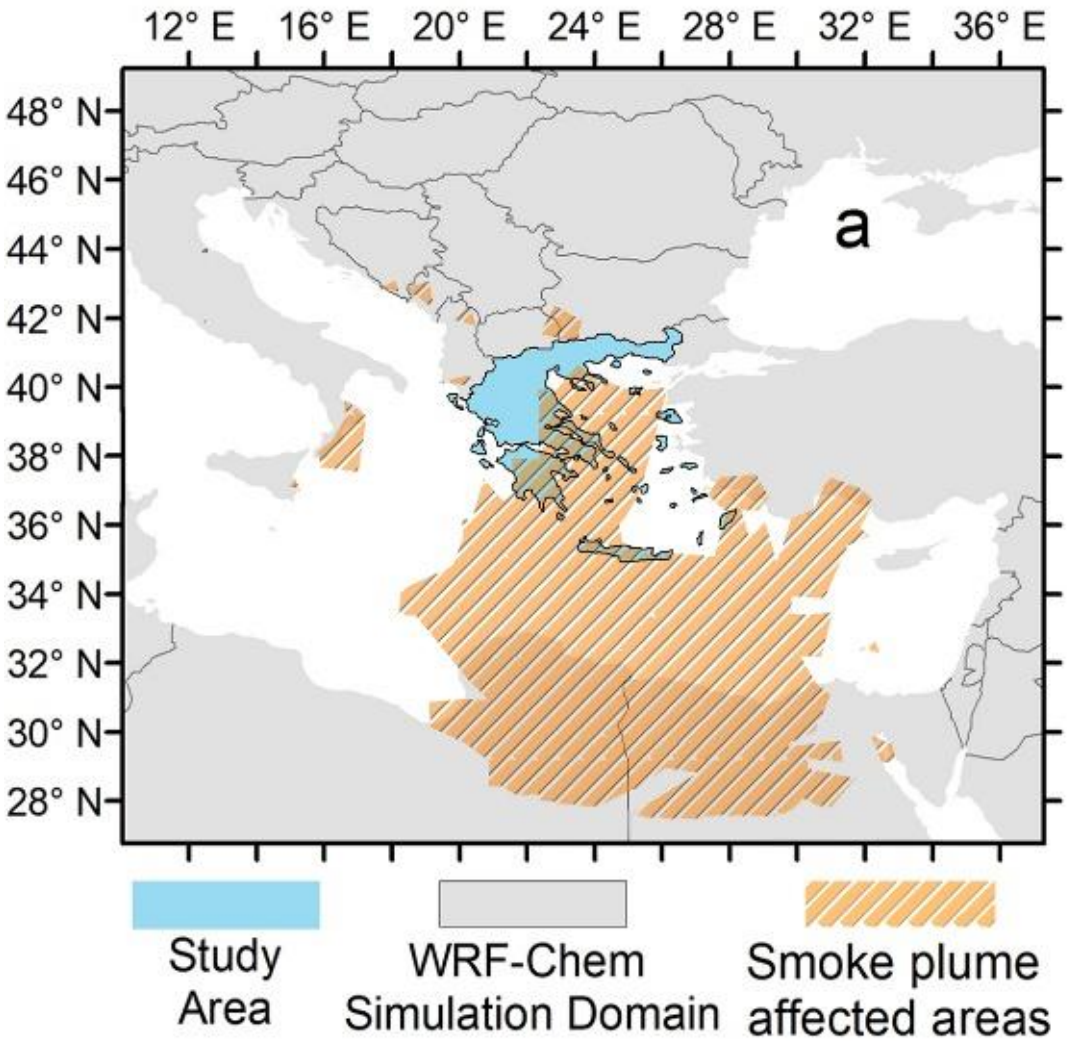

Figure 3.1. Panel (a): Study area in blue colour corresponding to the non-affected areas and the entire simulation domain in grey colour. Orange stripes inside the blue study area represent the wildfire smoke plume affected areas that were selected based on the methodology explained in subsection 3.2.3 in the South-eastern part of Greece.

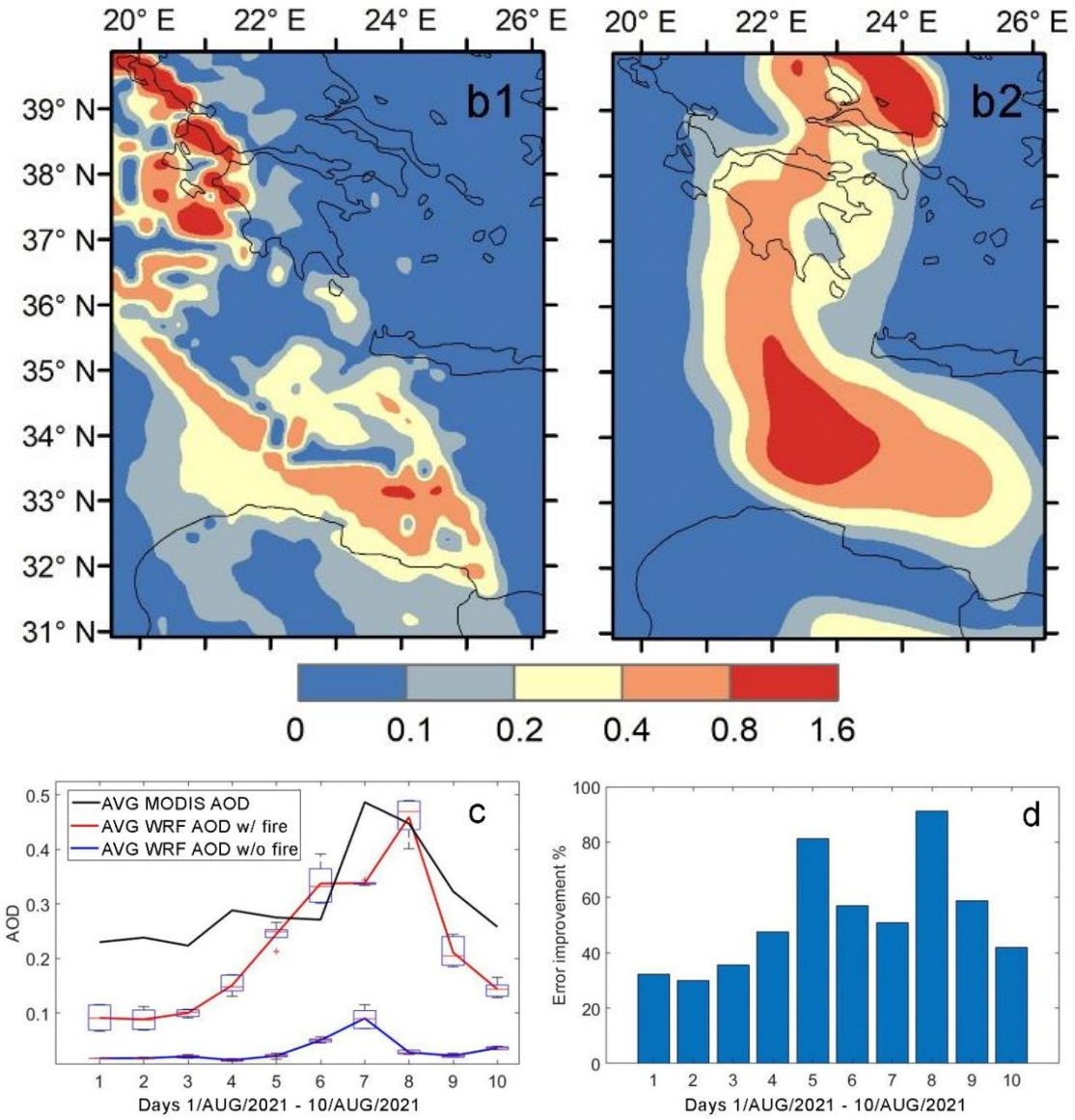

Figure 3.1. Comparison of WRF-Chem AOD output to MODIS observations. Panel (b1) shows a MODIS AOD snapshot for 8/8/2021 8:40 AM. Panel (b2) is a snapshot for the same day at 9:00 AM from WRF-Chem ensemble mean output from the simulation with fire emission data. Panel (c) shows comparison for all days, spatially averaged for the fire smoke affected areas in the Greek domain, for MODIS and for the two WRF-Chem simulations (averaged over all 10 ensemble members). The bars on top of the boxes represent the total spread of all 10 ensemble members for each of the 2 WRF-Chem simulations whereas the boxes indicate the spread of the middle 50% of the 10 ensemble members. Panel (d) shows the error improvement between the two WRF-Chem simulations (w/ minus w/o fire) when compared with the MODIS observations.

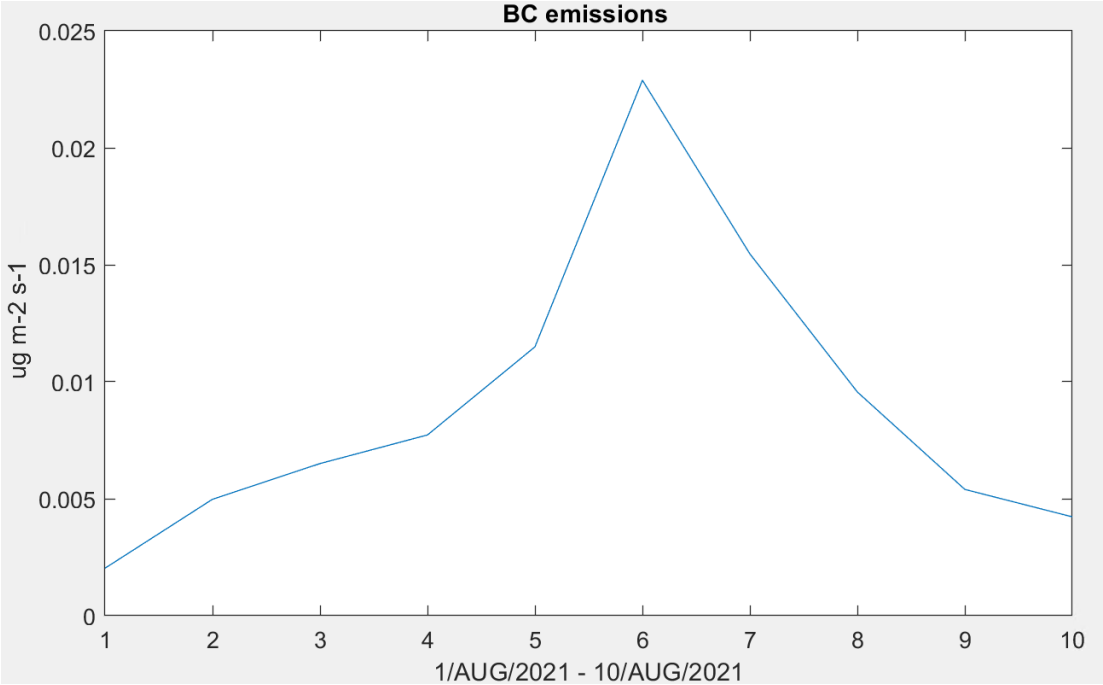

Figure 3.2. Time evolution of the spatially averaged Black Carbon emissions over the fire smoke affected areas in the Greek domain during the first 10 days of August.

Since our focus here is on meteorological effects of wildfire pollution, with a particular focus on the evolution of the heatwave that was ongoing in the country, we proceed to also assess the model skill in terms of capturing surface air temperature, and whether this skill improves when including wildfire emissions in the simulation. We compare to ERA5 reanalysis temperature data and to ground station temperature data from the NOANN network from the same wildfire-affected areas, as shown in Figure 3.3. From Figure 3.3c it is clear that using fire emissions, the WRF-Chem simulation performs better, as the correlation with observations strengthens in the wildfire-affected areas (applying the fire mask described in Subsection 3.2.3).

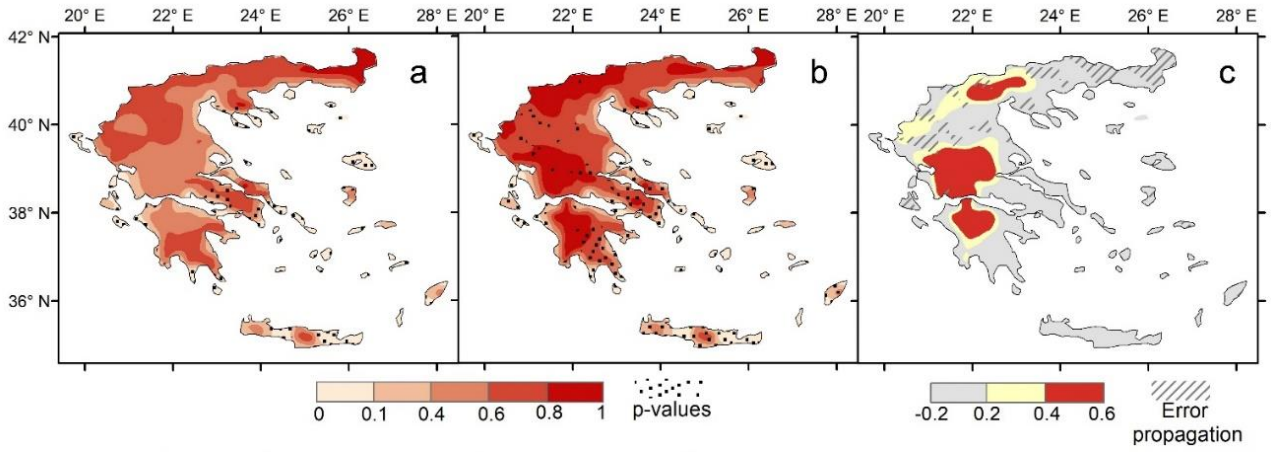

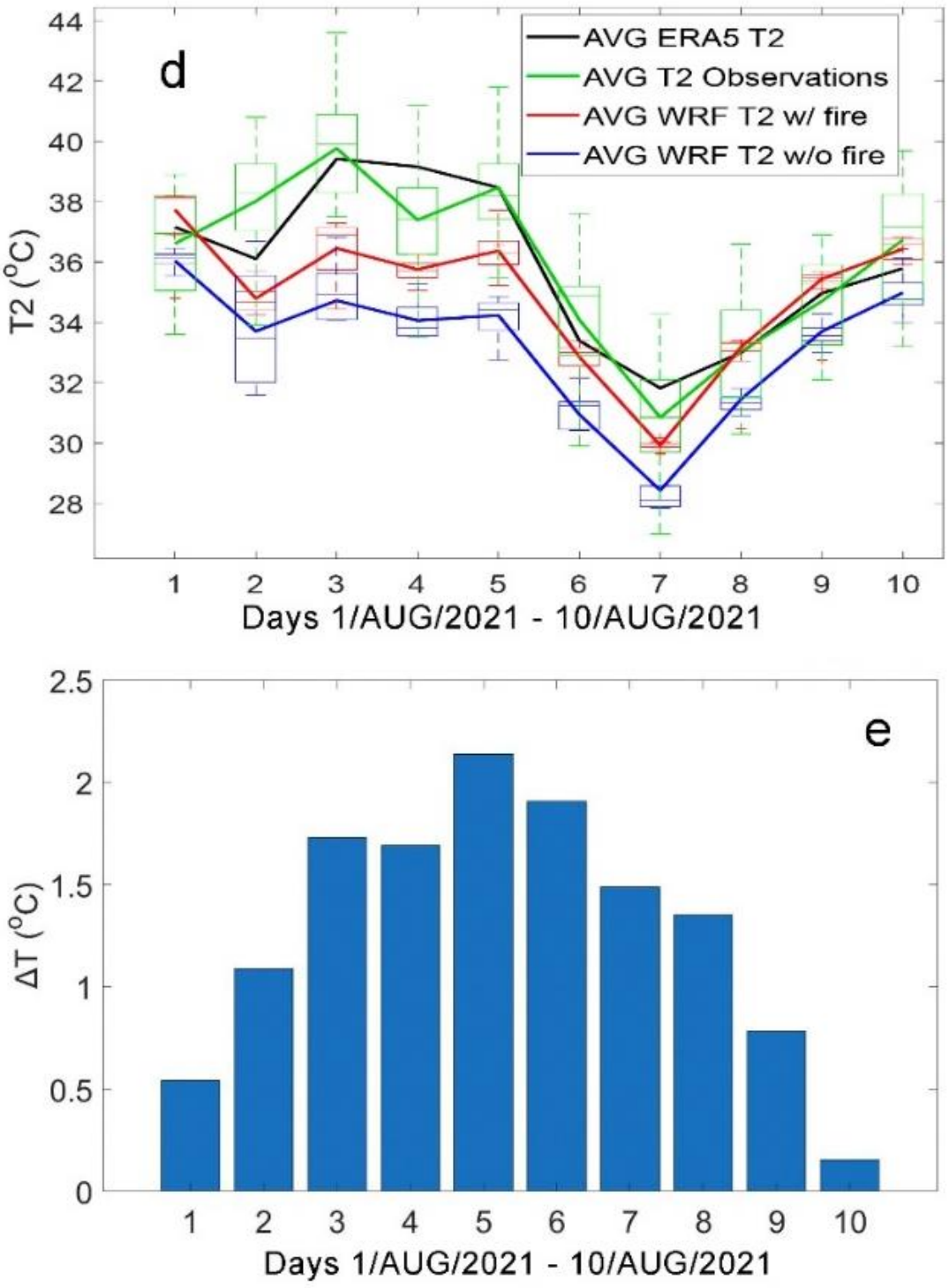

Figure 3.3. Comparison of WRF-Chem surface temperature output to ERA5 reanalysis and to ground station data (averaged over the domain). Panels (a) and (b) show the correlation between ERA5 and WRF-Chem 2m temperature, for the two simulations. Stippled regions are those with no significant difference between observed and simulated data as defined by the p-values < 0.05 (i.e. good agreement with observations). Panel (c) shows the difference between the two correlations in panel (a) and (b). Hatching indicates areas with differences that are not significant, using standard error propagation of the results from panels (a) and (b). Panel (d) shows the comparison of WRF-Chem simulations (averaged over all 10 ensemble members) with ERA5 data, spatially averaged for the wildfire smoke affected areas and for all days. The bars on top of the boxes represent the total spread of all 10 ensemble members for

each of the 2 WRF-Chem simulations, whereas the boxes indicate the spread of the middle 50% of the 10 ensemble members. Panel (e) shows the error improvement in temperature of the two WRF-Chem simulations relative to ERA5.

Additionally, the observed and simulated temperature values were averaged across the whole domain and their day-to-day evolution is shown in Figure 3.3d. First of all, we note that based on Figure 3.3d, the ERA5 and NOANN network temperatures agree very well for the region and period of interest. It is also apparent that including fire emissions in the model, results in better simulations of the average temperature and its variations, substantially improving the error, depicted in Figure 3.3e. Similarly, to AOD (Figure 3.1d), the error improvement is generally greater from August 4th to 8th, coinciding with the peak days of fire activity. During those core wildfire days, the simulation ignoring wildfire emissions' effects tends to underestimate temperatures by 2.5-4^{o}C (Figure 3.3d), while this error - which was calculated based on the temporal variation difference (ERA5-T2 w/ fire) - (ERA5-T2 w/o fire) - is reduced by 1.5-2^{o}C when including fire emissions clearly showcasing a fire impact (Figure 3.3e).

3.3.2 Physical mechanisms

We have established so far that WRF-Chem captures the levels and evolution of aerosol pollution and of temperature very well, and that this performance is strengthened when including wildfire emissions in the simulation. Therefore, our hypothesis that wildfire aerosols are important for accurately simulating weather conditions is supported by our results. We now delve further into the mechanisms that lead to the improved model performance when including fire emissions in the simulation. All difference maps in panels a-f as a result emerge from the perturbations to fire emissions. In Figure 3.5 panels (a, b), we show surface temperature and AOD in the two simulations and in panels b-f we explain the drivers influencing those temperature differences. On average, for all the areas affected by the wildfire smoke plume, there is an AOD increase between 0.1-1.5. From Figure 3.5a, it is seen that areas most affected by the smoke plume (as indicated in Figure 3.1a) are experiencing lower temperatures when including the fire emission effects, with decreases of up to 0.5 ^{o}C. At the same time, much of continental Greece that lies to the west of the smoke plume region is experiencing increases in temperature of up to 1.5 ^{o}C.

Wildfire smoke plume affected areas are experiencing lower temperatures since aerosols reduce shortwave radiation at the surface, as seen in Figure 3.5c. Longwave radiation changes were found to be much smaller than the changes in the shortwave as seen in Figure 3.4, meaning that the temperature changes seen in Figure 3.5a are explained predominantly by shortwave effects. The increases in surface temperatures

found in western areas of continental Greece (Figure 3.5a), which are not affected directly by the smoke plume (Figure 3.1a), occur due to a surplus of net shortwave radiation at the surface (Figure 3.5c). This appears to be due to the fact that fire aerosols cause a remote atmospheric circulation feedback away from the plume. Specifically, there are water vapour reductions (Figure 3.5d) causing the atmosphere to absorb less solar (shortwave) radiation, thus leading to more heating at the surface, explaining the higher surface temperatures seen in Figure 3.5a. Water vapour may be known more for its longwave effects, but it also absorbs substantially in the shortwave (Paynter and Ramaswamy, 2014; Haywood *et al.*, 2011). The areas experiencing higher temperatures also feature reduced cloudiness (Figure 3.5e), also contributing to increases in surface temperature.

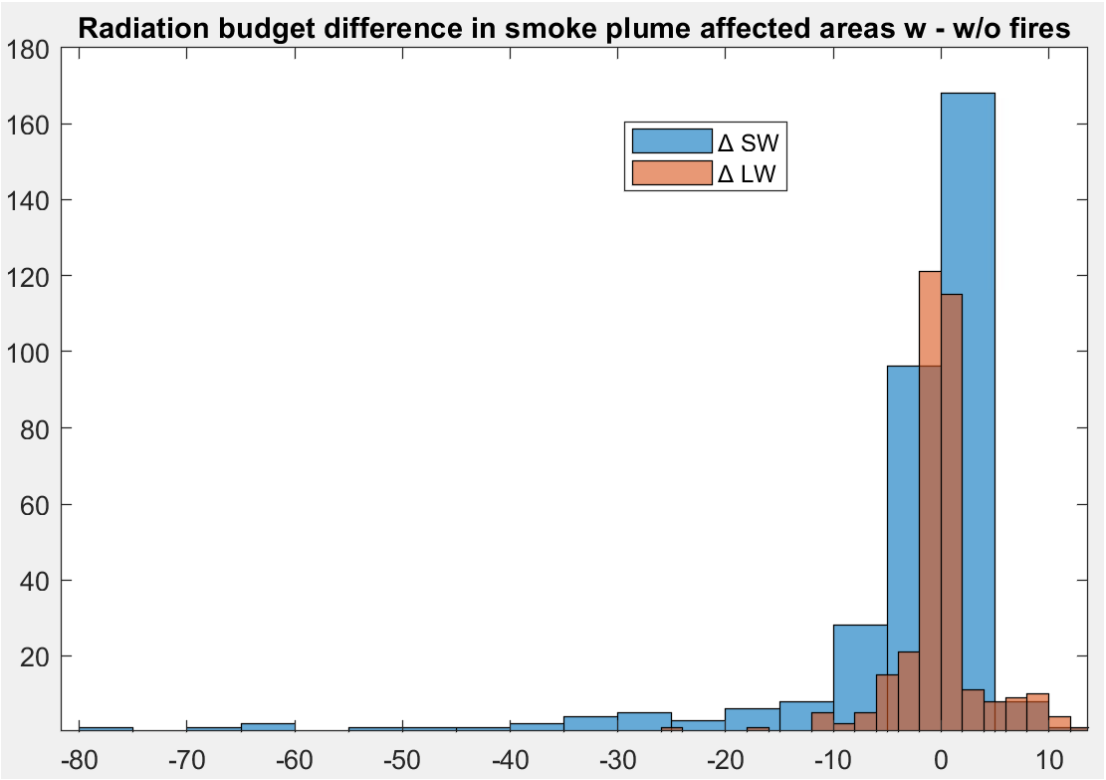

Figure 3.4. Ensemble mean differences in the longwave and shortwave radiation budget over the fire smoke affected areas in the Greek domain, between the WRF-Chem simulations with and without fire emissions:

We suggest that both the water vapour and the cloud reductions are causing the increases in shortwave radiation and temperature. An induced anticyclonic circulation pattern over most of central/western Greece when including fire emissions (Figure 3.5f), as seen in the wind field and the 850hPa geopotential height changes, appears to be the cause behind the water vapour and cloud reduction. The geopotential height of 850 hPa was chosen as it is widely used in atmospheric science to capture low to mid-troposphere processes, such as the development of weather systems close to the ground (Trigo *et al.*, 2006). This level provides a clearer picture of thermal advection and moisture transport, which are critical in identifying and understanding the

development of anticyclones. These features are not as clearly visible at higher levels, such as 500 hPa, making the 850 hPa data essential for understanding the dynamics and impacts of anticyclonic systems on weather (Richardson *et al.*, 2021;Zhang *et al.*, 2020). Higher geopotential heights are associated with higher underlying surface air pressures, and therefore with sunnier and drier weather conditions, therefore leading to lower water vapour abundances and less cloudiness (Fujita and Sato, 2017; Tang *et al.*, 2020).

The smoke plume, as seen in Figure 3.1a, whilst reducing the 2m temperature in the areas underneath, it also absorbs solar radiation due to the presence of black carbon thus heating the air within the plume. The heated air becomes more buoyant and rises as seen in the blue areas in Figure 3.5g, leading to a drop in surface pressure (Kochanski *et al.*, 2019; Liu, Goodrick and Heilman, 2014). Also dictated by the wind field circulation anomalies as seen in Figure 3.5f, the regions that lie further to the west of the smoke plume feature sinking air, to balance the rising air in the plume-dominated areas, thus increasing the surface pressure and creating the aforementioned anticyclone (Sharples, 2009; Sokolik *et al.*, 2019; Adam K Kochanski *et al.*, 2019;Kassomenos, 2010; Tomašević *et al.*, 2022). In general, heating perturbations such as that caused here by the smoke plume, can generate atmospheric waves, which are crucial in the mid-latitude circulation. The generated waves propagate through the atmosphere, transferring energy and momentum. This propagation can cause disturbances far from the initial perturbation site (Tomašević et al. 2022).

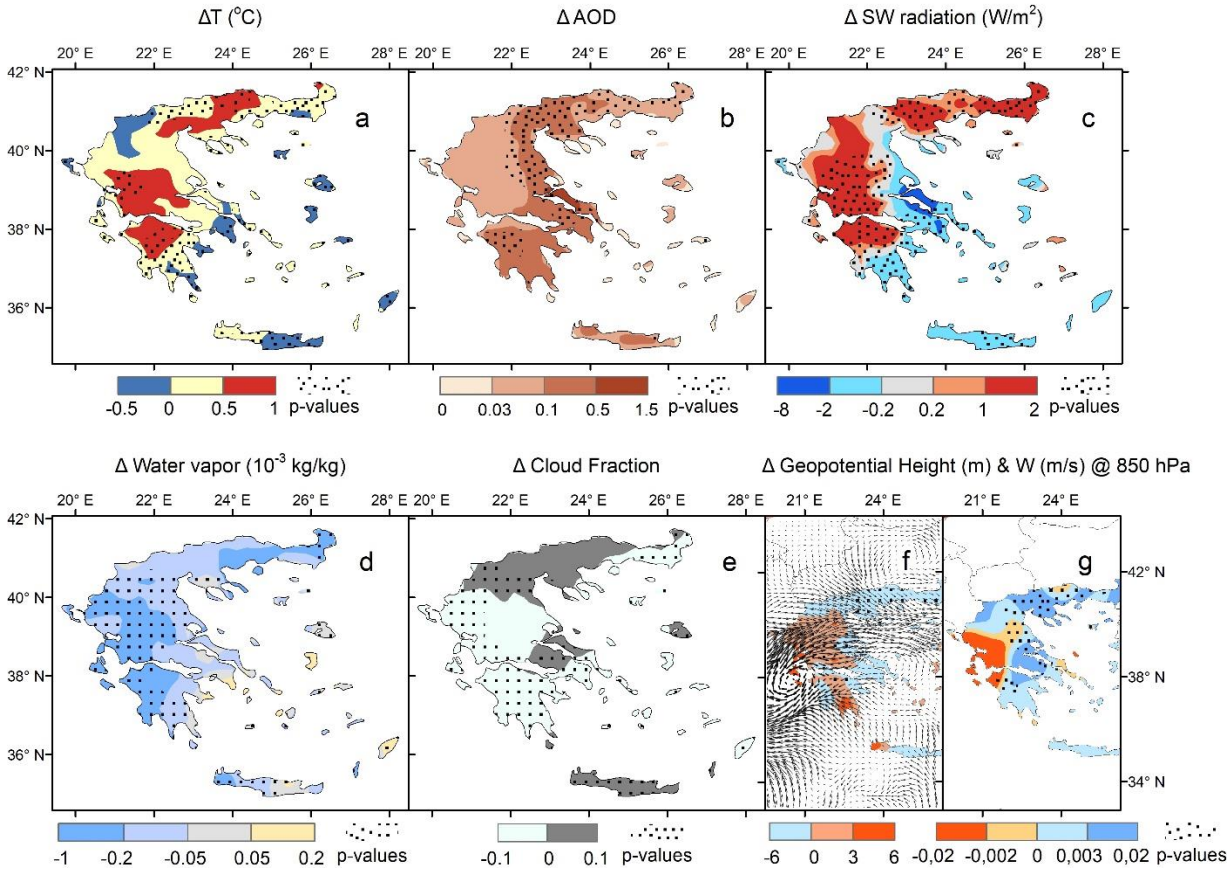

Figure 3.5. Ensemble mean differences in temperature, aerosol abundances and associated meteorological variables, between the WRF-Chem simulations with and without fire emissions: Panel (a): surface temperature difference at 14:00 (°C). Panel (b): AOD difference at 14:00. Panel (c): net downward shortwave radiation difference at the surface (W/m^2). Panel (d): surface water vapour difference (kg/kg). Panel (e): total cloud fraction difference expressed as areas with less cloud coverage during fire simulations (-0.1 - 0) and higher cloud coverage (0 - 0.1). Panel (f): difference in geopotential height and in the wind vector at 850 hPa. Panel (g): vertical wind speed changes at 850 hPa. Blue areas experience rising air and red areas sinking air.

Next, the effect of fire-emitted particles on the temporal evolution of temperature was studied. We examine this through performing regressions between daily temperature and AOD using output data from the simulation including fire emissions, as well as observational data (Figure 3.6). The wildfire-emitted particles in the plume, scatter some of the solar (shortwave) radiation back to space (mainly through organic carbon effects) and absorb some of the radiation (mainly black carbon). The absorption heats up the atmospheric column at the areas where the plume is located, while both the absorption and the scattering contribute to shortwave cooling of the Earth's surface (Liu et al. 2018; Voulgarakis and Field 2015). This cooling leads to the reduction of surface air temperatures near the locations of the wildfires and downwind from them Figure 3.5a.

When applying a wildfire smoke mask for the Greek domain (as explained in Subsection 3.2.3) and spatially averaging over the wildfire-affected and non-affected areas seen in Figure 3.1a (whilst considering all ensemble members), we find a clear difference in temperature tendencies with AOD. The wildfire-affected areas display a negative temperature tendency in this temporal analysis. On the contrary, for the non-affected areas, the same regression reveals a positive temperature tendency. These features are seen both in the regressions that use model results and in those using observational data from MODIS for the AOD and ERA5 for the temperature, suggesting that they represent realistic effects of wildfire aerosols on temperature.

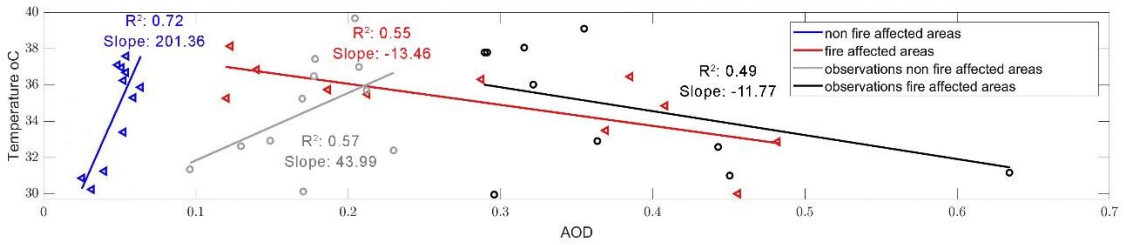

Figure 3.6. Temperature regression against AOD in the simulation including fire emissions and in observations. We find positive tendencies for areas in other parts of the country and negative tendencies for areas collocated with the smoke plume.

3.4 Conclusions

This study assessed the impact of the devastating Greek wildfires that occurred from August 4th to 8th 2021 on weather, through the radiative effects of the aerosol pollution caused by the fires. The research initially involved evaluating model-simulated aerosol optical depth (AOD), both with and without fire emissions, against MODIS satellite data. Results indicated that including fire emissions in the model improved the AOD error against the observations by an average of 50%, with the most significant improvements found during the core fire period.

When the simulated temperature output was spatially averaged and compared temporally to ERA5 and station data, it was found that the model's performance improved when including wildfire emissions, with the simulation error decreasing by 1.5-2 degrees C for the wildfire days. While temperatures were found to drastically decrease in the wildfire affected areas (by up to 0.5^{o}C), there were also even more drastic increases (by up to 1.5^{o}C) in the neighbouring continental Greek areas that lie to the west of the plume. These areas not directly affected by smoke radiative effects are found to be receiving a higher amount of shortwave radiation when wildfire emissions are activated. The remote feedback responsible for this increase in radiation is attributed to a combination of decreased atmospheric water vapour concentrations and cloud coverage, driven by an induced anticyclonic circulation over those areas. On the contrary, for the wildfire smoke plume-affected areas, temperatures were found to be lower when accounting for wildfire emissions because of the more straightforward scattering effect of wildfire smoke, causing negative surface radiative forcing and therefore driving the lower temperatures in those areas.

Our study is subject to certain limitations. Uncertainties in MODIS AOD measurements stem from several factors, including errors in instrument calibration, inaccuracies in cloud masking, incorrect assumptions about surface reflectance, and selection of aerosol models (whether fine or coarse). When compared to AERONET AOD there is a negative bias for the MODIS AOD datasets generated by the deep blue algorithm and the opposite is true for the MODIS AOD datasets from dark target algorithm and the merged dataset (Shi et al. 2019). We also note that to some extent the conclusions could be model-dependent, and therefore more studies of this kind are warranted in the future. Nevertheless, our study demonstrates a clear potential influence of intense wildfires on weather in a Mediterranean environment, with implications for better understanding of pollution-weather interactions and enhanced skill of weather forecasting. It also highlights the importance of accounting for indirect meteorological feedbacks occurring in the broader region of interest, and not only in the specific areas where the pollution from the wildfires is located.

Data availability statement

The data that support the findings of this study are openly available at the following URL/DOI:

Global Forecast System (GFS) WRF_Chem input data:
https://doi.org/10.5065/D65Q4T4Z

Biogenic/anthropogenic emissions WRF_Chem input data:
https://www.acom.ucar.edu/wrf-chem/download.shtml

Biomass burning emission WRF_Chem input data:
https://www.acom.ucar.edu/Data/fire/

MODIS AOD data:

https://doi.org/10.5067/MODIS/MCD19A2.006

ERA5 temperature data:

https://doi.org/10.24381/cds.adbb2d47

Ground stations temperature data:

https://meteosearch.meteo.gr/

Acknowledgments

This research was funded by the Leverhulme Centre for Wildfires, Environment, and Society through the Leverhulme Trust (grant number RC-2018-023). AV has also been supported by the AXA Research Fund (project 'AXA Chair in Wildfires and Climate') and by the Hellenic Foundation for Research and Innovation (Grant ID 3453). We also acknowledge the help of Ms Georgia Methimaki from the University of Athens for helping with the initial model setup.

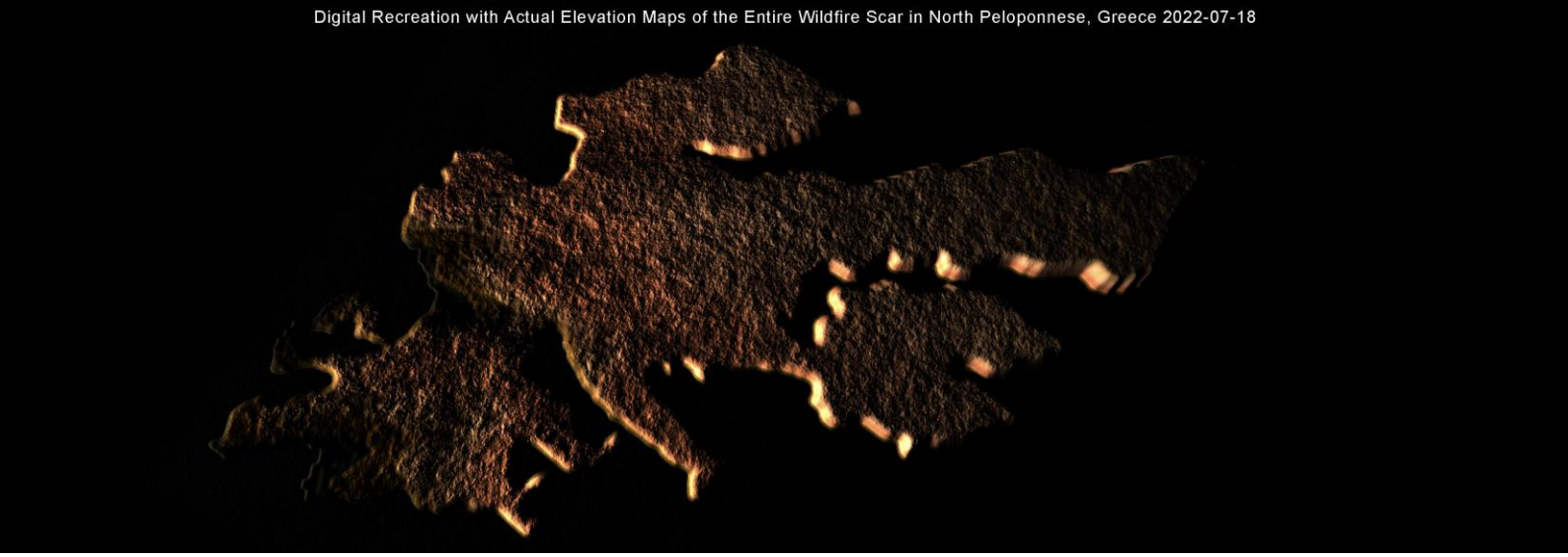

4. Automatic smoke plume detection using satellites

Abstract.

A large amount of aerosols is released by wildfires, which have an effect on the temperature and air pollution. This study evaluates the efficacy of satellite data in identifying and separating aerosols released by wildfires in Greece between 2000 and 2018. The MODIS satellite's Aerosol Optical Depth (AOD) and Thermal Anomalies products were employed, and their results were juxtaposed with the MERRA reanalysis data-derived Canadian Fire Weather Index (FWI). To precisely choose AOD values relevant to fires, a number of approaches were attempted. These included filtering AOD using the Absorptive AOD (AAOD) and Aerosol Index (AI) products. Using thermal anomalies to identify possible fire days and then filtering out non-fire days using the 99th percentile of AOD readings proved to be the most successful approach. The findings showed that this approach, especially in areas with a high fire frequency such as the Peloponnese, offered a good correlation between AOD and FWI. This study demonstrates how air pollutionevaluations and wildfire monitoring might be enhanced by combining thermal anomalies data with satellite-based AOD products.

4.1. Introduction

Aerosol is a general term for solid and gas particles suspended in air. Aerosols can have an important impact on regional and global atmospheric environments, climates, and ecosystems (Wu et al. 2020). Aerosols or 'particulate matter (PM)' are usually categorized based on their aerodynamic diameter, and the most widely monitored categories of aerosols are PM_{10} and $PM_{2.5}$. Particles with an aerodynamic diameter not exceeding 10µm are referred as PM_{10}. PM_{10} is primarily produced by industrial or agricultural production, construction, roadside dust, various industrial processes, and natural processes such as the resuspension of local soil and dust storms. Particles with an aerodynamic particle size not exceeding 2.5 µm are referred as $PM_{2.5}$ and are mainly derived from anthropogenic emissions. $PM_{2.5}$ is mainly produced by anthropogenic

combustion for transportation and energy production, and it is particularly important in environmental policy and public health (Xie et al. 2011).

Particulate air pollution is one of the major causes of death worldwide, with demonstrated adverse effects from both short-term and long-term exposure (Stafoggia et al. 2019). Wildfire-related aerosols can have catastrophic effects on a variety of human health issues, such as lung cancer, acute and chronic respiratory infections, and cardiovascular disorders (Cohen *et al.*, 2005; Jethva and Torres, 2019).

The most abundant pollutants emitted by fires in extratropical wildland areas, which includes typical wildland fires in the Mediterranean, are carbon monoxide (CO), particulate matter (aerosols, including organic carbon and black carbon, the latter also called 'soot'), methane (CH_4), NOx, and various non-methane hydrocarbons and volatile organic compounds (Knorr et al. 2016). Black carbon in particular results from the incomplete combustion of fossil fuels, biofuels and biomass and is responsible for scattering and absorbing portions of incoming solar rays, as well as absorbing radiation from the diffuse upward rays of scattered sunlight. The net effect is a warming of the atmosphere. It has been suggested that BC is the second most important component of global warming after CO_2 in terms of direct forcing (Galdos et al. 2013).

Aerosols are also being generated by burning fossil fuels and are affected by weather parameters such as temperature, wind speed, relative humidity and precipitation. Temperature is one of the main drivers responsible for wildfires, which release black carbon and other types of aerosols into the atmosphere. However, even without the presence of wildfires, there is also a natural source of aerosols, i.e. the biogenic volatile organic compounds (BVOC) which oxidate in the atmosphere forming semi- or non-volatile organic compounds. Consequently, these compounds can condense onto aerosol particles having the ability to act as cloud condensation nuclei and also correlate positively with temperature as they are emitted under warm and sunny conditions (Mielonen *et al.*, 2016; Scott *et al.*, 2014; Duncan *et al.*, 2009). When it comes to relative humidity, it is known that the volume of hydrophilic aerosols increases after water uptake thereby enhancing light scattering and consequently affecting the Earth/atmosphere radiation budget (Zang et al. 2019). Wind is responsible for the transportation of different types of aerosols. Definite correlation was found between surface wind speed and sea-salt aerosol concentration (Smirnov et al. 2003). For precipitation, ground based aerosol measurements have shown that it is a quick and effective scavenging process to the aerosols and their components in the air, resulting in a negative correlation with aerosol particle concentration (Tang et al., 2005).

Several studies have highlighted the good correlation between satellite aerosol products and their ground-level counterparts. Aerosol products from AERONET and specifically the AOD was found to have a significant level of correlation with the hygroscopic-corrected $PM_{2.5}$ concentration (Chew et al. 2016). The near-UV single scattering albedo from the Aura-OMI satellite was found to agree within ±0.03 with that of the SKYNET ground measurements (Hiren Jethva and Torres 2019). Aerosol

optical depth (AOD) from the OMI as well as the AERONET, was found to correlate well over burnt areas (H. Jethva and Torres 2011). Zeydan and Wang, (2019) used AOD data from the MODIS satellite and developed regression models to predict ground level concentrations of $PM_{2.5}$. Khoshsima et al. (2014) found that the AOD-PM_{10} correlation decreases with increasing relative humidity, while the AOD–PM_{10} correlation coefficient increases as wind speed increases.

Other studies have found that incorporating the FWI in fire emission models improves their ability to capture the variability and intensity of fire emissions (S. S. C. Wang et al. 2022). In adittion, it was found that when the FWI is integrated with fire radiative power observations the estimation of fire emissions is enhanced (Di Giuseppe et al. 2018). The present study aims to use the Canadian Fire Weather Index (FWI) which is metereologically-based to test its predictive power regarding the increses of fire-emitted aerosols. This is the first study using the highest values from a high resolution 1km AOD dataset that are also in close proximity to the Thermal Anomalies MODIS satelite product to effectively detect and isolate fire-emitted aerosols which are correlated with the FWI over the Greek domain.

4.2. Data and Methodology

4.2.1 MODIS Aerosol and Thermal Anomalies products

The satellite observed daily aerosol optical depth (AOD) and the thermal anomalies products from MODIS were used at a spatial resolution of 1km for the time period examined (2000-2018). Aerosol optical depth is a measure of aerosol abundances (e.g., urban haze, smoke, particles, desert dust, sea salt) distributed within a column of air from the Earth's surface to the top of the atmosphere. The AOD is a unitless property and it is equal to the negative natural logarithm of the light’s intensity at a specific wavelength after passing through the atmosphere over the same light’s intensity before entering the atmosphere. It is based on the principle that the suspended particles change the way that the atmosphere reflects and absorbs sunlight.

The thermal anomalies product from MODIS also has a 1km horizontal resolution and was used in combination with the AOD to more accurately detect fire-emitted aerosols for the same time period (2000-2018).

For a more accurate represantation of the likelihood of fire occurrence the FWI was calculated using reanalysis input data for the necessary weather variables such as noon values for temperature, relative humidity, wind speed and 24 hour precipitation.

4.2.2 Detection and isolation of fire emitted aerosols

One of the key challenges of determining the potential correlation between the FWI and the fire-emitted aerosols (i.e. AOD) was the accurate and reliable selection of the wildfire plumes. Selecting only the fire-influenced AOD values can be complicated. There are satellite products such as the OMI Absorptive AOD (AAOD) which isolates the optical thickness of absorbing-only aerosols, i.e. including mineral dust and black carbon (BC)or the Aerosol Index (AI), which is a qualitative index reflecting the presence of layers of aerosols with significant absorption. The main aerosol types that cause signals detected in the AI indeed include biomass burning, but also desert dust and volcanic ash plumes (Zhang and Liao 2016). These products were utilized initially as masks for fire-emitted aerosol. However, using these products lead to the selection of many days without actual fires but with equally high AOD values. It is clear from this result, that categorizing aerosol emissions cannot be done with absolute certainty using this simplistic method, as there can be sources producing highly absorptive aerosols other than wildfires, such as dust events.

A more robust and reliable way of selecting the AOD values from just the fire plumes is by first using the thermal anomalies product from MODIS to get a base selection of all days with potential fire occurrences. To limit the selection error of potential fire days, the MODIS AOD values higher than the daily 99^{th} percentile was used as a secondary step to filter out the additional days without actual fires that were previously selected by the thermal anomalies product. By using this method, the number of fire days gets reduced considerably, while increasing the accuracy of selecting actual fire days further.

4.2.3 Selection of the fire plume affected areas

After having a better selection of the potential fire days as described in Section 4.2.2, there can be still seen areas with high AOD values other than the ones affected by the smoke plumes. So, to restrict our selection to be as close as possible to the smoke plumes only, circular masks were generated with the center coordinates of the fire hotspots using the thermal anomalies product from MODIS and a radius equal to the length of the smoke plume corresponding to the 99^{th} percentile of the AOD values that has the closest proximity to the fire hotspot, as seen in Figure 4.1.

Figure 4.1 Isolation and selection of smoke plume affected areas based on the 99th percentile of the AOD values seen inside the red circles that are in close proximity to the thermal anomalies data representing wildfire centers marked with the green circles .

4.3. Results and discussion

4.3.1 Determining the optimal smoke plume selection methodology

One of the main objectives for this study was to accurately select the fire-emitted aerosols and the associated plume in an automated and accurate way. Initially, the correlation between the original AOD product from MODIS and the reanalysis FWI was performed and shown in Figure 4.2 subplot (a). Then the first selection stage of the potential fire days was performed by using the thermal anomalies product from MODIS. Using this product only, the days with detected hotspots from potential fires were selected and the AOD from all pixels from the entire domain within those time steps correlated with the corresponding FWI time steps in subplot (b), leading to stronger correlations between FWI and AOD. However, at this stage there are likely still selected days on which MODIS has falsely detected the presence of fires. This is why as a final stage, days with AOD values lower than the 99th percentile were removed from the previous selection. This resulted in a far stricter (and possibly more accurate) selection of fire-related AOD values, making the correlation with the corresponding FWI values even more well defined and stronger, as seen in subplot (c). Areas in subplot (c) with R greater than 0.8 inside the white rectangle correspond to the locations affected by the

catastrophic 2007 wildfires in the Peloponnese and Attica (Turquety et al. 2009). There are areas outside the white rectangle with equally high correlation that have high AOD values, likely due to dust, city air pollution or wind-driven transfer of fire-related aerosols from nearby burnt areas.

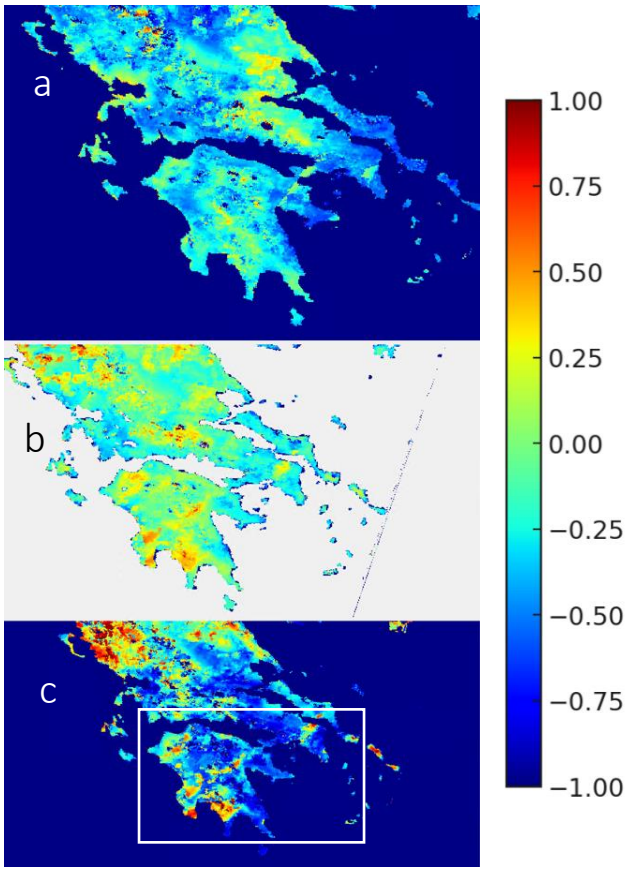

Figure 4.2. Temporal correlation between the different stages of fire related AOD isolation with the corresponding FWI. Subplot (a) is the original correlation between AOD (from MODIS) and FWI. Subplot (b) is the same correlation as subplot (a) but after selecting only the days with potential fire hotspots using the thermal anomalies product. Subplot (c) is the same correlation as subplot (b) but after further removing the days with AOD < 99th percentile of the entire domain of interest AOD values.

The methodology was expanded further to experiment with additional ways of filtering, in order to determine which one yields best results in selecting fire-related aerosols. Such methods included filtering the AOD results using the AAOD, the AI as well as the thermal anomalies. Figure 4.3 shows the correlation between FWI and AOD using the aforementioned methodologies. Subplot (a) is the correlation between AOD (from OMI) and FWI without any filters applied whereas subplot (b) is the correlation with the AOD (from MODIS) and FWI filtered using the Thermal Anomalies product. Subplot (c) is the correlation between the AOD (from OMI) and FWI filtered with the 95th percentile of the AI values whereas subplot (d) is the same concept as the subplots (c) but using the 95th percentile AAOD product (from OMI) instead of the AOD. This product already consists of the most absorptive aerosol values thus it doesn't need any additional filtering.

Comparing the results from the AOD correlations to the AAOD ones (subplots c and d) it can be seen they have a lot of similarities. The map in subplot (a), even though featuring lower R values, it also has similar pattern as the correlations in subplots (c) and (d), which means that by filtering the AOD results the pattern stays the same, but the correlation strengthens. The areas with high correlations are limited, whereas on the other hand in subplot (b) (using the thermal anomalies product from MODIS for filtering) they are more clearly defined and likely correspond better to the actual fire plume locations, especially the areas in the white rectangle thus this is the chosen filtering process. The highest correlation is observed for the areas in Peloponnese, Attica and Evia that experienced the catastrophic wildfires of 2007, with R values exceeding 0.8. For two representative areas with high R values in Peloponnese, the scatter plots (e and f) were created respectively by averaging the values inside the orange squares. Both these scatter plots show the clear positive correlation between FWI and AOD. Even though the areas with R>0.8 are limited, these also correspond to actual burnt areas, meaning that the FWI can potentially predict these specific high-aerosol events well.

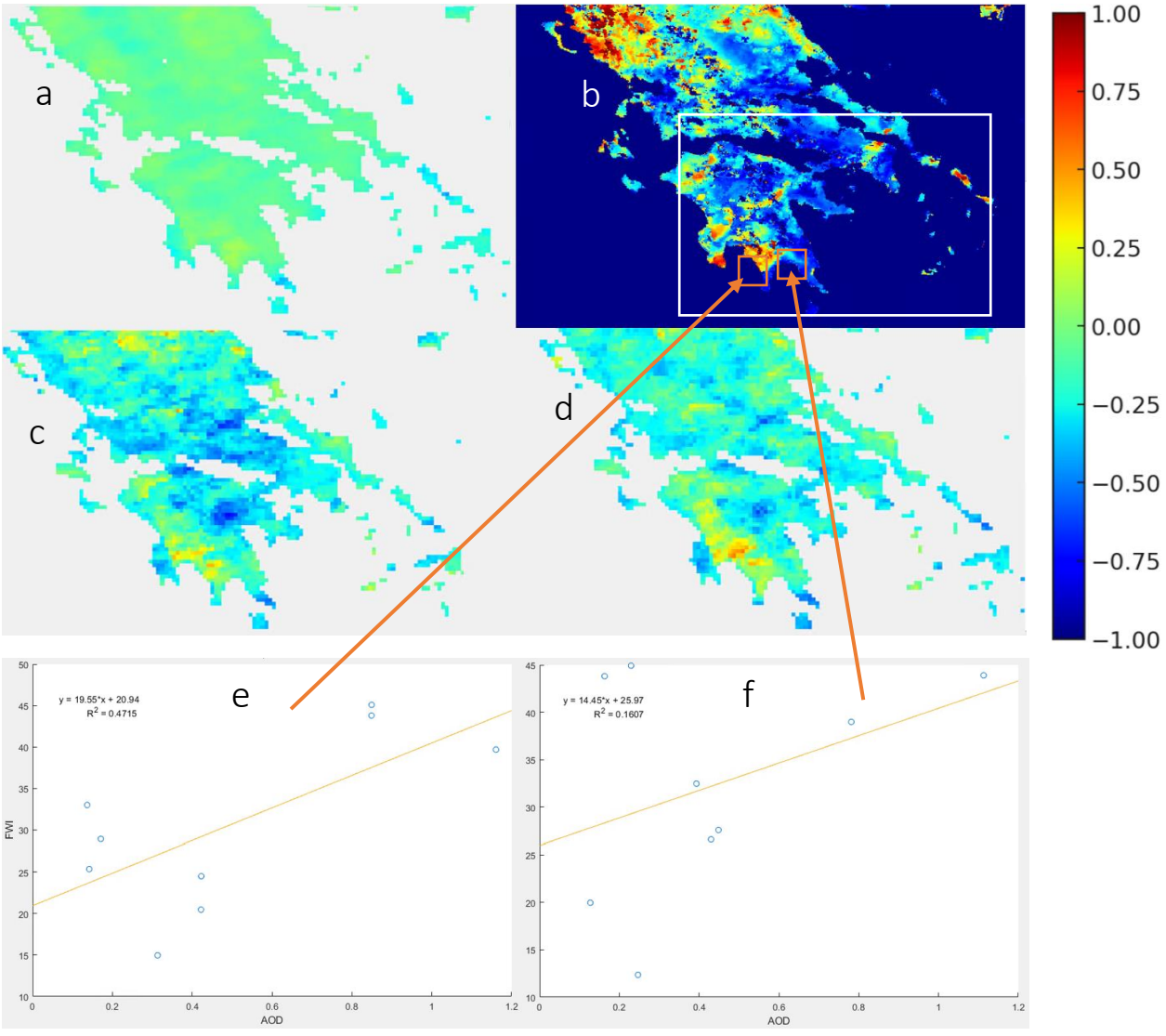

Figure 4.3. Correlations between different types of AOD products with the reanalysis FWI together with their trend lines (yellow lines). Subplot (a) is the correlation of the AOD from OMI with the FWI. Subplot (b) is the correlation between the AOD from MODIS and the FWI, filtered using the thermal anomalies product. Subplot (c) is the correlation between the MODIS AOD and FWI filtered with the 95th percentile of the AI values; whereas subplot (d) is the same concept as subplot (c) but using the 95th percentile of the AAOD instead of the AOD. Subplots (e and f) are scatterplots of two representative areas with high R values in Peloponnese and their respective trend lines.

4.3.2 AOD correlations with weather variables

Having found in Figure 4.3 that using the thermal anomalies product yields the best selection of fire-related AOD, that method was used in Figure 4.4 for to study further the correlations between AOD and the reanalysis weather variables that were used for the FWI calculation. This way the influence of weather and on aerosol concentrations and overall the aerosol-weather interactions can be better understood.

Subplot (a) is the correlation with relative humidity, which for the most areas without fires has a positive correlation with AOD. That is in line with the findings from other papers as aerosol's volume increases under the presence of humidity, which greatly affects the scattering of light (Zang *et al.*, 2019; Khoshsima *et al.*, 2014).

Subplot (b) showcases the correlation with precipitation. This plot mainly shows positive correlations with AOD except for the burnt areas as those did not receive any precipitation. However, that subplot is not conducive of the actual events as in reality there was not any precipitation events during the specific selected time steps. In addition, the areas showing signs of precipitation only appear to have received up to 5mm of rain which could be within the reanalysis margin of error and thus no concrete conclusions can be drawn.

Subplot (c) is the correlation with wind speed. Most of the burnt areas have negative correlation with AOD since this variable is responsible for particle transportation in the atmosphere leading to aerosol dilution reducing their concentration (Smirnov et al. 2003) (Khoshsima et al. 2014).

Subplot (d) is the correlation of temperature with the AOD. Even though temperature is the main driver of forest fires (M. D. Flannigan et al. 2016), it mostly has positive correlation with AOD for all areas. This is happening as all selected days are during summer season when Greece has consistently high temperatures.

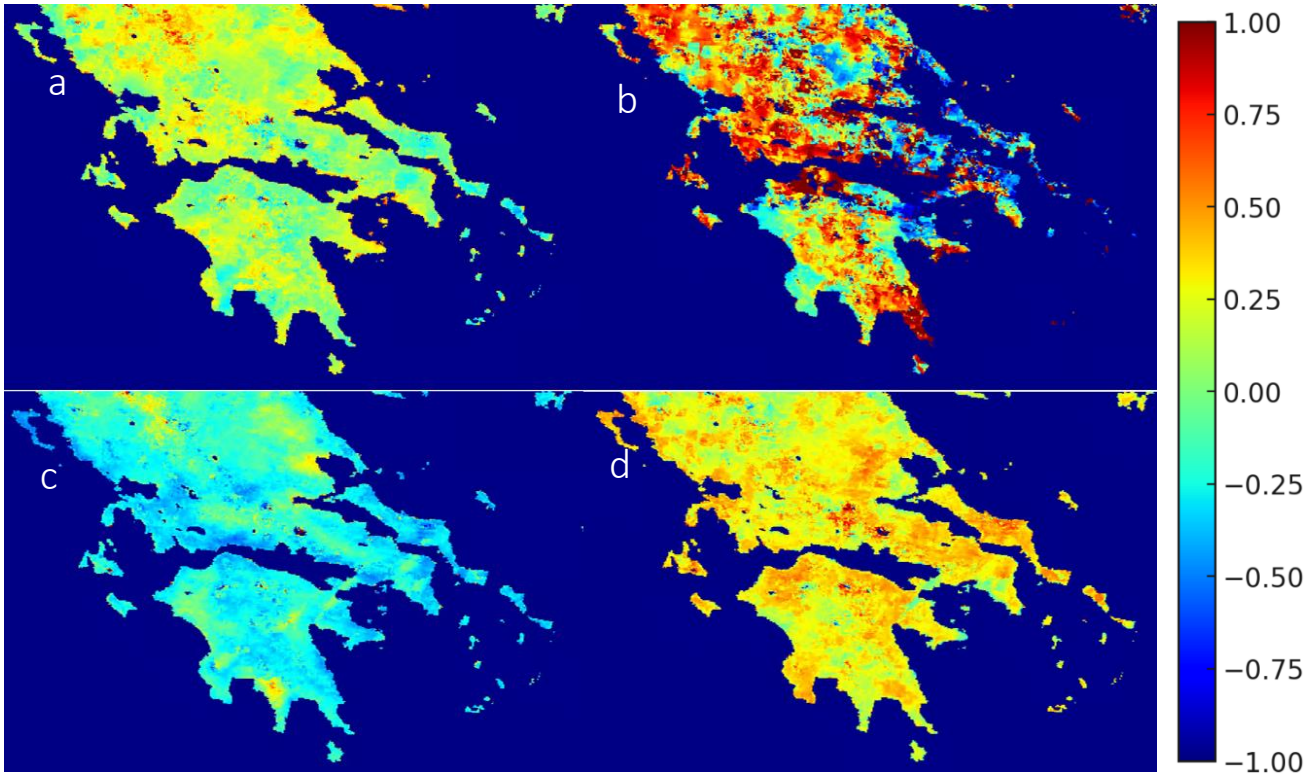

Figure 4.4. Correlations between AOD (from MODIS) and relative humidity in subplot (a), precipitation in subplot (b), wind speed in subplot (c) and temperature in subplot (d) filtered using the Thermal Anomalies product.

So far the analysis was focused on the entire domain of interest and was determined that there are areas where an AOD increase can be predicted by observing an increase in the FWI. However, even though the correct days with actual fire occurances were selected, it is aparent in Figure 4.2 subplot (c) that there are additional areas with high AOD values. That is why the areas affected by the fire plume only were selected using the methodology described in Section 4.2.3. Using only the areas with the white pixels inside the red circles as seen in Figure 4.1, the scatterplots of the AOD versus the FWI as well as the meteorological variables used for the FWI calculation were created and presented in Figure 4.5. In this figure, mainly the days of the catastrophic 2007 wildfires are shown with red circles as those were the only cloud free fire days since MODIS masks out cloud covered areas. These specific 2007 wildfires are of great importance as they represent the only 4-day event of consecutive wildfires in the period 2000-2018, with the fifth circle 27/08/2007 being the day that fires ended whilst leaving the atmosphere saturated with smoke.

Thus this 5-day event is a great case study as the wildfire aerosols gradually started emitting on 23/08/2007 and gradually faded on 27/08/2007. In subplot (a), the direct FWI and AOD correlation is even more clear, especially on the fifth day when wildfires ended, and both the FWI and the AOD decreased. That decrease can be explained by the weather variables on that day: the wind speed decreased (subplot (b)) limiting further wildfire spread; temperature dropped by 6 degrees (subplot (d)) and most importantly relative humidity increased from 20% to 45% (subplot (c)).

It is also interesting that all fire affected areas have an FWI value greater than 30 as seen in subplot (a). This specific value of FWI=30 was determined by Karali et al. (2014) for Greece as a general representative threshold for fire danger using forest service fire records. In this study we have proved the validity of their findings using a more general methodology that can be implemented for any country.

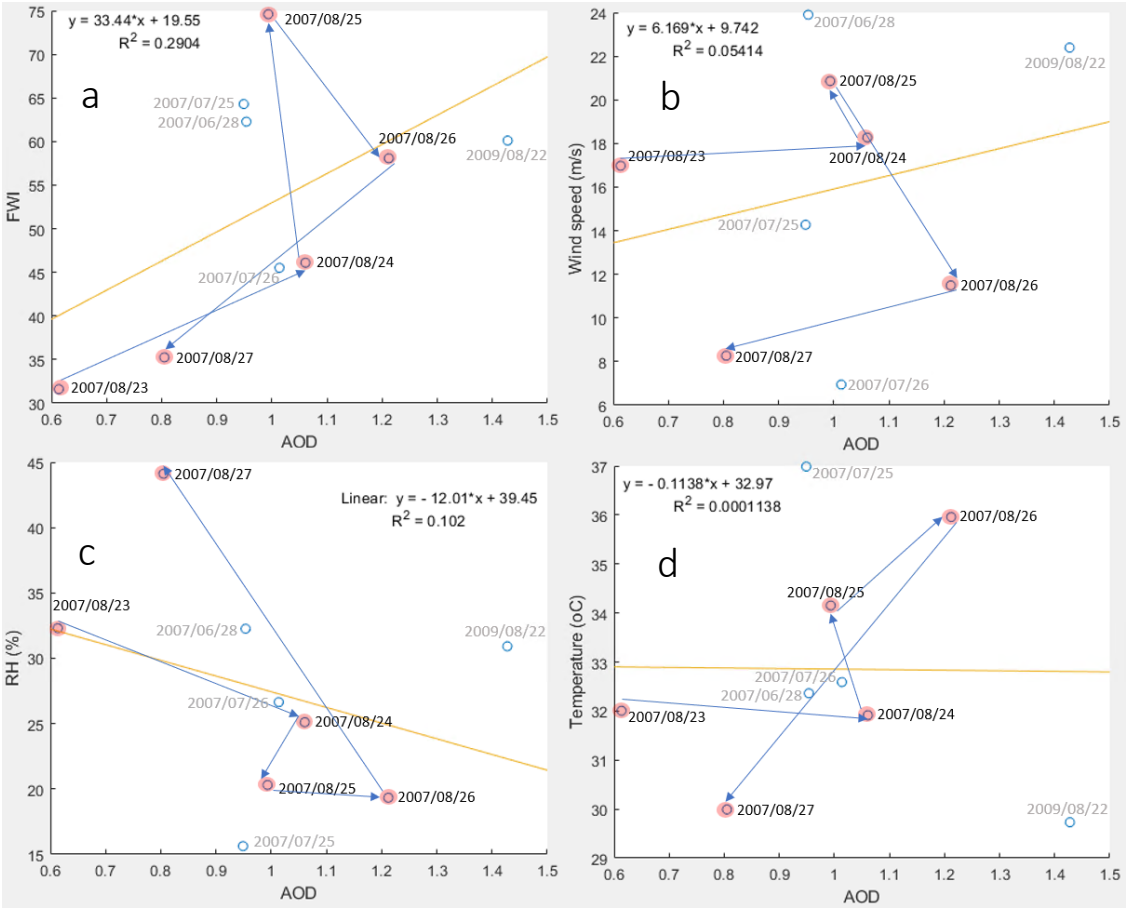

Figure 4.5. Average regressions between AOD from the areas affected by fire plumes directly and the corresponding FWI together with their trend lines (yellow lines) in subplot (a), wind speed in subplot (b), relative humidity in subplot (c) and temperature in subplot (d). Red dots represent the consecutive days with the 2007 catastrophic wildfires.

4.4 Conclusions

The present study evaluated different aerosol products from the OMI and MODIS satellites and made comparisons with the Canadian fire weather index as it was calculated from MERRA reanalysis weather variables. Moreover, correlations between the aforementioned products were conducted and compared, to find the most reliable wildfire smoke plume selection process. When the AOD product is filtered using the thermal anomalies product from MODIS, we achieved the most accurate selection of fire days and a stronger correlation with the FWI. Additional methodologies of filtering the AOD values were tested using the 95^{th} percentile of the AAOD or the AI values which yielded similar results, but not as strong or as accurate correlations.

Based on the correlation between AOD and FWI using the thermal anomalies method, a few key areas showcase a strong correlation. It was determined that only the areas with R>0.8 have a positive trend, so it can be concluded that the FWI has the ability to represent potential areas with fire activity accurately. The majority of those areas are in the Peloponnese which is known for high fire frequency especially during the summer months. Using the methodology for selecting just the AOD values from the fire plume, the direct correlation between FWI and AOD was clear and was also found that all fire affected areas had FWI>30 which represents the generally accepted national fire danger threshold.

Using the final selection with actual smoke plume from wildfire events and applying it to several meteorological variables as well as the FWI, it was found that the areas underneath the smoke plume were experiencing increasing FWI, temperatures and wind speed in conjunction with lower humidity as wildfires were increasing in size and intensity. All those parameters led to exacerbating wildfire events.

This study is subject to certain limitations. MODIS has a cloud mask. One major constraint is the presence of cloud cover, which can obscure satellite observations and lead to gaps in data. Additionally, small fires less than 0.1 km^2 that do not generate significant thermal anomalies or aerosol emissions and are smaller than the detection threshold of MODIS spatial resolution might not be detected, thereby underestimating the total number of fire events. These limitations suggest that while the current approach is effective, there is room for improvement through the integration of additional satellite products with higher sensitivity and the additional use of in-situ information from ground-based observations.

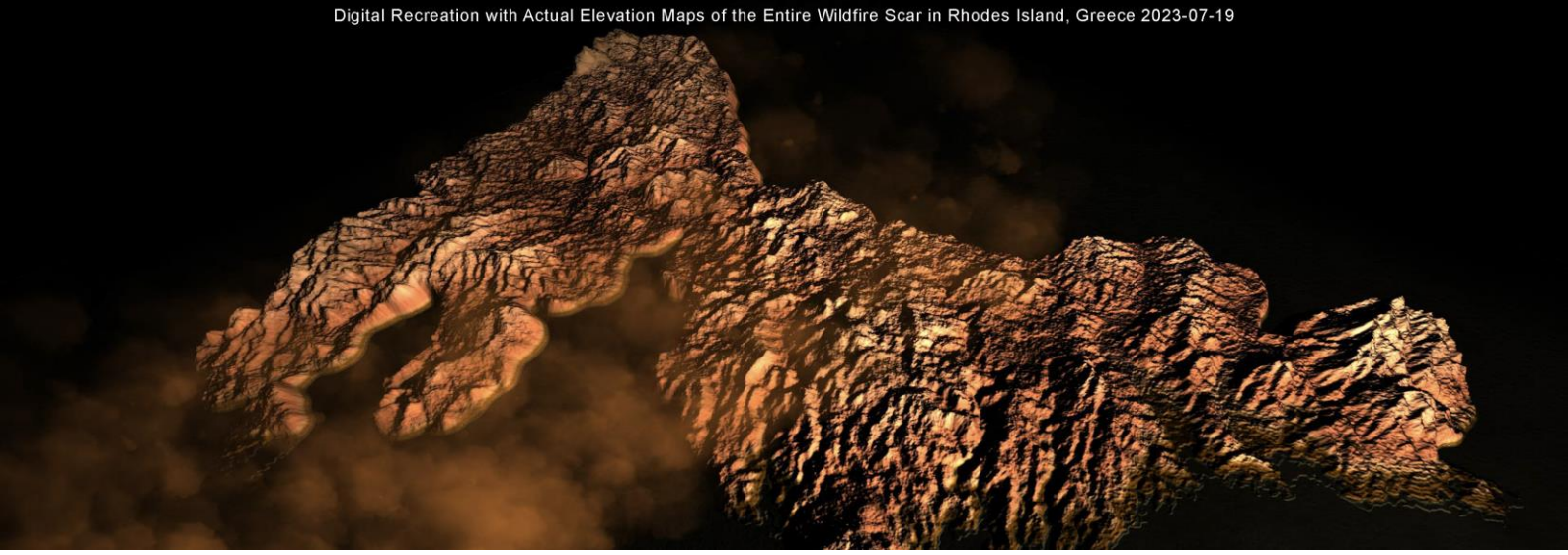

5. Estimating future burnt area changes over Greece using the JULES-INFERNO model

This chapter is based on a manuscript that has been submitted for publication

Abstract

Our previous studies (Chapter 2 and Rovithakis et al., 2022) have shown that climatic conditions in the Mediterranean and specifically over Greece are expected to change, resulting in an increase in fire season length which implies increases in burnt area. Our research presented in the current chapter employs the Joint UK Land Environment Simulator (JULES) to investigate the repercussions of climate change and future vegetation changes on future burnt area using UKESM1-0-LL gridded data from the ISIMIP3b model run. In the present study, the modelled burnt area is validated against satellite observations from Copernicus. We use three Shared Socioeconomic Pathways (SSPs) consisting of an optimistic emissions scenario where emissions peak and decline beyond 2020 (SSP126) a middle-of-the-road scenario (SSP370) and a pessimistic scenario, in terms of mitigation where emissions continue to rise throughout the century (SSP585). Our results show increased burnt area in the future compared to the present-day period in response to overall drier climatological conditions. When compared with the ISIMIP results with dynamic vegetation the overall burnt area was smaller. The biggest burnt area increases were found to be in south Greece particularly in Peloponnese due to higher future availability of heat resistant (unaffected by the drier future climatic conditions) needle leaf trees and the smallest decreases in the agricultural areas of northern Greece due to a reduction in the aforementioned tree category.

5.1 Introduction

For some ecosystems wildfires can have a positive impact serving as a catalyst for plant life regeneration (Littell et al. 2010). However, for the vulnerable ecosystems wildfires can have devastating effects (Andela et al. 2018). Furthermore, can cause negative consequences when it comes to the atmospheric environment (Voulgarakis and Field 2015), human health (Chuvieco et al. 2018) and the economy (Nielsen-Pincus, Moseley, and Gebert 2014). Future temperature projections between 2 - 5^{o}C (Zittis et al. 2019) in conjunction with decreasing precipitation trends have shown to increase future fire season length up to a month for some areas over Greece, a Mediterranean type environment (Rovithakis et al. 2022)Studying and understanding how the future burnt area might evolve is important for providing insight to the potential future effects of wildfires. Apart from the better known impacts on infrastructure, ecosystems, air quality and health, fires can also affect local temperatures due to radiation forcing resulting from their emissions (M. G. Tosca, D. J. Diner, M.J.Garay 2014; Tosca, Randerson, and Zender 2013; Jiang et al. 2020). Moreover, their ability to affect soil structure is making it more susceptible to runoff thus increasing the future likelihood of flash flooding and further infrastructure destruction (Neary et al. 2012; Langmann et al. 2009; Pfister, Wiedinmyer, and Emmons 2008). The Mediterranean basin and specifically Greece is one of the most sensitive to global warming regions, while at the same time being in the crossroads of many different atmospheric pollution types such as fine anthropogenic aerosols and ozone precursors from Europe, desert dust from North Africa and the Middle East, and maritime aerosols from the Mediterranean Sea and the Atlantic Ocean (Kalivitis et al. 2007).

When it comes to the potential future land surface changes, several models are projecting a forested area decrease in the tropics (Moritz et al. 2012). Over the Mediterranean region, landscape fragmentation is projected to increase thus resulting in a negative wildfire feedback (Riva et al. 2016). However, fire suppression tactics over the region cause unmanaged vegetation overgrowth and subsequently higher intensity future wildfires (Salis et al. 2022). In addition, this region is projected to have similar agricultural expanse due to improved technology balancing the effects of climate change (Eglin et al. 2010). The region's intensive agricultural activity will lead to an even more fire sensitive ecosystem and in these human influenced areas fire can increase the landscape's homogeneity thus increasing the extent of future burnt area (Loepfe et al. 2010).

Other studies on the effects of land use/land cover changes on wildfires on a global level found decreasing fire emissions in response to harvested land cover change and increases in response to future climate change (Kloster et al. 2012). In the United States, in regions where urbanized areas replace forests and grasslands, a future land use/land cover pattern leads to increased surface temperature and vapour pressure deficit, along with reduced precipitation compared to the current land use/land cover

pattern. Conversely, in regions where croplands replace forests, the opposite trend is observed. These alterations in local and regional atmospheric conditions result in extended fire season and more frequent and intense wildfires (Zhong *et al.*, 2021; Bryant and Westerling, 2014). Mediterranean type ecosystems, have experienced increased fire occurrence in response to changes in the agricultural/forest interface and urban/forest interface (Gallardo et al. 2016). This paper aims to investigate the implications of changing versus static land use on future burnt area trends in Greece. Through a combination of modelling techniques and data analysis, we aim to provide insights into the potential impacts of land use change on wildfire occurrence and extent.

5.2 Data and JULES model setup

For this study, the JULES-INFERNO model was utilized to perform future burnt area simulations with static vegetation to be compared with the equivalent JULES- INFERNO output with dynamically changing vegetation. The latter have recently been completed as part of the ISIMIP3b modelling experiment contributed by our collaborator Dr Chantelle Burton from UK MetOffice. Comparison of our fixed-vegetation simulations with the ISIMIP simulations, will isolate the role of climate-driven flammability changes from the role of climate-driven dynamic vegetation changes in driving future burned area changes in the area of Greece.

The Joint UK Land Environment Simulator (JULES) is an advanced land surface model (LSM) developed to simulate the dynamics of terrestrial hydrology, vegetation, carbon storage, and the surface exchange of water, energy, and carbon, as outlined by Clark et al. (2011). Moreover, JULES integrates the INteractive Fire and Emission algoRithm for Natural environments (INFERNO), which estimates fuel flammability based on a simplified fire count model influenced by monthly average temperature, relative humidity, and precipitation. This algorithm also considers human population density and lightning as sources of ignition. In INFERNO, upper soil moisture reflects the residual effects of past precipitation, which contrasts with immediate rainfall that acts as a quick fire suppressant. Here, traditional measures of vegetation density are replaced by a fuel load index reliant on leaf carbon and decomposable plant matter, or litter. INFERNO's ignition processes include variables for both anthropogenic and natural causes, specifically lightning, as detailed by Mangeon et al. (2016). Within JULES, the dynamic global vegetation model (DGVM) named TRIFFID (Top-down Representation of Interactive Foliage and Flora Including Dynamics) is integral for simulating the carbon cycle and the distribution of various plant functional types (PFTs) (Burton et al. 2019).

Here, the domain covers the entire globe, with a resolution of 0.5°. The simulations cover 3 10-year periods, i.e. a reference 1980-1990 and two future ones 2030-2040 and 2080-2090. For these simulations, the same ISIMIP3b JULES configuration was utilized (u-cc669 at vn6.2) in conjunction with the ISIMIP3b input and prescribed data at 0.5° but without the dynamic vegetation model TRIFFID in order to compare it with the existing ISIMIP3b simulations involving dynamic vegetation.

For model evaluation purposes, we performed two additional simulations (with and without dynamic vegetation) driven by weather variables generated from the ISIMIP3a modelling experiment based on observational datasets for the period 2004-2019. The simulated burnt area from these simulations was validated against GFED5 burnt area observations for the period 2004-2019. This period was chosen in order to be in line with Y. Chen et al. (2023), as they found data from this period to be more consistent since both MODIS Terra and Aqua data were available. GFED5 is the newest dataset which uses the Terra and Aqua combined monthly burned area product (MCD64A1) as the base for calculating the 2001–2020 burned area, in combination with the fine-resolution burned area images from Landsat or Sentinel-2 and MODIS active fire data (Chen et al. 2023).

Output files from JULES-INFERNO with dynamic vegetation include various classes representing distinct land cover types and vegetation functional types. For instance, variable 'evgndltr' denotes the total evergreen needle leaf trees along with the litter (fallen leaves and needles) associated with them. The class 'evgbdltr' indicates the evergreen broadleaf trees including their associated litter. 'C4grass' refers to grasses utilizing the C4 photosynthetic pathway, typically found in warmer climates and more efficient in photosynthesis under high temperatures and intense light than C3 grasses. Conversely, 'C3grass' represents grasses using the C3 photosynthetic pathway, which are more prevalent in cooler, wetter environments and less efficient under high temperatures and light conditions compared to C4 grasses. 'C4crop' signifies crops that follow the C4 photosynthetic pathway, resembling C4 grasses in their efficiency under high-temperature and light conditions. 'C3crop' pertains to crops employing the C3 photosynthetic pathway, common in cooler, wetter environments, and less efficient under high temperatures and light compared to C4 crops. 'Dcdndltr' represents the total deciduous needleleaf trees including litter associated with these trees. 'Dcdcldbdltr' representing the total deciduous broadleaf trees including litter associated with these trees and the 'total' representing the total vegetation, including all the different types of vegetation classes (Best *et al.*, 2011; Clark *et al.*, 2011; Mangeon *et al.*, 2016).

5.3 Results

5.3.1 Model performance

We first examined the performance of JULES-INFERNO simulation with static and dynamically changing vegetation in terms of simulating burnt area, against GFED5 observations for years 2004-2019. For this comparison, atmospheric forcings from actual observations (ISIMIP3a) were utilised as input data to calculate burnt area in the simulation with static vegetation, while readily available burnt area output from ISIMIP3a was obtained for the corresponding simulation with dynamically changing vegetation.

A limiting factor is that fire models (such as JULES-INFERNO) only rely on weather conditions and vegetation quantities to calculate burnt area, without any information on actual fire ignitions, a factor that is impossible to predict, due to its stochastic nature. This, in turn, makes it impossible to predict the extremely high 2007 actual burnt area seen Figure 5.1 panel (d) to its full extent.

Even though there is biases of the simulations when compared to the GFED5 observations, the former can still capture the general burnt area behaviour with an acceptable correlation for the majority of the areas in the Greek domain as seen in Figure 5.1 panels a and b. These two panels have remarkably similar correlation, with panel b representing the correlation with dynamically changing vegetation being slightly worse as seen in Figure 5.1 panel c which is the difference of dynamic minus static vegetation. That can be attributed to the additional degree of freedom in the dynamic vegetation simulation. The simulation with prescribed static vegetation uses observations to constrain the vegetation quantities, and since during the relatively short period of 2004-2019 the vegetation remains fairly steady, that simulation has slightly better correlation. The simulation with dynamic vegetation involves an additional uncertainty that leads to a departure from the true state, and the consequent bias.

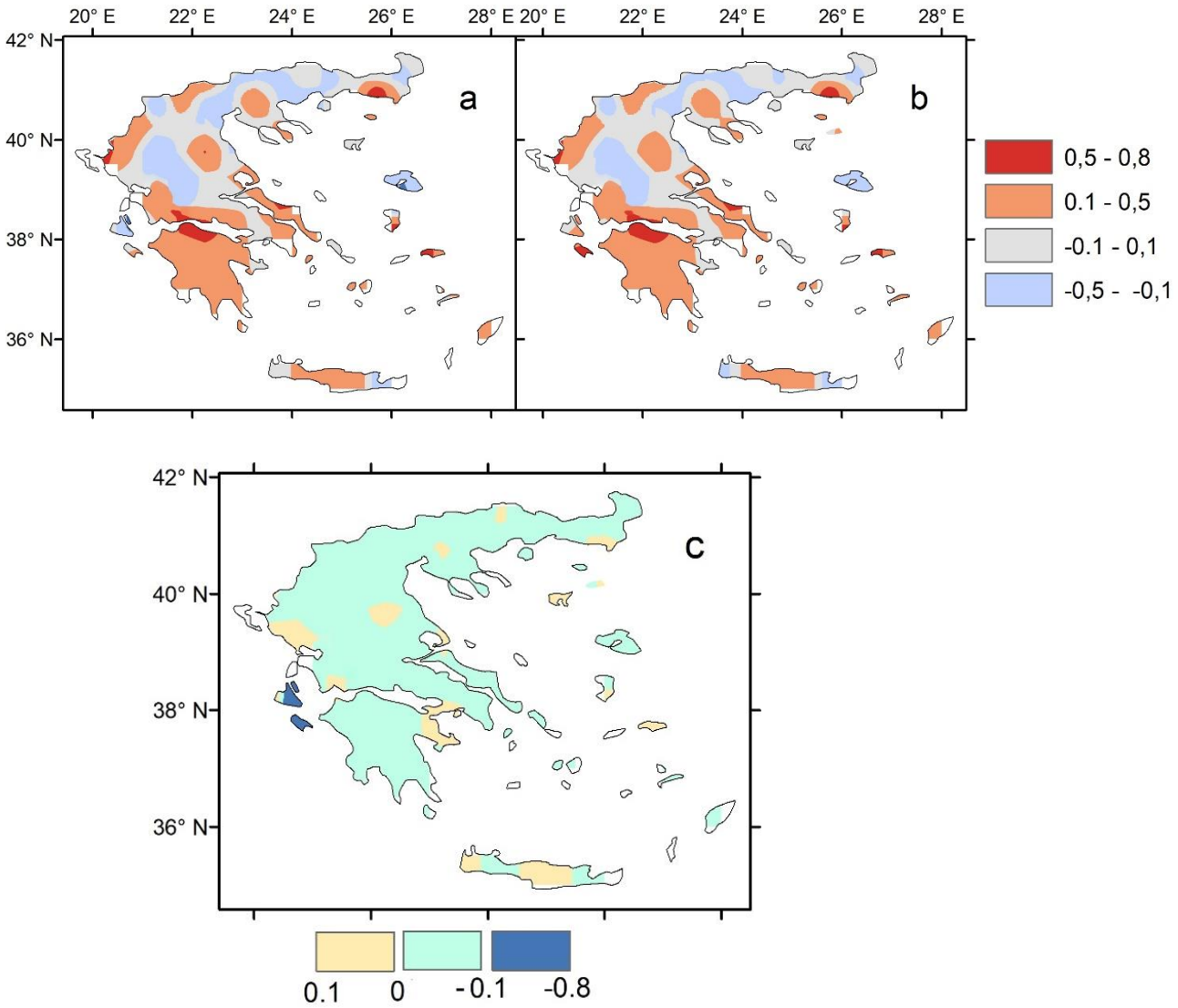
20° E
22° E
24° E
26° E
28° E
42° N
40° N
38° N
36° N
a
b
0,5 - 0,8
0.1 - 0,5
-0.1 - 0,1
-0,5 - -0,1
c
0.1
0
- 0.1
-0.8
d
GFED BA
BA inferno static
BA inferno dynamic
Total BA (km²)
2200
2000
1800
1600
1400
1200
1000
800
600
400
200
2005
2007
2009
2011
2013
2015
2017
2019

Figure 5.1. Panels (a) and (b) show the correlation between GFED5 and JULES-INFERNO Burnt Area, for the simulation with static vegetation cover and the one with dynamically changing, respectively for the period (2004-2019). Panel (c) shows the difference between the two correlations (panel (b) - (a)). Panel (d) shows comparison for all years for the domain-wide spatial average, between the GFED observations and the simulated Burnt Areas with static and dynamically changing vegetation cover.

To further assess the model's performance with static and dynamic vegetation, its output was compared with GFED burnt area observations, shown in Figure 5.2. The modelled annual mean burned area panel a1 shows significant burning in central and northern Greece. The GFED data panel a3 also indicate high burned areas in continental Greece but show a more pronounced hot spot in central Greece than the model. All of the winter and spring panels (b1-b3, c1-c3) for modelled and observed burned area show little burning activity across Greece in those seasons. The summer season shows the best agreement between modelled and GFED data (panels d1-d3) with the main burnt areas appearing in central and southern Greece. Both modelled panel e1 and GFED panel e3 data during the Autumn season show reduced burned areas compared to summer but still indicate notable activity in central Greece. September basically influences the entire Autumn season mean as this is the last month with burned areas.

For the panels f1-j3 of the figure 5.2, we show results for one by one the months of the fire season (May-September). May panels f1-f2 show minimal activity in both datasets, with slightly more pronounced burning in central Greece areas. Burnt area starts increasing in June panels g1-g2, with GFED data showing more substantial activity in central Greece. July panels h1-h2 show significant burnt areas in central and southern Greece, with the GFED data showing more widespread burning. August panels i1-i2 feature the peak burning activity of all months, particularly in central Greece, in both the observations and the model. During September, which is the final month with wildfire activity panels j1-j2, burnt areas are reduced in magnitude and exist mainly in continental Greece.

Overall, the most significant burned areas are consistently observed in central Greece. This pattern holds true across annual, seasonal, and monthly means. Northern Greece shows some activity, especially in autumn, which is also reflected in annual means. Southern Greece, including parts of the Peloponnese, also experiences notable burning, particularly during the summer months. The modelled BA consistently shows lower values than the areas with peak values in GFED5 data and higher values in other areas compared to the GFED observed burnt area. This discrepancy arises because the model estimates Burnt Area based on weather parameters such as temperature, humidity, precipitation, and wind speed, without accounting for specific ignitions which can lead to more uniform spatial distribution. The simulation with dynamic vegetation in all panels a2-e2 and f2-j2 shows even lower values than those with static vegetation. However, these lower values are even more concentrated in the areas mostly affected by fire. Despite the lower values, the model captures the overall spatial pattern of burnt areas, with central Greece being the most affected region. One key area where the model overestimates burnt area is Crete. Although Crete experiences high temperatures, it lacks substantial vegetation to sustain large wildfires, which the model does not account for, leading to this overestimation. This highlights the importance of

integrating more comprehensive data, including vegetation and fuel loads, to improve the accuracy of wildfire risk models since in panels d2, e2 and g2-j2 these areas are dramatically reduced.

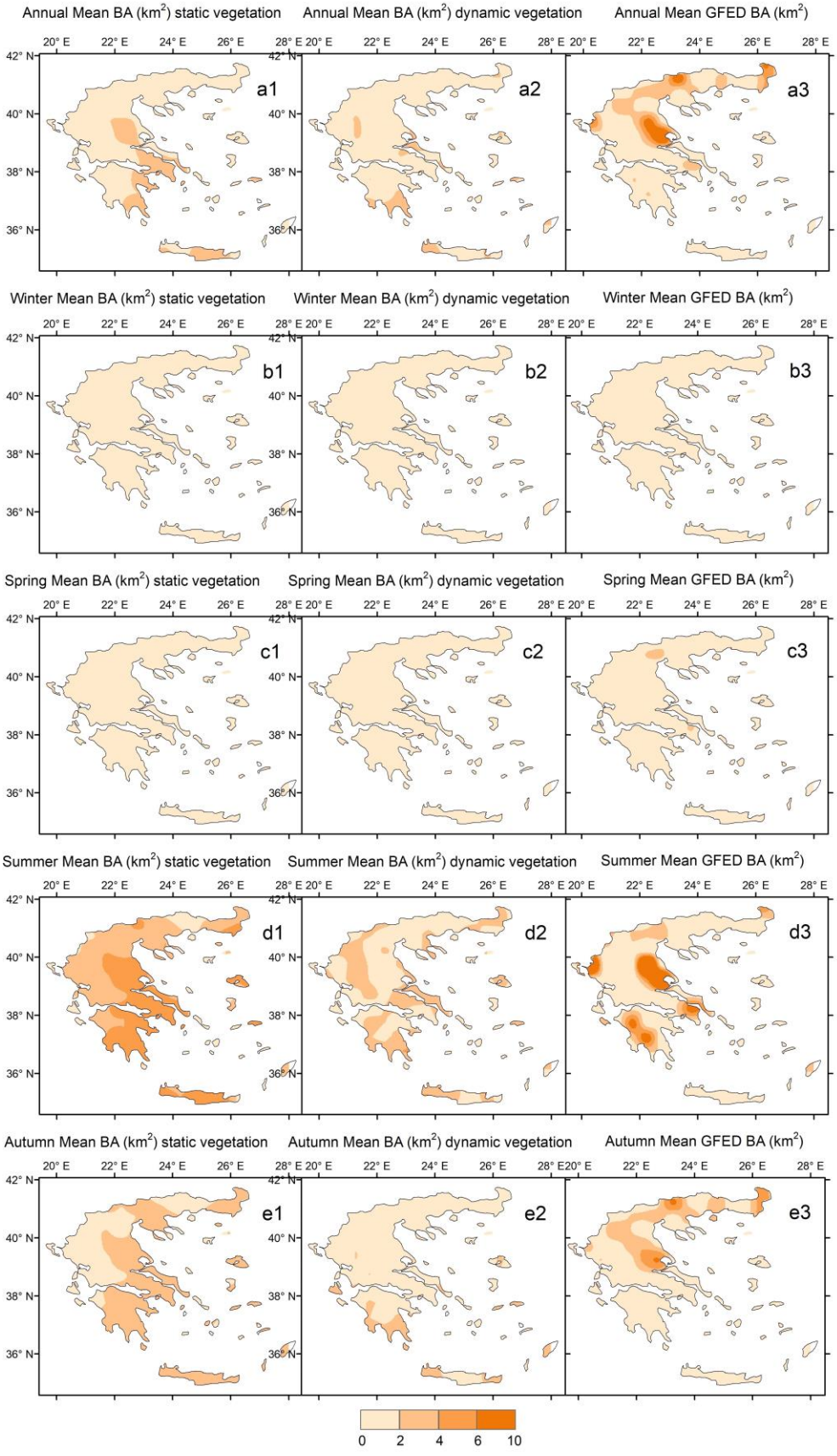

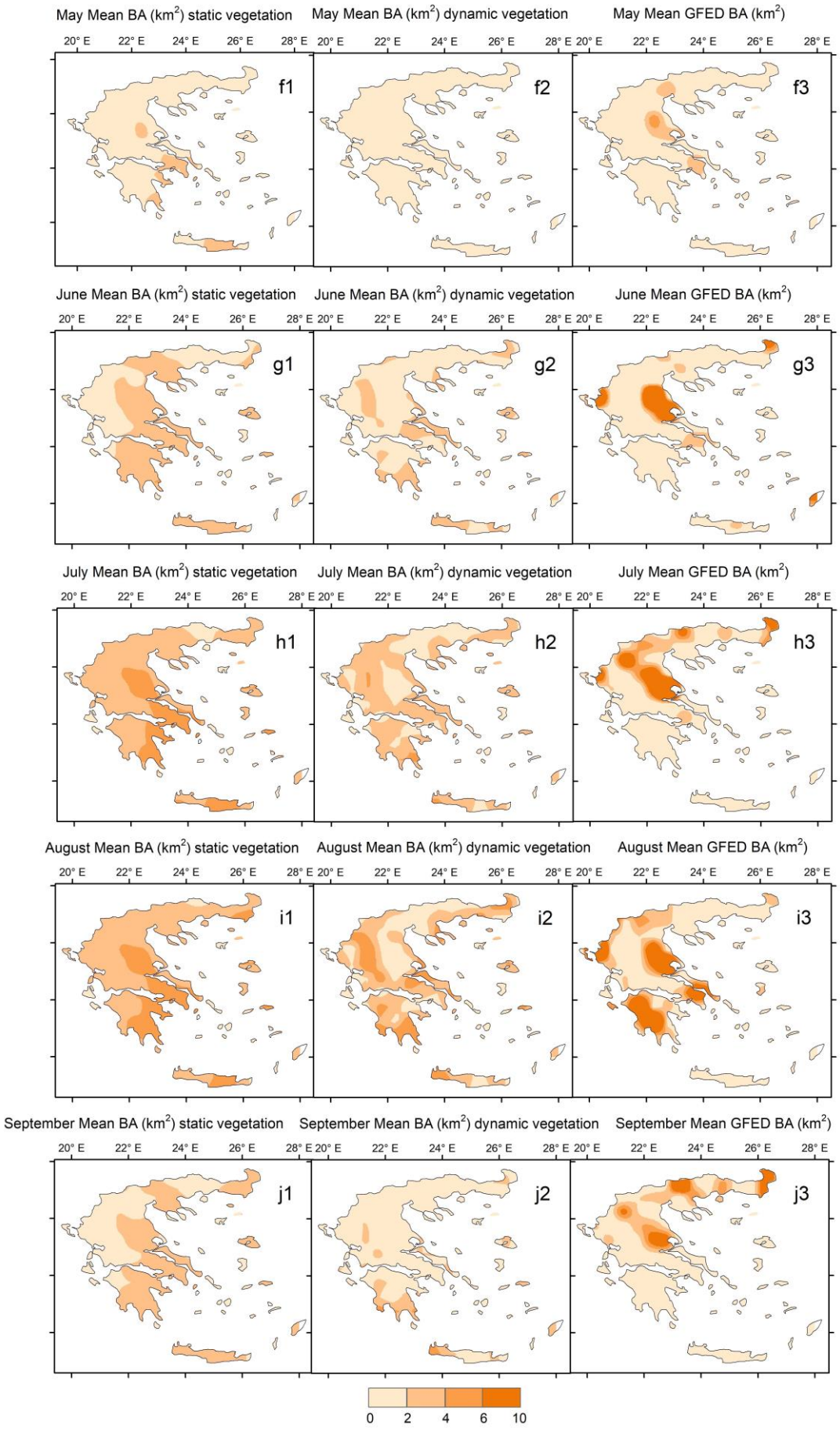
May Mean BA (km2) static vegetation
May Mean BA (km2) dynamic vegetation
May Mean GFED BA (km2)
June Mean BA (km2) static vegetation
June Mean BA (km2) dynamic vegetation
June Mean GFED BA (km2)
July Mean BA (km2) static vegetation
July Mean BA (km2) dynamic vegetation
July Mean GFED BA (km2)
August Mean BA (km2) static vegetation
August Mean BA (km2) dynamic vegetation
August Mean GFED BA (km2)
September Mean BA (km2) static vegetation
September Mean BA (km2) dynamic vegetation
September Mean GFED BA (km2)
20° E
22° E
24° E
26° E
28° E
f1
f2
f3
g1
g2
g3
h1
h2
h3
i1
i2
i3
j1
j2
j3
0
2
4
6
10

Figure 5.2. Spatial distribution of the mean burned area (BA) in Greece from 2004 to 2019. Each pair of panels compares the modelled BA with static vegetation (left) and the one with dynamic vegetation (middle) with the Global Fire Emissions Database (GFED) observed BA (right). Panels (a1-a3) Annual mean BA (b1-b3) Winter mean BA (c1c3) Spring mean BA (d1-d3) Summer mean BA (e1-e3) Autumn mean BA (f1-f3) May mean BA (g1-g3) June mean BA (h1-h3) July mean BA (i1-i3) August mean BA (j1-j3) September mean BA.

5.3.2 Future changes and climatic drivers

For the first experiment with static vegetation, the only factors that can influence burnt area are the climatological conditions. Future changes in these variables in the various scenarios are presented in Figures 5.3 and 5.4. Burnt area is projected to increase for all areas in Greece in the distant future when compared to the reference period for all future scenarios except for the optimistic SSP126, which projects a small decrease for some areas of up to 0.1 km^2. A similar pattern as that for the SSP126 distant future panel emerges for all SSP scenarios for the near future (panels a1-c1). Out of the panels (a1-c2) we see higher burnt area increases mainly in eastern continental Greece. Those increases get more pronounced in the distant future for SSP370 and SSP585 (b2-c2) reaching up to 2.5 km^2 additional burnt area compared to the reference period.

When it comes to the drivers of burnt area change, we see that temperature panels (d1-f2) do not follow the east west divide present in burnt area changes seen in the top panels of Fig. 5.3. Instead, it demonstrates a latitudinal gradient with higher temperature changes of up to 9^oC occurring in northern Greece, explaining the somewhat boosted increases of burnt area in that area.

The relatively minor distant future burnt area decreases in SSP126 (panel a2) can be explained by the domination of wetter conditions in the corresponding areas since this scenario is the most optimistic one resulting in more stable climate conditions similar to the reference period. These optimistic climatic conditions are expressed as more precipitation (panels g2 and j2, respectively).

However, overall, the changes in precipitation panels (j1-l2) are small and thus contribute less in burnt area changes. One example of that small contribution can be seen in panel l2 where under the most pessimistic scenario the northeastern edge of Greece is projected to experience more precipitation in addition to increases in burnt area seen in panel c2.

Soil moisture is an additional metric that is being influenced by various weather variables. Precipitation directly adds water to the soil, making it the most immediate and obvious factor affecting soil moisture levels. Temperature plays a crucial role as higher temperatures increase the rate of evaporation from the soil and transpiration from plants, both of which reduce soil moisture and increase vegetation flammability. Additionally, humidity levels, which are influenced by temperature and precipitation patterns, affect soil moisture through their impact on evaporation rates. All those effects from these weather parameters are reflected in panels (m1-o1) and (m2-p2) as northern and central Greece appears to have the biggest decrease in soil moisture as a response to drier weather conditions in those areas.

Greece being located in the southeastern Mediterranean region is expected to experience the effects of tropical expansion and consequent sub-tropical drying (Feng and Fu, 2013;Senande-Rivera, Insua-Costa and Miguez-Macho, 2022), explaining the aforementioned latitudinal gradient and drier future conditions favouring the overall burnt area increases. This expansion appears to have greater impact in northern Greece since those areas historically are not as adapted to drier conditions.

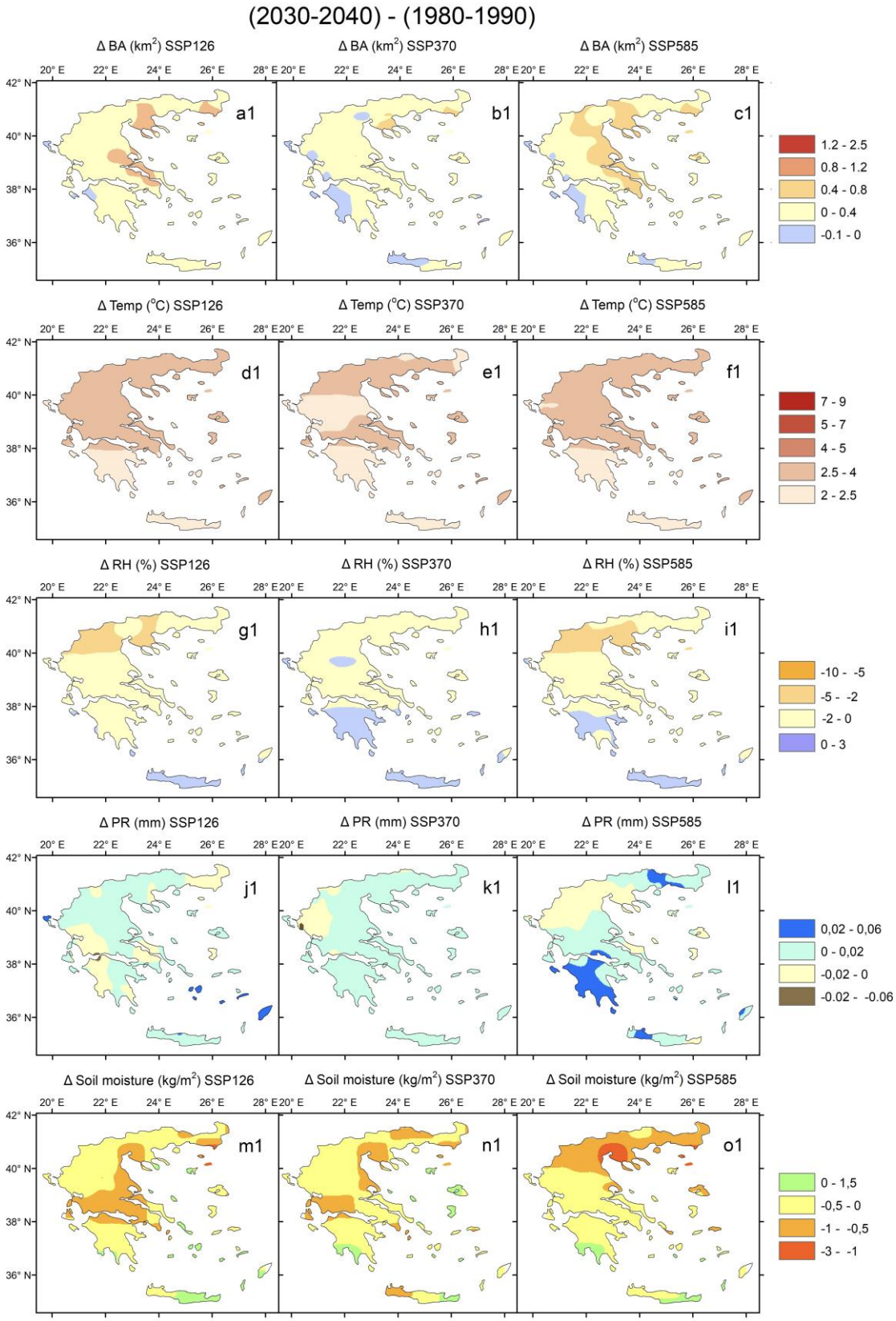

Figure 5.3. Burned area and climate variable changes for the three SSP scenarios between the near future and the reference period (panels a1-l1). Burnt Area differences 1st row. Temperature differences 2nd row. Relative humidity differences 3rd row. Precipitation differences 4th row. Soil moisture differences 5th row.

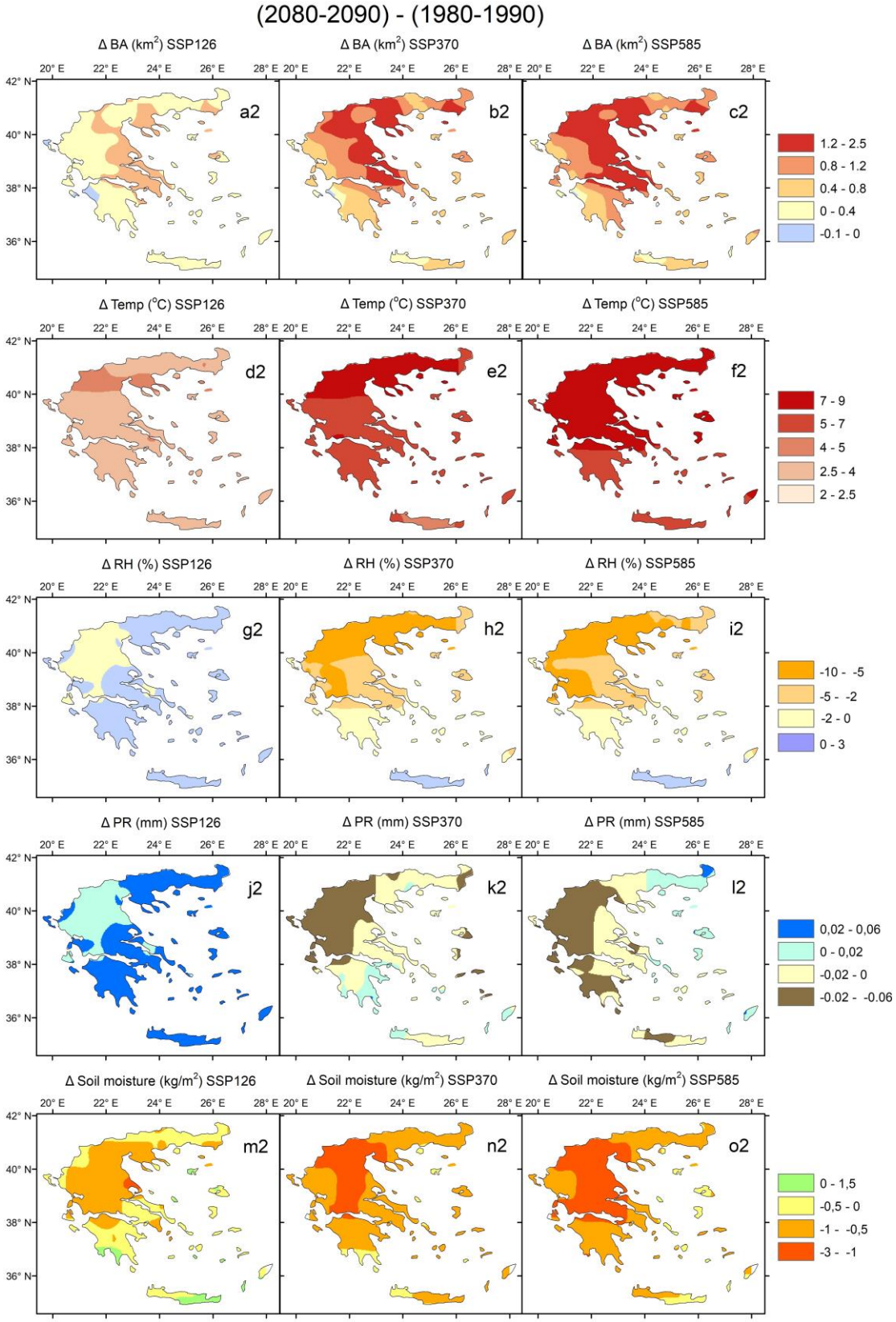

Figure 5.4. Burned area and climate variable changes for the three SSP scenarios between the near future and the reference period (panels a2-l2). Burnt Area differences 1st row.

Temperature differences 2nd row. Relative humidity differences 3rd row. Precipitation differences 4th row. Soil moisture differences 5th row.

5.3.3 Frequency of High Burnt Area events and Connection of Burnt Area and FWI

To better understand the evolution of different burnt area sizes, Figure 5.5 was made where it is evident that the majority of the burnt area changes in Greece fall in the 0-1 km² bin, across all scenarios and periods, suggesting that most areas will see little to no change in burnt area size.

Also, a substantial number of instances is represented by the small burnt area reduction bin (-1-0 km²). In that category, the number of instances is dominated by the SSP126 scenario as it suggests that mitigation efforts and lower emissions can lead to a reduction in the areas burnt by wildfires.

The number of instances with higher burnt area bins (1-2 km², 2-3 km² and 3-4 km²) in comparison to the reference period follow a similar pattern in the higher emission scenarios SSP585 and SSP370 for the late century (2080-2090). Especially concerning is the presence of around 1000 instances across Greece in the timespan of 10 years (2080-2090) with burnt area of 4 km² larger than in the reference period (1980-1990). This emphasizes the potential exacerbation of wildfire activity under high greenhouse gas emissions, which could lead to more extensive and possibly more destructive wildfires.

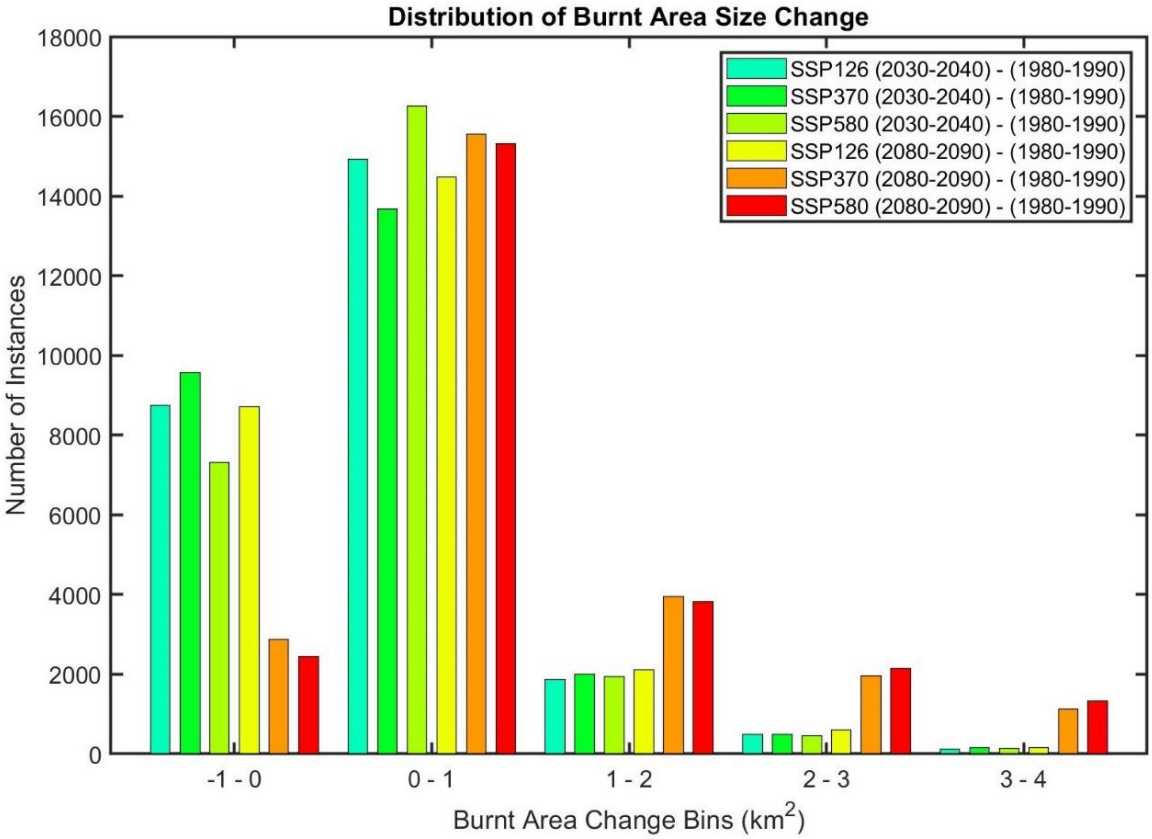

Figure 5.5. Distribution of Burnt Area size changes under different SSP Scenarios for future periods (2030-2040 and 2080-2090) compared to the reference period (1980-1990).

The distribution of the areas mostly affected by high burnt area events greater than 12 km² corresponding to the 99th percentile of all burnt area values during the reference period 1980-1990 can be seen in Figure 5.6. Panels a, b, and c show a clear pattern for the most affected areas to be in eastern continental Greece, with the most pessimistic SSP585 future scenario showcasing the highest extent of the areas, with up to 100 additional events with burnt area greater than 12 km² during the two future decades 2030-2040 and 2080-2090, compared to the reference period 1980-1990.

In the monthly burnt area frequency analysis, it can be observed that the number of high burnt area events in the period 2080-2090 (panel e) practically doubles compared to the period 2030-2040 (panel d). The highest frequency of those catastrophic events occurs in July (7th month) and August (8th month) across all scenarios. It is notable to mention that even though all emission scenarios in the period 2030-2040 do not predict any high burnt area events in May and September, this behaviour completely changes in the period 2080-2090 for all emission scenarios except the SSP126, with September having 20 more high burnt area events across Greece. May, on the other hand, does not demonstrate any change. That potential increase in catastrophic events towards the end of the fire season is in line with the findings from our previous paper (Rovithakis et al. 2022), where we showed that the fire season length is expected to increase by up to a month, with the future October being like the current September.

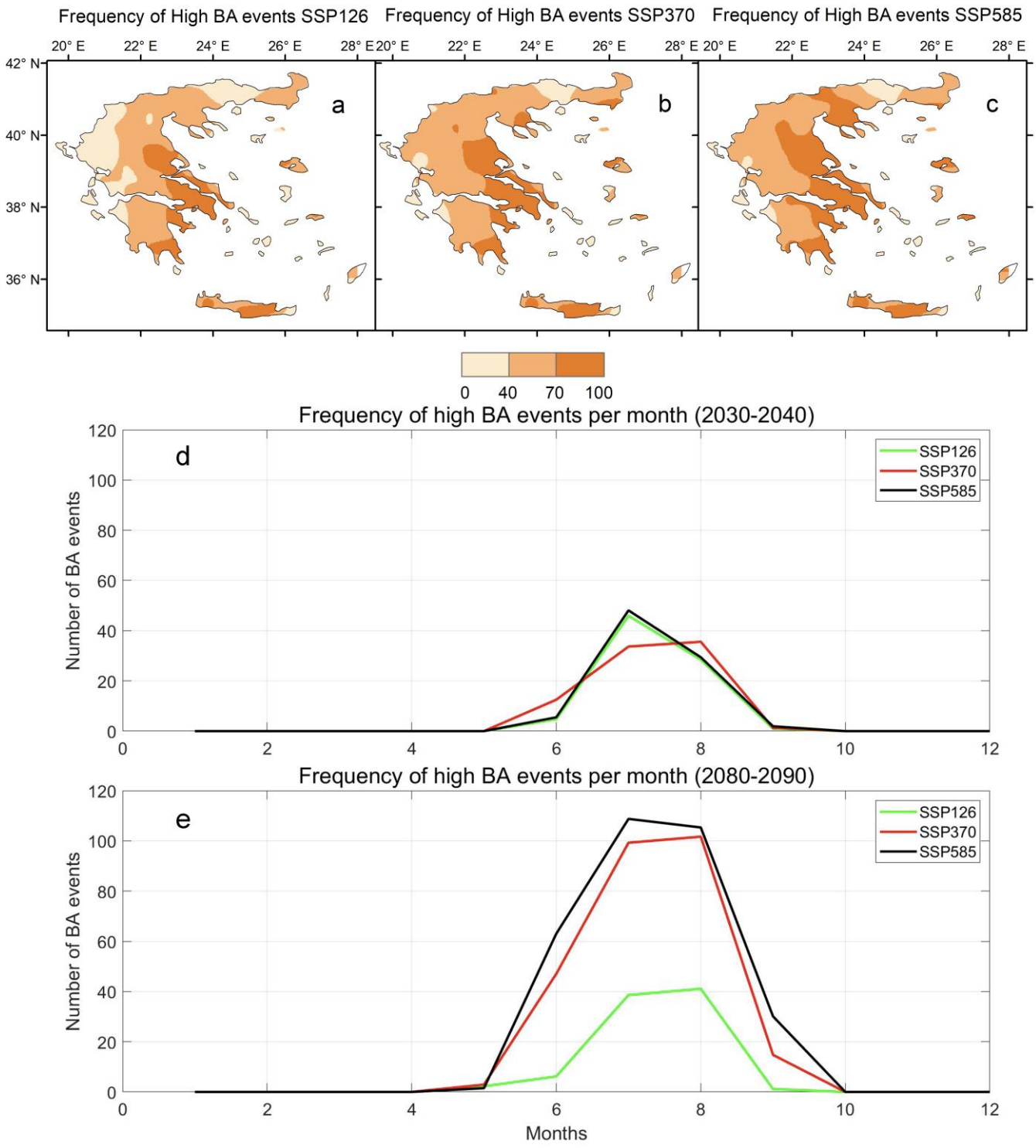

Figure 5.6. Frequency of high Burned Area (BA) Events greater than the 99th percentile of the historical period in Greece under Different SSP Scenarios. Panels a, b, and c show the spatial distribution of the frequency of high BA events for the periods 2030-2040 and 2080-2090 under SSP126, SSP370, and SSP585 scenarios, respectively. Panels (d) and (e) display the temporal distribution of the frequency of high BA events per month aggregated for all of Greece for the periods 2030-2040 and 2080-2090 respectively under the same SSP scenarios.

By temporally averaging the burnt area results for all SSP scenarios for the reference (1981-1990) and the 2 future periods (2031-2040) and (2081-2090), we compare them with the Canadian Fire Weather Index (FWI) results from our previous study (Rovithakis et al. 2022) for the equivalent time periods in Figure 5.7. A similar pattern is observed where the reference period has the lowest values, the SSP585 in the distant future the highest and the rest have similar values, demonstrating the FWI's good skill in terms of capturing burnt area tendencies as seen in Figure 5.7.

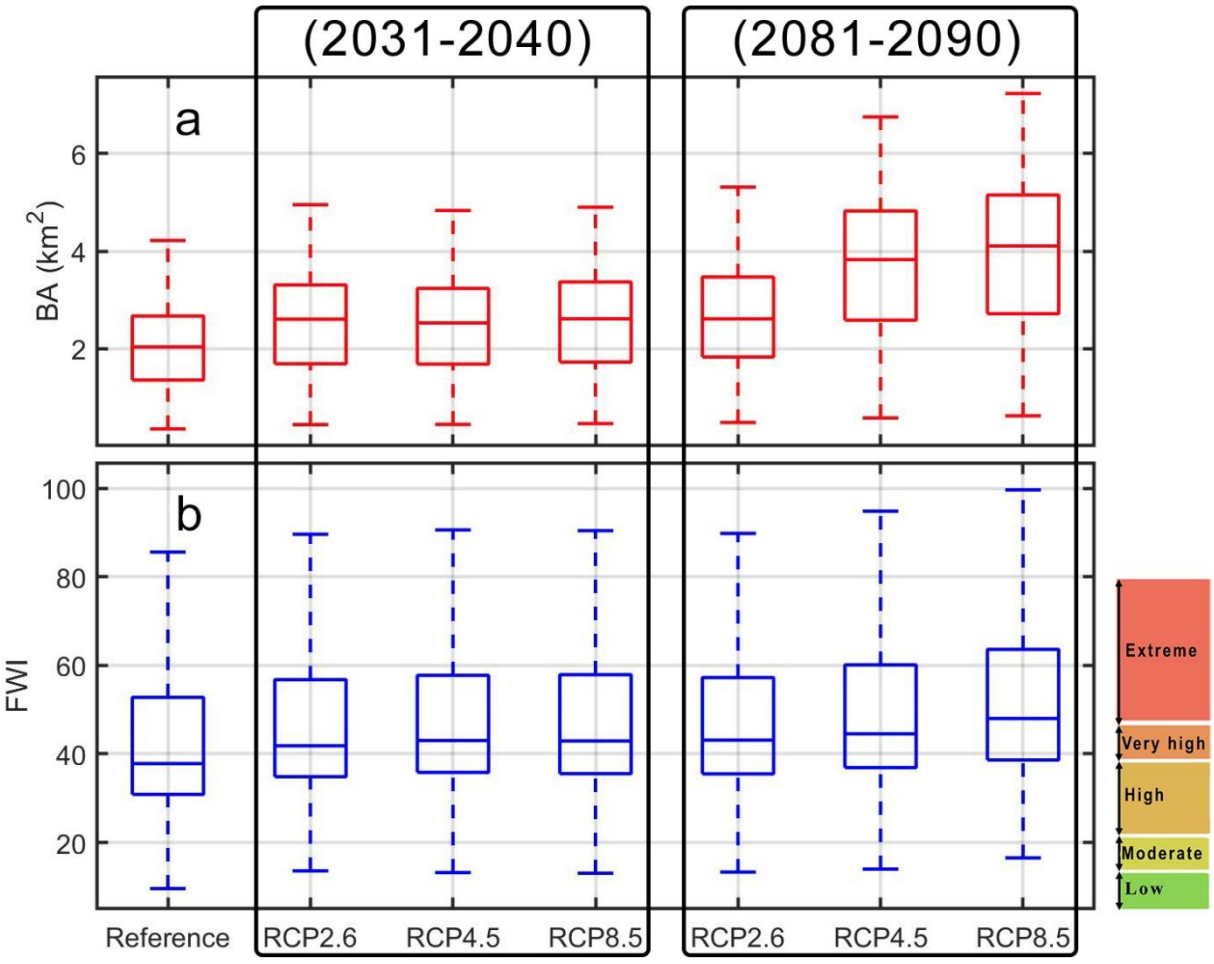

Figure 5.7. Boxplots showing the evolution of burnt area for the three SSP scenarios using JULES-INFERNO (panel a), compared to the FWI for the same time periods as calculated from our previous study (Rovithakis et al. 2022) (panel b).

5.3.4 The role of static vs dynamic vegetation on Burnt Area

As mentioned earlier, we also use simulations provided by Chantelle Burton from the MetOffice to see the effects of dynamic vegetation. Since those simulations start from 2015, we show the Burnt Area correlations with different weather variables for the fire season months for the two future periods 2081-2090 and 2031-2040 in Figure 5.8. Overall, it can be seen that higher temperatures and wind speeds, as well as lower

relative humidity and precipitation lead to increased future burnt area across Greece in both simulations with static and dynamic vegetation.

Specifically, northern Greece features similarly high positive correlations between temperature (panels a and b) and wind speed (panels c and d) with burned areas, and strong negative correlations with relative humidity (panels e and f) and precipitation (panels g and h) in both simulations. This suggests that hotter, windier, and drier conditions significantly contribute to larger burned areas in these regions.

Central Greece also follows a similar pattern, but with slightly reduced correlation strengths between all-weather variables except for relative humidity panel d when dynamic vegetation is considered. This indicates that vegetation changes can mitigate some of the impacts of weather parameters on burned areas.

Southern Greece, including the Peloponnese, features strong correlations of burnt area changes with relative humidity (panels e and f) and precipitation (panels g and h) changes, but slightly weaker compared with central Greece, and less so with wind speed (panels c and d). On the other hand, the correlation with temperature (panels a and b) is stronger than the equivalent in central Greece.

The weaker correlation between wind speed and burned area in the Peloponnese could be explained by the region's unique geographical conditions and morphology. The Peloponnese is characterized by mountainous terrain and fragmented landscapes, which can disrupt wind patterns and reduce the continuous spread of fires. Studies have shown that complex topography can lead to variable wind directions and speeds (Moritz et al. 2014; Keeley and Zedler 2009). This effect is particularly evident in regions with significant elevation changes and irregular landscapes, which are common in the Peloponnese.

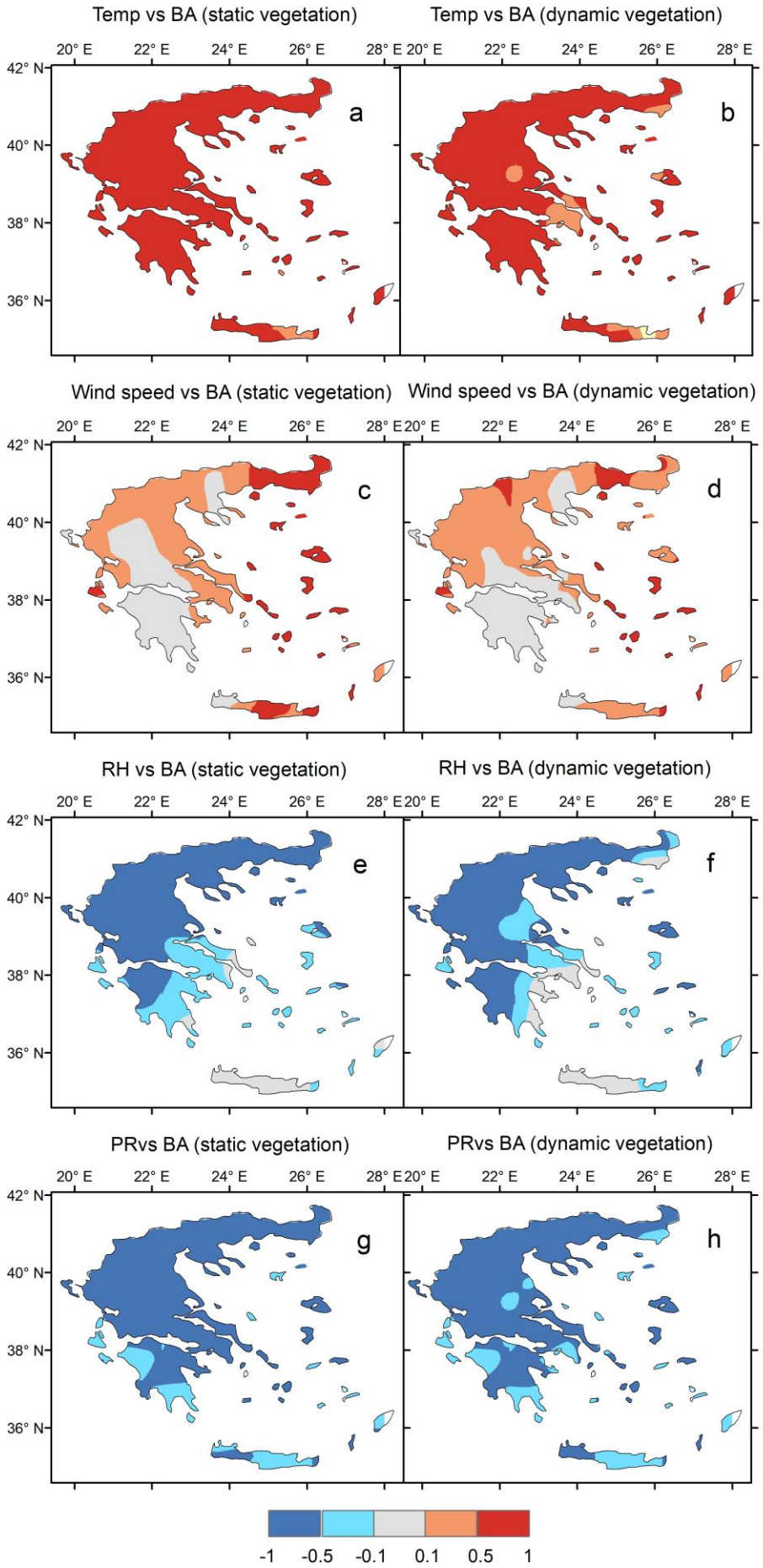
Temp vs BA (static vegetation)
Temp vs BA (dynamic vegetation)
Wind speed vs BA (static vegetation)
Wind speed vs BA (dynamic vegetation)
RH vs BA (static vegetation)
RH vs BA (dynamic vegetation)
PRvs BA (static vegetation)
PRvs BA (dynamic vegetation)
20° E
22° E
24° E
26° E
28° E
42° N
40° N
38° N
36° N
a
b
c
d
e
f
g
h
-1
-0.5
-0.1
0.1
0.5
1

Figure 5.8. Spatial correlations between burned area (BA) and various weather variables during fire season months across Greece. Panels show comparisons between the model using static (left column) and dynamic (right column) vegetation conditions in the JULES-INFERNO model. Panels a and b show the correlation between temperature and burnt area. Panel c and d show the correlation between wind speed and burnt area. Panel e and f show the correlation between relative humidity and burnt area. Panel g and h show the correlation between precipitation and burnt area.

Subsequently, we use the simulations with dynamic vegetation to examine burnt area change between the distant and the near future (2081-2090) – (2031-2040) in order to compare these results with those for the simulations with static vegetation (Figure 5.9). Comparing panels (a-c) with (d-f), two main things become apparent: the simulation with dynamic vegetation has somewhat smaller burnt area changes overall and the areas experiencing the highest burnt area in panels (b) and (c) due to the previously described climatological effects are experiencing less burnt area in the distant future compared to the near future as seen in panels (e) and (f). The overall difference between the simulations with static and dynamic vegetation in panels (g-i) does not change drastically from the panels (a-c) due to the smaller values of burnt area changes in panels (d-f). To explain the drastic difference in burnt area pattern between panels (b-c) and (h-i), these areas were grouped under the name NG (North Greece) spatially averaged and compared with the spatially averaged areas with similar pattern between these four panels grouped under the name SG (South Greece) as seen in panel (i), based on the carbon mass availability in different vegetation types seen in Figure 5.10 panels (j-o).

Figure 5.10 panels (j-o) consist of different types of grass and trees. The latter clearly have a longer periodicity than grass types since forests have a greater resilience to yearly weather fluctuations. In addition, the NG areas with the deep red colour coincide nicely with the biggest agricultural fields in Greece and thus these areas will experience a decreasing tendency in evergreen needleleaf trees (black line) as seen in panels (j-l). Other than this reduction, grass type of vegetation has the second highest carbon mass overall. On the other hand, SG areas not only show a small increasing tendency in the same type of evergreen needle leaf trees, which is a dry resistant vegetation category, but also have the second highest carbon mass stored in evergreen broad leaf trees (red line), showcasing an increasing tendency explaining the dynamic vegetation burnt area increases in SG areas in panels (e-f).

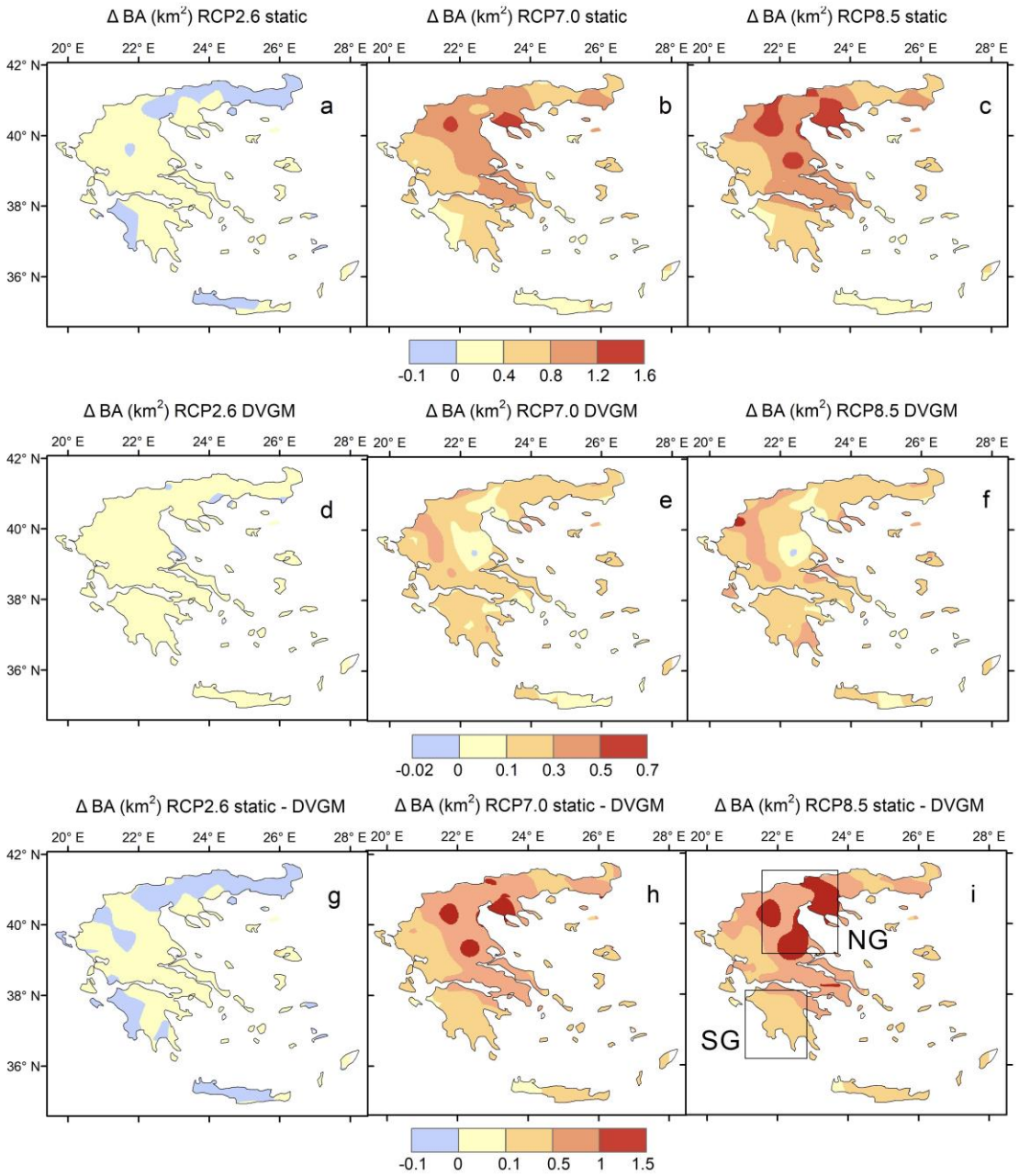

Figure 5.9. Burnt Area differences between distant future and near future from the simulation with static vegetation for the 3 SSP scenarios panels (a-c). Burnt Area differences between distant future and near future from the simulation with dynamic vegetation for the 3 SSP scenarios panels (d-f). Panels (g-i) show Burnt Area differences between the simulation with static and dynamic changing vegetation. We observe two areas (NG and SG) within the domain with the highest and lowest differences respectively in panel (i).

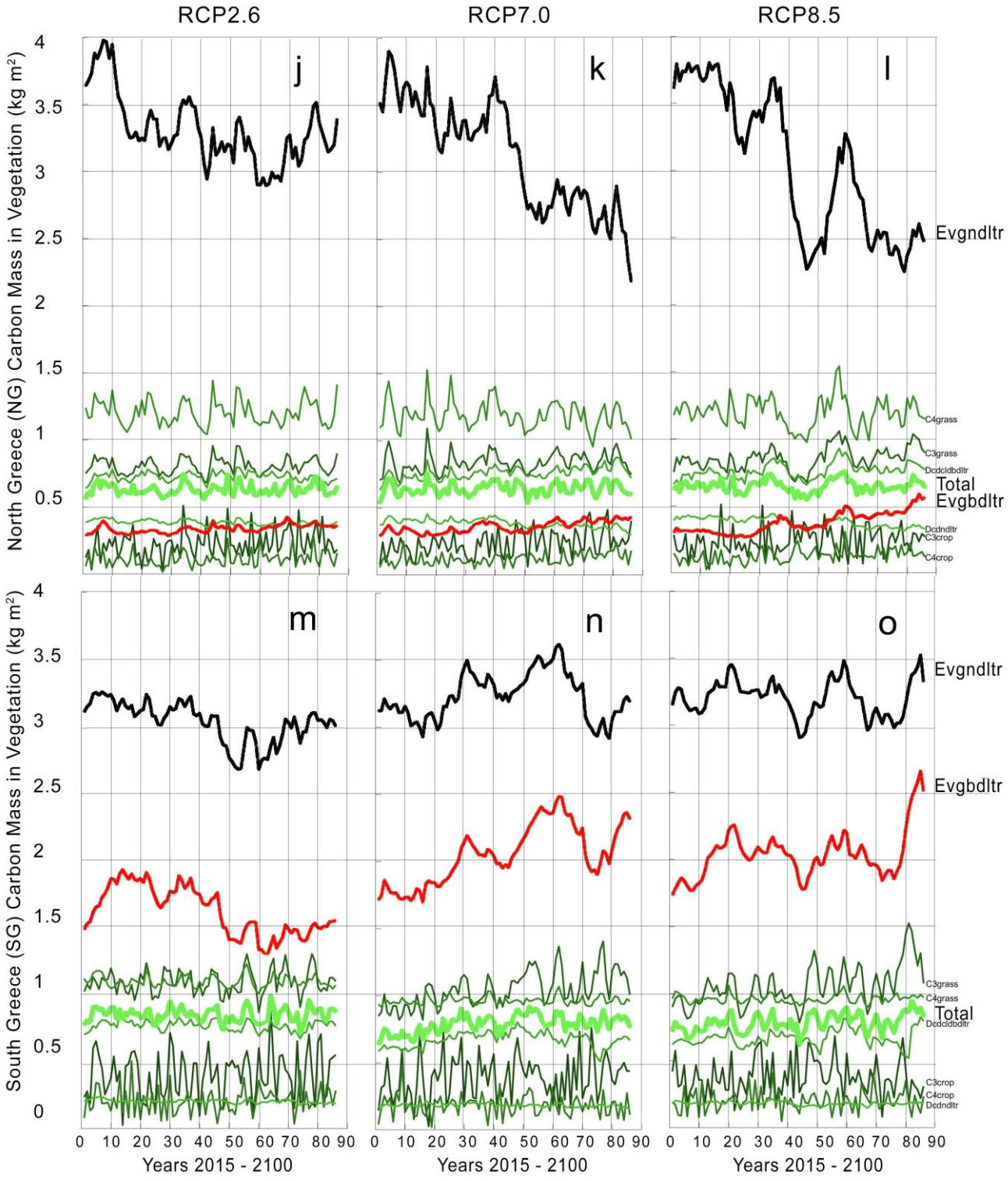

Figure 5.10. To explain the highest and lowest differences respectively in Figure 5.9 panel (i) for the areas NG and SG, panels (j-o) show comparisons of JULES variable 'carbon mass in vegetation' for the years 2015-2100 to see the entire variable's evolution and for the three SSP scenarios spatially, averaged for NG (top row) and for SG (bottom row).

5.4 Conclusions

The present study evaluated future burnt area changes with static vegetation as well as assessing the importance of dynamically changing vegetation . The model-simulated burnt area with static and dynamically changing vegetation was evaluated against GFED5 observations. It was found that overall, the two simulations can capture the general trend of the observed burnt area, even though years with anomalously high burnt area cannot be captured due to the lack of fire emission data in the simulations. In both simulations, the majority of correlation values were greater than 0.5, with slightly lower values for the dynamic vegetation simulation.

Future climate change plays a crucial role in shaping future wildfire activity. While a substantial portion of areas may remain stable in terms of burning, there is 1000 instances with 4 km² larger burnt area under high emission scenarios. This highlights the importance of climate mitigation efforts to reduce emissions and the associated impacts on wildfire regimes. Additionally, the areas experiencing the highest frequency of catastrophic wildfire events are distributed mainly in eastern continental Greece. Thus, these areas need even better fire management strategies and preparedness measures. Additionally, a shift towards more catastrophic Burnt Area events has been observed for the month of September.

It was found that higher temperatures and lower relative humidity consistently correlate with larger burned areas across Greece, with some regional variations. The impact of wind speed and precipitation also varies geographically, but generally it was seen that higher wind speeds and lower precipitation are associated with increased Burnt Areas, especially in the northern and central regions. The shift from static to dynamic vegetation seems to reduce the strength of these correlations slightly.

The simulation with static vegetation for the two future periods projected increases of average burnt area of 0.8 km^2 for the entire domain on average, with the highest values of up to 2.5 km^2 in the eastern continental Greece. That was only in response to drier climatological conditions in this region in the distant future, with temperature changes of up to 9 ^oC, up to 10% lower relative humidity, and slightly reduced precipitation. When burnt area is solely calculated on climatological conditions, it was found that the FWI index can reflect similar changes. On the other hand, allowing the vegetation to change dynamically led to a smaller overall distant future burnt area change of 0.3 km^2 on average for the entire domain since fire is no longer igniting in areas already burnt, as well as decreases of up to 0.02 km^2 for the main agricultural areas of Greece. Those burnt area decreases were due to the decreases of needleleaf trees, as those areas are categorized as agricultural land, which consequently led to less area available to be burnt in the distant future.

Our study is subject to certain limitations. The sources of uncertainties in GFED5 Burnt Area include instrument calibration errors. When compared to GFED5, whilst the two simulations manage to capture the overall trend, there is also a bias mainly due to the inevitable lack of realistic fire ignition data leading to a less accurate depiction of reality. We also note that to some extent the conclusions could be model-dependent, and therefore more studies of this kind are warranted in the future. Nevertheless, our study demonstrates the threat for increased burnt areas in the area of Greece in the future, as well as a clear potential influence of the vegetation changes in shaping the future trends in burning.

Data-code availability statement

The data that support the findings of this study are openly available at the following URL/DOI:

Input weather variables:
https://data.isimip.org/search/tree/ISIMIP3b/InputData/climate/atmosphere/ukesm1-0-ll/

GFED5 Burnt Area observations:

https://doi.org/10.5281/zenodo.7668423

The JULES code used in these experiments is freely available on the JULES trunk from version 4.8 (revision 6925) onwards. The rose suite used for these experiments is u-cc669 at vn6.2 (located in the repository at trac/rosesu/log/a/p/8/4/5 r69824). Both the suite and the JULES code are available on the JULES FCM repository: https://code.metoffice.gov.uk/trac/jules (registration required).

Acknowledgments

This research was funded by the Leverhulme Centre for Wildfires, Environment, and Society through the Leverhulme Trust (grant number RC-2018-023). We also acknowledge the help of Dr Matthew Kasoar from Imperial College London for helping with the initial model setup, Dr Eleanor Burke, and Dr Chantelle Burton from UK MetOffice for providing the Burnt Area simulations with dynamic vegetation.

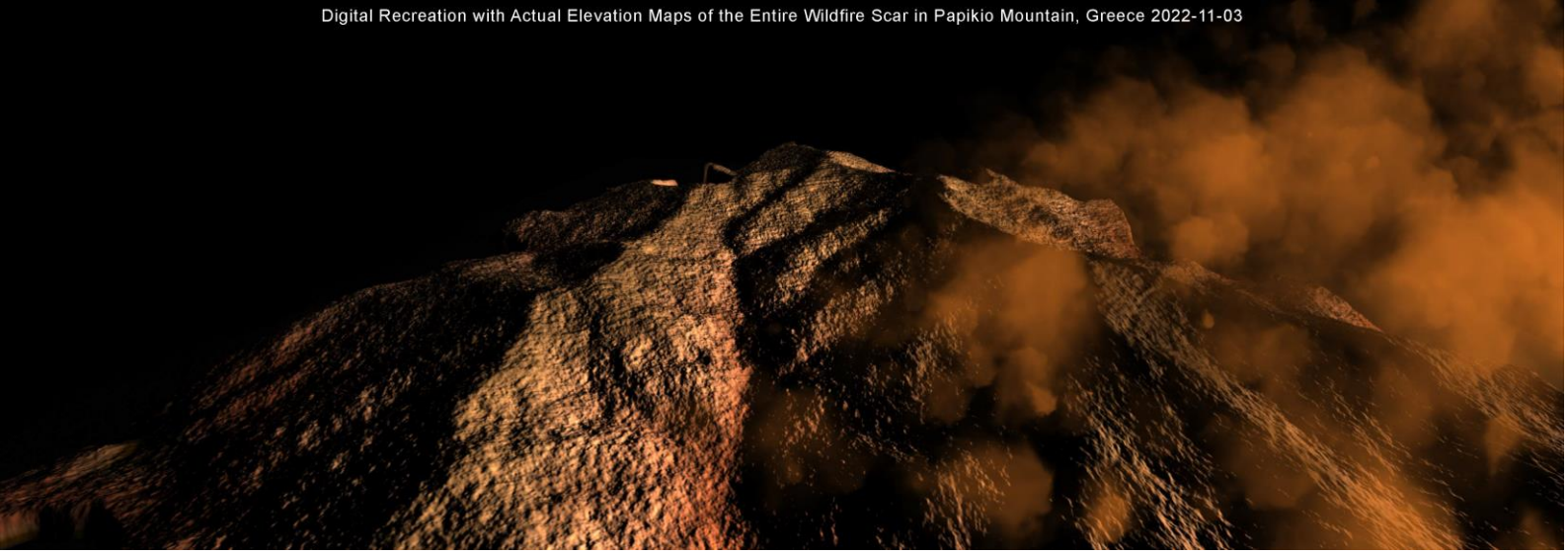

6. Conclusions

The four main scientific studies collectively provide a comprehensive understanding of the multifaceted challenges posed by climate change and wildfires in Mediterranean regions, with a specific focus on Greece. Each one contributes valuable insights into various aspects of wildfire dynamics, impacts, and management strategies.

The first paper, "Future Climate Change Impact on Wildfire Danger over the Mediterranean: The Case of Greece," highlights the significant increase in wildfire danger due to projected climate change scenarios. Using the Canadian Fire Weather Index (FWI) and regional climate models, the study reveals a stark future where Greece faces up to 40 additional days of critical fire danger annually by the late 21st century under the SSP585 scenario. This increase is not uniform across the country, with high-risk areas such as Crete, the Aegean Islands, Attica, and parts of the Peloponnese being particularly vulnerable. The extension of the fire season and the associated health impacts from particulate emissions underscore the urgent need for robust fire management and mitigation strategies. These findings stress the importance of regional adaptation plans tailored to local climatic and environmental conditions, in order to effectively address the heightened fire risks posed by climate change.

The second study, "Wildfire Aerosols and Their Impact on Weather: A Case Study of the August 2021 Fires in Greece Using the WRF-Chem Model," delves into the atmospheric effects of wildfire aerosols and their feedback on local weather conditions. The study's findings indicate that wildfire aerosols significantly alter atmospheric dynamics by reducing surface solar radiation, which lowers surface temperatures for the areas underneath the smoke plume. This research highlights the necessity of incorporating aerosol data into weather forecasting models to enhance the precision of weather predictions during wildfire events. Improved accuracy in forecasting can aid emergency response efforts and inform public health agencies, ultimately contributing to better preparedness and resilience against wildfire events.

The third study," Automatic smoke plume detection using satellites" assessed aerosol products from the MODIS and OMI satellites and contrasted them with the MERRA

reanalysis data-derived Canadian Fire Weather Index (FWI). The best fire day selection and greatest connection with FWI were obtained by filtering AOD using MODIS thermal anomalies; areas with a correlation coefficient (R) greater than 0.8, especially in the Peloponnese region, were shown to be at high risk of fire. Other filters produced good but marginally less accurate results, such as the 95th percentile of AAOD or AI. Elevated temperatures, wind speeds, reduced humidity, and rises in fire hazard (over 30, signifying extreme fire danger) were all noted under plumes of wildfire smoke.

The fourth research project, titled "Estimating future burnt area changes over Greece using the JULES-INFERNO model". By utilizing the Joint UK Land Environment Simulator (JULES), the study examines the effects of static versus dynamic vegetation in future Burnt Area. Overall, Burnt Area in the future is expected to increase due to a combination of drier climatological conditions as well as heat resistant native plant species except for the main agricultural areas in Greece, where burnt area is expected to decrease.

The insights gained from these studies collectively emphasize the complexity of wildfire management in the context of a changing climate. As climate change continues to alter weather patterns and increase fire risks, it is imperative to develop and implement comprehensive fire management strategies that are adaptive and region-specific. Policymakers must prioritize the integration of advanced climate and weather modelling tools, such as the FWI, WRF-Chem, and JULES, into fire management planning. These tools can provide critical predictions and guide effective interventions to mitigate wildfire risks.

Furthermore, we highlight the importance of a multi-faceted approach to wildfire management that includes both preventative measures, such as fuel reduction, and responsive measures, such as accurate weather forecasting and emergency response. Public awareness and community engagement are also essential components of effective wildfire management, as local populations play a crucial role in both prevention and response efforts.

7. Future Research

While these studies provide valuable insights, further research is essential to deepen our understanding and improve wildfire management strategies. Future research may focus on:

1. Long-term Climate Projections:

Enhancing the accuracy and granularity of climate models to better predict long-term fire danger trends in specific regions. This includes refining future emission scenarios and exploring additional pathways that reflect varying degrees of climate action and policy implementation. In addition there is a growing need for more and better tailored fire danger models since nowadays wildfires are occurring even in the northern latitudes claiming the lives of people and destroying infrastructure and venerable ecosystems which is why the research we are conducting at the Atmospheric Environment and Climate Change Lab at the Technical University of Crete is so important.

2. Aerosol-Climate Interactions:

Investigating the complex interactions between wildfire aerosols and climate, particularly their impact on regional and global climate systems. This includes studying the feedback loops between aerosols, cloud formation, and precipitation patterns over longer timeframes and diverse geographic areas.

3. Integrated Fire Management Systems:

Developing integrated fire management systems that combine advanced modelling tools, real-time data, and community-based monitoring. These systems should facilitate proactive fire risk assessment, early warning, and coordinated response efforts. The early detection and warning category is especially important in combating Wildfires. Current wildfire detection technologies, such as sensor networks, UAVs, and satellite surveillance, face several limitations including limited range, dependency on proximity to fires, and reduced effectiveness under dense smoke or cloud cover. However, by using a LiDAR system mounted on watch towers a non-fire atmospheric profile can be created, optimized for different weather conditions and times of day, enabling real-time fire detection. It also offers significant advantages, including automation, a large operational range of 1-20 km, and ease of integration with existing watchtowers. It can consistently perform regardless of human operation, time of day, or weather conditions. Once a fire is detected, UAVs can be deployed to accurately locate and track the fire front, enhancing overall fire management and response strategies. This project aims to improve the accuracy and efficiency of wildfire monitoring, helping to mitigate the adverse effects of wildfires.

By addressing these research areas, scientists and policymakers can enhance their ability to predict, prevent, and respond to wildfires, reducing the adverse impacts on ecosystems, human health, and economy. Continuous investment in research and innovation will be crucial to building resilient communities in the face of an increasingly volatile climate.

Bibliography

Abatzoglou, John T., A. Park Williams, and Renaud Barbero. 2019. "Global Emergence of Anthropogenic Climate Change in Fire Weather Indices." *Geophysical Research Letters* 46 (1): 326–36. https://doi.org/10.1029/2018GL080959.

Abatzoglou, John T., A. Park Williams, Luigi Boschetti, Maria Zubkova, and Crystal A. Kolden. 2018. "Global Patterns of Interannual Climate–Fire Relationships." *Global Change Biology* 24 (11): 5164–75. https://doi.org/10.1111/gcb.14405.

Adams, Joan Duncan. 2001. "Reinterpreting Evaluation Classics in the Modern Age." *Journal of Continuing Higher Education* 49 (2): 14–22. https://doi.org/10.1080/07377366.2001.10400427.

Akagi, S. K., R. J. Yokelson, C. Wiedinmyer, M. J. Alvarado, J. S. Reid, T. Karl, J. D. Crounse, and P. O. Wennberg. 2011. "Emission Factors for Open and Domestic Biomass Burning for Use in Atmospheric Models." *Atmospheric Chemistry and Physics* 11 (9): 4039–72. https://doi.org/10.5194/acp-11-4039-2011.

Alkhatib, Ahmad A.A. 2014. "A Review on Forest Fire Detection Techniques." *International Journal of Distributed Sensor Networks* 2014. https://doi.org/10.1155/2014/597368.

Amatulli, Giuseppe, Andrea Camia, and Jesús San-Miguel-Ayanz. 2013. "Estimating Future Burned Areas under Changing Climate in the EU-Mediterranean Countries." *Science of the Total Environment*. https://doi.org/10.1016/j.scitotenv.2013.02.014.

Amiridis, V., D. S. Balis, E. Giannakaki, A. Stohl, S. Kazadzis, M. E. Koukouli, and P. Zanis. 2009. "Optical Characteristics of Biomass Burning Aerosols over Southeastern Europe Determined from UV-Raman Lidar Measurements." *Atmospheric Chemistry and Physics* 9 (7): 2431–40. https://doi.org/10.5194/acp-9-2431-2009.

Andela, Niels, Douglas C. Morton, Louis Giglio, Ronan Paugam, Yang Chen, Stijn Hantson, Guido R. van der Werf, and James T. Randerson. 2018. "The Global Fire Atlas of Individual Fire Size, Duration, Speed, and Direction." *Earth System Science Data Discussions*, no. August 2018: 1–28. https://doi.org/10.5194/essd-2018-89.

Andreae, M O, and P Merlet. 2001a. "Emission of Trace Gases and Aerosols from Biomass Burning." *GLOBAL BIOGEOCHEMICAL CYCLES* 15 (4): 955–66.

Andreae, M O, and P Merlet. 2001a. "Emission of Trace Gases and Aerosols from Biomass Burning." GLOBAL BIOGEOCHEMICAL CYCLES 15 (4): 955–66.

Ayugi, Brian, Guirong Tan, Gnim Tchalim Gnitou, Moses Ojara, and Victor Ongoma. 2020. "Historical Evaluations and Simulations of Precipitation over East Africa from Rossby Centre Regional Climate Model." *Atmospheric Research* 232 (August 2019): 104705. https://doi.org/10.1016/j.atmosres.2019.104705.

Baker, Aaron D, and Stephen F Austin. 2021. "The Effect of Initial Conditions on the Weather Research and Forecasting Model The Effect of Initial Conditions on the

Weather Research and Forecasting Model."

Bar-Massada, Avi, Volker C. Radeloff, and Susan I. Stewart. 2014. "Biotic and Abiotic Effects of Human Settlements in the Wildland-Urban Interface." *BioScience* 64 (5): 429–37. https://doi.org/10.1093/biosci/biu039.

Barrett, K., A. D. McGuire, E. E. Hoy, and E. S. Kasischke. 2011. "Potential Shifts in Dominant Forest Cover in Interior Alaska Driven by Variations in Fire Severity." *Ecological Applications* 21 (7): 2380–96. https://doi.org/10.1890/10-0896.1.

Bartok, Blanka, Adrian Sorin Telcian, Christian Săcărea, Csaba Horvath, Adina Eliza Croitoru, and Vlad Stoian. 2021. "Regional Climate Models Validation for Agroclimatology in Romania." *Atmosphere* 12 (8). https://doi.org/10.3390/atmos12080978.

Bedia, J., S. Herrera, A. Camia, J. M. Moreno, and J. M. Gutiérrez. 2014. "Forest Fire Danger Projections in the Mediterranean Using ENSEMBLES Regional Climate Change Scenarios." *Climatic Change* 122 (1–2): 185–99. https://doi.org/10.1007/s10584-013-1005-z.

Bento-Gonçalves, António, António Vieira, Xavier Úbeda, and Deborah Martin. 2012. "Fire and Soils: Key Concepts and Recent Advances." *Geoderma* 191: 3–13. https://doi.org/10.1016/j.geoderma.2012.01.004.

Bessie, W. C., and E. A. Johnson. 1995. "The Relative Importance of Fuels and Weather on Fire Behavior in Subalpine Forests." *Ecology* 76 (3): 747–62. https://doi.org/10.2307/1939341.

Best, M. J., M. Pryor, D. B. Clark, G. G. Rooney, R .L. H. Essery, C. B. Ménard, J. M. Edwards, et al. 2011. "The Joint UK Land Environment Simulator (JULES), Model Description – Part 1: Energy and Water Fluxes." *Geoscientific Model Development* 4 (3): 677–99. https://doi.org/10.5194/gmd-4-677-2011.

Bistinas, I., S. P. Harrison, I. C. Prentice, and J. M.C. Pereira. 2014. "Causal Relationships versus Emergent Patterns in the Global Controls of Fire Frequency." *Biogeosciences* 11 (18): 5087–5101. https://doi.org/10.5194/bg-11-5087-2014.

Bond, T. C., S. J. Doherty, D. W. Fahey, P. M. Forster, T. Berntsen, B. J. Deangelo, M. G. Flanner, et al. 2013. "Bounding the Role of Black Carbon in the Climate System: A Scientific Assessment." *Journal of Geophysical Research Atmospheres* 118 (11): 5380–5552. https://doi.org/10.1002/jgrd.50171.

Bowman, David M.J.S., and Fay H. Johnston. 2005. "Wildfire Smoke, Fire Management, and Human Health." *EcoHealth* 2 (1): 76–80. https://doi.org/10.1007/s10393-004-0149-8.

Bradshaw, L, J Deeming, R Burgan, and J Cohen. 1984. *The 1978 National Fire-Danger Rating System: Technical Documentation*. Vol. 169. US Department of Agriculture, Forest Service, Intermountain Forest and Range ….

Bryant, Benjamin P., and Anthony L. Westerling. 2014. "Scenarios for Future Wildfire Risk in California: Links between Changing Demography, Land Use, Climate, and Wildfire." *Environmetrics* 25 (6): 454–71. https://doi.org/10.1002/env.2280.

Burton, Chantelle, Richard Betts, Manoel Cardoso, R. Ted Feldpausch, Anna Harper, Chris D. Jones, Douglas I. Kelley, Eddy Robertson, and Andy Wiltshire. 2019. "Representation of Fire, Land-Use Change and Vegetation Dynamics in the Joint UK Land Environment Simulator Vn4.9 (JULES)." *Geoscientific Model Development* 12 (1): 179–93. https://doi.org/10.5194/gmd-12-179-2019.

Buscarino, Arturo, Carlo Famoso, Luigi Fortuna, Mattia Frasca, and Maria Gabriella Xibilia. 2015. "Complexity in Forest Fires: From Simple Experiments to Nonlinear Networked Models." *Communications in Nonlinear Science and Numerical Simulation* 22 (1–3): 660–75. https://doi.org/10.1016/j.cnsns.2014.10.007.

Buxton, Michael, Rachel Haynes, David Mercer, and Andrew Butt. 2011. "Vulnerability to Bushfire Risk at Melbourne's Urban Fringe: The Failure of Regulatory Land Use Planning." *Geographical Research* 49 (1): 1–12. https://doi.org/10.1111/j.1745-5871.2010.00670.x.

Bytnerowicz, Andrzej, Dan Cayan, Philip Riggan, Susan Schilling, Philip Dawson, Mary Tyree, Lynn Wolden, Robert Tissell, and Haiganoush Preisler. 2010. "Analysis of the Effects of Combustion Emissions and Santa Ana Winds on Ambient Ozone during the October 2007 Southern California Wildfires." *Atmospheric Environment* 44 (5): 678–87. https://doi.org/10.1016/j.atmosenv.2009.11.014.

Calkin, David E., Jack D. Cohen, Mark A. Finney, and Matthew P. Thompson. 2014. "How Risk Management Can Prevent Future Wildfire Disasters in the Wildland-Urban Interface." *Proceedings of the National Academy of Sciences of the United States of America* 111 (2): 746–51. https://doi.org/10.1073/pnas.1315088111.

Carreiras, Manuela, Antonio José Dinis Ferreira, Sandra Valente, Luuk Fleskens, Óscar Gonzales-Pelayo, José Luis Rubio, Cathelijne R. Stoof, Celeste Oliveira A. Coelho, Carla Sofia Santos Ferreira, and Coen J. Ritsema. 2014. "Comparative Analysis of Policies to Deal with Wildfire Risk." *Land Degradation and Development* 25 (1): 92–103. https://doi.org/10.1002/ldr.2271.

Carvalho, A. C., A. Carvalho, H. Martins, C. Marques, A. Rocha, C. Borrego, D. X. Viegas, and A. I. Miranda. 2011. "Fire Weather Risk Assessment under Climate Change Using a Dynamical Downscaling Approach." *Environmental Modelling and Software*. https://doi.org/10.1016/j.envsoft.2011.03.012.

Chapin, F. Stuart, Amy L. Lovecraft, Erika S. Zavaleta, Joanna Nelson, Martin D. Robards, Gary P. Kofinas, Sarah F. Trainor, Garry D. Peterson, Henry P. Huntington, and Rosamond L. Naylor. 2006. "Policy Strategies to Address Sustainability of Alaskan Boreal Forests in Response to a Directionally Changing Climate." *Proceedings of the National Academy of Sciences of the United States of America* 103 (45): 16637–43. https://doi.org/10.1073/pnas.0606955103.

Chapin, F. Stuart, Sarah F. Trainor, Orville Huntington, Amy L. Lovecraft, Erika Zavaleta, David C. Natcher, A. David McGuire, et al. 2008. "Increasing Wildfire in Alaska's Boreal Forest: Pathways to Potential Solutions of a Wicked Problem." *BioScience* 58 (6): 531–40. https://doi.org/10.1641/B580609.

Chen, D., Z. Liu, C. S. Schwartz, J. D. Cetola, Y. Gu, and L. Xue. 2014. "The Impact of Aerosol Optical Depth Assimilation on Aerosol Forecasts and Radiative Effects

during a Wild Fire Event over the United States." *Geoscientific Model Development* 7 (6): 2709–15. https://doi.org/10.5194/gmd-7-2709-2014.

Chen, Yang, Joanne Hall, Dave Van Wees, Niels Andela, Stijn Hantson, Louis Giglio, Guido R. Van Der Werf, Douglas C. Morton, and James T. Randerson. 2023. "Multi-Decadal Trends and Variability in Burned Area from the Fifth Version of the Global Fire Emissions Database (GFED5)." *Earth System Science Data* 15 (11): 5227–59. https://doi.org/10.5194/essd-15-5227-2023.

Chew, Boon Ning, James R. Campbell, Edward J. Hyer, Santo V. Salinas, Jeffrey S. Reid, Ellsworth J. Welton, Brent N. Holben, and Soo Chin Liew. 2016. "Relationship between Aerosol Optical Depth and Particulate Matter over Singapore: Effects of Aerosol Vertical Distributions." *Aerosol and Air Quality Research* 16 (11): 2818–30. https://doi.org/10.4209/aaqr.2015.07.0457.

Chokkavarapu, Nagaveni, and Venkata Ravibabu Mandla. 2019. "Comparative Study of GCMs, RCMs, Downscaling and Hydrological Models: A Review toward Future Climate Change Impact Estimation." *SN Applied Sciences* 1 (12): 1–15. https://doi.org/10.1007/s42452-019-1764-x.

Chuvieco, Emilio, Louis Giglio, and Chris Justice. 2008. "Global Characterization of Fire Activity: Toward Defining Fire Regimes from Earth Observation Data." *Global Change Biology* 14 (7): 1488–1502. https://doi.org/10.1111/j.1365-2486.2008.01585.x.

Chuvieco, Emilio, Joshua Lizundia-Loiola, Maria Lucrecia Pettinari, Ruben Ramo, Marc Padilla, Kevin Tansey, Florent Mouillot, et al. 2018. "Generation and Analysis of a New Global Burned Area Product Based on MODIS 250 m Reflectance Bands and Thermal Anomalies." *Earth System Science Data* 10 (4): 2015–31. https://doi.org/10.5194/essd-10-2015-2018.

Clark, D. B., L. M. Mercado, S. Sitch, C. D. Jones, N. Gedney, M. J. Best, M. Pryor, et al. 2011. "The Joint UK Land Environment Simulator (JULES), Model Description – Part 2: Carbon Fluxes and Vegetation Dynamics." *Geoscientific Model Development* 4 (3): 701–22. https://doi.org/10.5194/gmd-4-701-2011.

Cohen, Aaron J., H. Ross Anderson, Bart Ostro, Kiran Dev Pandey, Michal Krzyzanowski, Nino Künzli, Kersten Gutschmidt, et al. 2005. "The Global Burden of Disease Due to Outdoor Air Pollution." *Journal of Toxicology and Environmental Health - Part A*. https://doi.org/10.1080/15287390590936166.

De, D. K., O. C. Olawole, E. S. Joel, U. I. Ikono, S. O. Oyedepo, O. F. Olawole, O. Obaseki, et al. 2019. "Twenty-First Century Technology of Combating Wildfire." *IOP Conference Series: Earth and Environmental Science* 331 (1). https://doi.org/10.1088/1755-1315/331/1/012015.

Diapouli, Evangelia, Athina Cerise Kalogridis, Christina Markantonaki, Stergios Vratolis, Prodromos Fetfatzis, Cristina Colombi, and Konstantinos Eleftheriadis. 2017. "Annual Variability of Black Carbon Concentrations Originating from Biomass and Fossil Fuel Combustion for the Suburban Aerosol in Athens, Greece." *Atmosphere* 8 (12). https://doi.org/10.3390/atmos8120234.

Dimitrakopoulos, A. P. 2002. “Mediterranean Fuel Models and Potential Fire Behaviour in Greece.” *International Journal of Wildland Fire* 11 (2): 127–30. https://doi.org/10.1071/WF02018.

Dimitrakopoulos, A. P., A. M. Bemmerzouk, and I. D. Mitsopoulos. 2011. “Evaluation of the Canadian Fire Weather Index System in an Eastern Mediterranean Environment.” *Meteorological Applications* 18 (1): 83–93. https://doi.org/10.1002/met.214.

Dowdy, Andrew J, Graham a Mills, Klara Finkele, and William De Groot. 2009. *Australian Fire Weather as Represented by the McArthur Forest Fire Danger Index and the Canadian Forest Fire Weather Index*. *Citeseer*. http://citeseerx.ist.psu.edu/viewdoc/download?doi=10.1.1.307.8282&rep=rep1&type=pdf.

Driscoll, Don A., David B. Lindenmayer, Andrew F. Bennett, Michael Bode, Ross A. Bradstock, Geoffrey J. Cary, Michael F. Clarke, et al. 2010. “Fire Management for Biodiversity Conservation: Key Research Questions and Our Capacity to Answer Them.” *Biological Conservation* 143 (9): 1928–39. https://doi.org/10.1016/j.biocon.2010.05.026.

Duncan, Bryan N., Yasuko Yoshida, Megan R. Damon, Anne R. Douglass, and Jacquelyn C. Witte. 2009. “Temperature Dependence of Factors Controlling Isoprene Emissions.” *Geophysical Research Letters*. https://doi.org/10.1029/2008GL037090.

Dupuy, Jean luc, Hélène Fargeon, Nicolas Martin-StPaul, François Pimont, Julien Ruffault, Mercedes Guijarro, Carmen Hernando, Javier Madrigal, and Paulo Fernandes. 2020. “Climate Change Impact on Future Wildfire Danger and Activity in Southern Europe: A Review.” *Annals of Forest Science*. Springer. https://doi.org/10.1007/s13595-020-00933-5.

Eglin, T., P. Ciais, S. L. Piao, P. Barre, V. Bellassen, P. Cadule, C. Chenu, et al. 2010. “Historical and Future Perspectives of Global Soil Carbon Response to Climate and Land-Use Changes.” *Tellus, Series B: Chemical and Physical Meteorology* 62 (5): 700–718. https://doi.org/10.1111/j.1600-0889.2010.00499.x.

Feng, S., and Q. Fu. 2013. “Expansion of Global Drylands under a Warming Climate.” *Atmospheric Chemistry and Physics* 13 (19): 10081–94. https://doi.org/10.5194/acp-13-10081-2013.

Fernandes, Paulo M. 2013. “Fire-Smart Management of Forest Landscapes in the Mediterranean Basin under Global Change.” *Landscape and Urban Planning* 110 (1): 175–82. https://doi.org/10.1016/j.landurbplan.2012.10.014.

Fernandez, D, M Erena, and J Pecci. 2012. “Use of Remote Sensing for the Calculation of Biophysical Indicators.” *Otions Méditerranéennes. Series B: Studies and Research* 67 (December): 55–63. http://om.ciheam.org/om/pdf/b67/00006596.pdf.

Field, Robert D. 2020. “Using Satellite Estimates of Precipitation for Fire Danger Rating.” *Satellite Precipitation Measurement* 2: 1131–54.

Flannigan, M. D., B. M. Wotton, G. A. Marshall, W. J. de Groot, J. Johnston, N. Jurko, and A. S. Cantin. 2016. "Fuel Moisture Sensitivity to Temperature and Precipitation: Climate Change Implications." *Climatic Change* 134 (1–2): 59–71. https://doi.org/10.1007/s10584-015-1521-0.

Flannigan, Mike, Alan S. Cantin, William J. De Groot, Mike Wotton, Alison Newbery, and Lynn M. Gowman. 2013. "Global Wildland Fire Season Severity in the 21st Century." *Forest Ecology and Management*. https://doi.org/10.1016/j.foreco.2012.10.022.

Forkel, Renate, Alessandra Balzarini, Rocio Baró, Roberto Bianconi, Gabriele Curci, Pedro Jiménez-Guerrero, Marcus Hirtl, et al. 2015. "Analysis of the WRF-Chem Contributions to AQMEII Phase2 with Respect to Aerosol Radiative Feedbacks on Meteorology and Pollutant Distributions." *Atmospheric Environment* 115: 630–45. https://doi.org/10.1016/j.atmosenv.2014.10.056.

French, Nancy H.F., Pierre Goovaerts, and Eric S. Kasischke. 2004. "Uncertainty in Estimating Carbon Emissions from Boreal Forest Fires." *Journal of Geophysical Research D: Atmospheres* 109 (14): 1–12. https://doi.org/10.1029/2003JD003635.

Fujita, Mikiko, and Tomonori Sato. 2017. "Observed Behaviours of Precipitable Water Vapour and Precipitation Intensity in Response to Upper Air Profiles Estimated from Surface Air Temperature." *Scientific Reports* 7 (1): 5–10. https://doi.org/10.1038/s41598-017-04443-9.

Galdos, Marcelo, Otávio Cavalett, Joaquim E.A. Seabra, Luiz Augusto Horta Nogueira, and Antonio Bonomi. 2013. "Trends in Global Warming and Human Health Impacts Related to Brazilian Sugarcane Ethanol Production Considering Black Carbon Emissions." *Applied Energy* 104: 576–82. https://doi.org/10.1016/j.apenergy.2012.11.002.

Gallardo, Marta, Israel Gómez, Lara Vilar, Javier Martínez-Vega, and Maria Pilar Martín. 2016. "Impacts of Future Land Use/Land Cover on Wildfire Occurrence in the Madrid Region (Spain)." *Regional Environmental Change* 16 (4): 1047–61. https://doi.org/10.1007/s10113-015-0819-9.

Giannakopoulos, Christos, and Anna Karali. n.d. "Fire Danger Indicators for Europe from 1970 to 2098 Derived from Climate Projections." Copernicus Climate Change Service. https://doi.org/10.24381/cds.ca755de7.

Giannakopoulos, Christos, Effie Kostopoulou, Konstantinos V. Varotsos, Kostas Tziotziou, and Achilleas Plitharas. 2011. "An Integrated Assessment of Climate Change Impacts for Greece in the near Future." *Regional Environmental Change* 11 (4): 829–43. https://doi.org/10.1007/s10113-011-0219-8.

Giannaros, Theodore M., Vassiliki Kotroni, and Konstantinos Lagouvardos. 2021. "Climatology and Trend Analysis (1987–2016) of Fire Weather in the Euro-Mediterranean." *International Journal of Climatology* 41 (S1): E491–508. https://doi.org/10.1002/joc.6701.

Giannaros, Theodore M., Georgios Papavasileiou, Konstantinos Lagouvardos, Vassiliki Kotroni, Stavros Dafis, Athanasios Karagiannidis, and Eleni Dragozi. 2022.

"Meteorological Analysis of the 2021 Extreme Wildfires in Greece: Lessons Learned and Implications for Early Warning of the Potential for Pyroconvection." *Atmosphere* 13 (3). https://doi.org/10.3390/atmos13030475.

Giuseppe, Francesca Di, Samuel Rémy, Florian Pappenberger, and Fredrik Wetterhall. 2018. "Using the Fire Weather Index (FWI) to Improve the Estimation of Fire Emissions from Fire Radiative Power (FRP) Observations." *Atmospheric Chemistry and Physics* 18 (8): 5359–70. https://doi.org/10.5194/acp-18-5359-2018.

Goss, Michael, Daniel L. Swain, John T. Abatzoglou, Ali Sarhadi, Crystal A. Kolden, A. Park Williams, and Noah S. Diffenbaugh. 2020. "Climate Change Is Increasing the Likelihood of Extreme Autumn Wildfire Conditions across California." *Environmental Research Letters* 15 (9): 94016. https://doi.org/10.1088/1748-9326/ab83a7.

Grell, Georg A., Steven E. Peckham, Rainer Schmitz, Stuart A. McKeen, Gregory Frost, William C. Skamarock, and Brian Eder. 2005. "Fully Coupled 'Online' Chemistry within the WRF Model." *Atmospheric Environment* 39 (37): 6957–75. https://doi.org/10.1016/j.atmosenv.2005.04.027.

Grgurić, Sanja, Josip Križan, Goran Gašparac, Oleg Antonic, Zdravko Spiric, Rodelise E. Mamouri, A. Christodoulou, et al. 2014. "Relationship between MODIS Based Aerosol Optical Depth and PM10 over Croatia." *Central European Journal of Geosciences* 6 (1): 2–16. https://doi.org/10.2478/s13533-012-0135-6.

Grillakis, Manolis G. 2019. "Increase in Severe and Extreme Soil Moisture Droughts for Europe under Climate Change." *Science of The Total Environment*, January. https://doi.org/10.1016/J.SCITOTENV.2019.01.001.

Grillakis, Manolis, Apostolos Voulgarakis, Anastasios Rovithakis, Konstantinos D. Seiradakis, Aristeidis Koutroulis, Robert D. Field, Matthew Kasoar, Athanasios Papadopoulos, and Mihalis Lazaridis. 2022. "Climate Drivers of Global Wildfire Burned Area." *Environmental Research Letters* 17 (4). https://doi.org/10.1088/1748-9326/ac5fa1.

Groot, William De., Robert D. Field, Michael A. Brady, Orbita Roswintiarti, and Maznorizan Mohamad. 2007. "Development of the Indonesian and Malaysian Fire Danger Rating Systems." *Mitigation and Adaptation Strategies for Global Change* 12 (1): 165–80. https://doi.org/10.1007/s11027-006-9043-8.

Guion, Antoine, Solène Turquety, Jan Polcher, Romain Pennel, Sophie Bastin, and Thomas Arsouze. 2022. "Droughts and Heatwaves in the Western Mediterranean: Impact on Vegetation and Wildfires Using the Coupled WRF-ORCHIDEE Regional Model (RegIPSL)." *Climate Dynamics* 58 (9–10): 2881–2903. https://doi.org/10.1007/s00382-021-05938-y.

Hartung, Carl, Richard Han, Carl Seielstad, and Saxon Holbrook. 2006. "FireWxNet: A Multi-Tiered Portable Wireless System for Monitoring Weather Conditions in Wildland Fire Environments," 28–41. https://doi.org/10.1145/1134680.1134685.

Haywood, Jim M., Nicolas Bellouin, Andy Jones, Olivier Boucher, Martin Wild, and Keith P. Shine. 2011. "The Roles of Aerosol, Water Vapor and Cloud in Future Global

Dimming/Brightening." *Journal of Geophysical Research Atmospheres* 116 (20): 1–14. https://doi.org/10.1029/2011JD016000.

Hazeleger, W., X. Wang, C. Severijns, S. Ştefănescu, R. Bintanja, A. Sterl, K. Wyser, et al. 2012. "EC-Earth V2.2: Description and Validation of a New Seamless Earth System Prediction Model." *Climate Dynamics* 39 (11): 2611–29. https://doi.org/10.1007/s00382-011-1228-5.

Hersbach, Hans, Bill Bell, Paul Berrisford, Shoji Hirahara, András Horányi, Joaquín Muñoz-Sabater, Julien Nicolas, et al. 2020. "The ERA5 Global Reanalysis." *Quarterly Journal of the Royal Meteorological Society* 146 (730): 1999–2049. https://doi.org/10.1002/qj.3803.

Holling, C. S., and Gary K. Meffe. 1996. "Command and Control and the Pathology of Natural Resource Management." *Conservation Biology* 10 (2): 328–37. https://doi.org/10.1046/j.1523-1739.1996.10020328.x.

Holz, Andrés, Thomas Kitzberger, Juan Paritsis, and Thomas T. Veblen. 2012. "Ecological and Climatic Controls of Modern Wildfire Activity Patterns across Southwestern South America." *Ecosphere* 3 (11): 1–25. https://doi.org/10.1890/ES12-00234.1.

Hurteau, Matthew D., George W. Koch, and Bruce A. Hungate. 2008. "Carbon Protection and Fire Risk Reduction: Toward a Full Accounting of Forest Carbon Offsets." *Frontiers in Ecology and the Environment* 6 (9): 493–98. https://doi.org/10.1890/070187.

Hyslop, Nicole Pauly. 2009. "Impaired Visibility: The Air Pollution People See." *Atmospheric Environment* 43 (1): 182–95. https://doi.org/10.1016/j.atmosenv.2008.09.067.

Iles, Carley E., Robert Vautard, Jane Strachan, Sylvie Joussaume, Bernd R. Eggen, and Chris D. Hewitt. 2020. "The Benefits of Increasing Resolution in Global and Regional Climate Simulations for European Climate Extremes." *Geoscientific Model Development* 13 (11): 5583–5607. https://doi.org/10.5194/gmd-13-5583-2020.

Jacob, Daniela, Juliane Petersen, Bastian Eggert, Antoinette Alias, Ole Bøssing Christensen, Laurens M Bouwer, Alain Braun, et al. 2013. "EURO-CORDEX: New High-Resolution Climate Change Projections for European Impact Research." *Regional Environmental Change* 14 (2): 563–78. https://doi.org/10.1007/s10113-013-0499-2.

Jacob, Daniela, Claas Teichmann, Stefan Sobolowski, Eleni Katragkou, Ivonne Anders, Michal Belda, Rasmus Benestad, et al. 2020. "Regional Climate Downscaling over Europe: Perspectives from the EURO-CORDEX Community." *Regional Environmental Change* 20 (2). https://doi.org/10.1007/s10113-020-01606-9.

Jaffe, Dan, William Hafner, Duli Chand, Anthony Westerling, and Dominick Spracklen. 2008. "Interannual Variations in PM2.5 Due to Wildfires in the Western United States." *Environmental Science and Technology* 42 (8): 2812–18. https://doi.org/10.1021/es702755v.

Jeong, Jaein I., Rokjin J. Park, and Daeok Youn. 2008. "Effects of Siberian Forest Fires on

Air Quality in East Asia during May 2003 and Its Climate Implication." *Atmospheric Environment* 42 (39): 8910–22. https://doi.org/10.1016/j.atmosenv.2008.08.037.

Jethva, H., and O. Torres. 2011. "Satellite-Based Evidence of Wavelength-Dependent Aerosol Absorption in Biomass Burning Smoke Inferred from Ozone Monitoring Instrument." *Atmospheric Chemistry and Physics* 11 (20): 10541–51. https://doi.org/10.5194/acp-11-10541-2011.

Jethva, Hiren, and Omar Torres. 2019. "A Comparative Evaluation of Aura-OMI and SKYNET near-UV Single-Scattering Albedo Products." *Atmospheric Measurement Techniques* 12 (12): 6489–6503. https://doi.org/10.5194/amt-12-6489-2019.

Jiang, Yiquan, Xiu Qun Yang, Xiaohong Liu, Yun Qian, Kai Zhang, Minghuai Wang, Fang Li, Yong Wang, and Zheng Lu. 2020. "Impacts of Wildfire Aerosols on Global Energy Budget and Climate: The Role of Climate Feedbacks." *Journal of Climate* 33 (8): 3351–66. https://doi.org/10.1175/JCLI-D-19-0572.1.

Jolly, W. Matt, Mark A. Cochrane, Patrick H. Freeborn, Zachary A. Holden, Timothy J. Brown, Grant J. Williamson, and David M.J.S. Bowman. 2015. "Climate-Induced Variations in Global Wildfire Danger from 1979 to 2013." *Nature Communications* 6 (May): 1–11. https://doi.org/10.1038/ncomms8537.

Julien, Boulange, Hanasaki Naota, Veldkamp Ted, Schewe Jacob, and Shiogama Hideo. 2018. "Magnitude and Robustness Associated with the Climate Change Impacts on Global Hydrological Variables for Transient and Stabilized Climate States." *Environmental Research Letters* 13 (6). https://doi.org/10.1088/1748-9326/aac179.

Kalivitis, N., E. Gerasopoulos, M. Vrekoussis, G. Kouvarakis, N. Kubilay, N. Hatzianastassiou, I. Vardavas, and N. Mihalopoulos. 2007. "Dust Transport over the Eastern Mediterranean Derived from Total Ozone Mapping Spectrometer, Aerosol Robotic Network, and Surface Measurements." *Journal of Geophysical Research Atmospheres* 112 (3): 1–9. https://doi.org/10.1029/2006JD007510.

Karali, A., M. Hatzaki, C. Giannakopoulos, A. Roussos, G. Xanthopoulos, and V. Tenentes. 2014. "Sensitivity and Evaluation of Current Fire Risk and Future Projections Due to Climate Change: The Case Study of Greece." *Natural Hazards and Earth System Sciences* 14 (1): 143–53. https://doi.org/10.5194/nhess-14-143-2014.

Kasischke, S. Eric, L. N Christensen, and J. Brian Stocks. 1995. "FIRE , GLOBAL WARMING , AND THE CARBON BALANCE OF BOREAL FORESTS." *Ecologica! Applications* 5 (2): 437–51.

Kaskaoutis, D. G., Shailesh Kumar Kharol, N. Sifakis, P. T. Nastos, Anu Rani Sharma, K. V.S. Badarinath, and H. D. Kambezidis. 2011. "Satellite Monitoring of the Biomass-Burning Aerosols during the Wildfires of August 2007 in Greece: Climate Implications." *Atmospheric Environment* 45 (3): 716–26. https://doi.org/10.1016/j.atmosenv.2010.09.043.

Kassomenos, Pavlos. 2010. "Synoptic Circulation Control on Wild Fire Occurrence." *Physics and Chemistry of the Earth* 35 (9–12): 544–52. https://doi.org/10.1016/j.pce.2009.11.008.

Keeley, Jon E., and Paul H. Zedler. 2009. “Large, High-Intensity Fire Events in Southern California Shrublands: Debunking the Fine-Grain Age Patch Model.” *Ecological Applications* 19 (1): 69–94.

Khoshsima, M., F. Ahmadi-Givi, A. A. Bidokhti, and S. Sabetghadam. 2014. “Impact of Meteorological Parameters on Relation between Aerosol Optical Indices and Air Pollution in a Sub-Urban Area.” *Journal of Aerosol Science* 68: 46–57. https://doi.org/10.1016/j.jaerosci.2013.10.008.

Kirchmeier-Young, Megan C., Francis W. Zwiers, Nathan P. Gillett, and Alex J. Cannon. 2017. “Attributing Extreme Fire Risk in Western Canada to Human Emissions.” *Climatic Change* 144 (2): 365–79. https://doi.org/10.1007/s10584-017-2030-0.

Kitzberger, Thomas, Ezequiel Aráoz, Juan H. Gowda, Mónica Mermoz, and Juan M. Morales. 2012. “Decreases in Fire Spread Probability with Forest Age Promotes Alternative Community States, Reduced Resilience to Climate Variability and Large Fire Regime Shifts.” *Ecosystems* 15 (1): 97–112. https://doi.org/10.1007/s10021-011-9494-y.

Kjellström, Erik, Lars Bärring, Grigory Nikulin, Carin Nilsson, Gunn Persson, and Gustav Strandberg. 2016. “Production and Use of Regional Climate Model Projections – A Swedish Perspective on Building Climate Services.” *Climate Services* 2–3: 15–29. https://doi.org/10.1016/j.cliser.2016.06.004.

Kloster, S., N. M. Mahowald, J. T. Randerson, and P. J. Lawrence. 2012. “The Impacts of Climate, Land Use, and Demography on Fires during the 21st Century Simulated by CLM-CN.” *Biogeosciences* 9 (1): 509–25. https://doi.org/10.5194/bg-9-509-2012.

Knist, Sebastian, Klaus Goergen, Erasmo Buonomo, Ole Bøssing Christensen, Augustin Colette, Rita M. Cardoso, Rowan Fealy, et al. 2016. “Land-atmosphere Coupling in EURO-CORDEX Evaluation Experiments.” JGR Atmospheres. https://doi.org/10.1002/ 2016JD025476.

Knorr, Wolfgang, Frank Dentener, Stijn Hantson, Leiwen Jiang, Zbigniew Klimont, and Almut Arneth. 2016. “Air Quality Impacts of European Wildfire Emissions in a Changing Climate.” *Atmospheric Chemistry and Physics* 16 (9): 5685–5703. https://doi.org/10.5194/acp-16-5685-2016.

Kochanski, A. K., D. V. Mallia, M. G. Fearon, J. Mandel, A. H. Souri, and T Brown. 2019. “JGR Atmospheres - 2019 - Kochanski - Modeling Wildfire Smoke Feedback Mechanisms Using a Coupled Fire-Atmosphere Model With.Pdf.” *Journal OfGeophysical Research* 124: 9099–9116. https://doi.org/doi.org/10.1029/2019JD030558.

Kochanski, Adam K, Derek V Mallia, Matthew G Fearon, Jan Mandel, Amir H Souri, and Tim Brown. 2019. “Modeling Wildfire Smoke Feedback Mechanisms Using a Coupled Fire-Atmosphere Model With a Radiatively Active Aerosol Scheme.” *Journal OfGeophysical Research* 124: 9099–9116. https://doi.org/https://doi.org/10.1029/2019JD030558.

Kottek, Markus, Jürgen Grieser, Christoph Beck, Bruno Rudolf, and Franz Rubel. 2006.

"World Map of the Köppen-Geiger Climate Classification Updated." *Meteorologische Zeitschrift* 15 (3): 259–63. https://doi.org/10.1127/0941-2948/2006/0130.

Krawchuk, Meg A., and Max A. Moritz. 2011. "Constraints on Global Fire Activity Vary across a Resource Gradient." *Ecology* 92 (1): 121–32. https://doi.org/10.1890/09-1843.1.

Krawchuk, Meg A., Max A. Moritz, Marc André Parisien, Jeff Van Dorn, and Katharine Hayhoe. 2009. "Global Pyrogeography: The Current and Future Distribution of Wildfire." *PLoS ONE* 4 (4). https://doi.org/10.1371/journal.pone.0005102.

Krüll, Wolfgang, Robert Tobera, Ingolf Willms, Helmut Essen, and Nora Von Wahl. 2012. "Early Forest Fire Detection and Verification Using Optical Smoke, Gas and Microwave Sensors." *Procedia Engineering* 45: 584–94. https://doi.org/10.1016/j.proeng.2012.08.208.

Lagouvardos, K., V. Kotroni, T. M. Giannaros, and S. Dafis. 2019. "Meteorological Conditions Conducive to the Rapid Spread of the Deadly Wildfire in Eastern Attica, Greece." *Bulletin of the American Meteorological Society* 100 (11): 2137–45. https://doi.org/10.1175/BAMS-D-18-0231.1.

Langmann, Bärbel, Bryan Duncan, Christiane Textor, Jörg Trentmann, and Guido R. van der Werf. 2009. "Vegetation Fire Emissions and Their Impact on Air Pollution and Climate." *Atmospheric Environment* 43 (1): 107–16. https://doi.org/10.1016/j.atmosenv.2008.09.047.

Lazaridis, M., M. Latos, V. Aleksandropoulou, O. Hov, A. Papayannis, and K. Tørseth. 2008. "Contribution of Forest Fire Emissions to Atmospheric Pollution in Greece." *Air Quality, Atmosphere and Health* 1 (3): 143–58. https://doi.org/10.1007/s11869-008-0020-0.

Le, By, Yang Sim, C I D Imperial, and Project Physics. 2017. "Fire Spread Modelling : An Overview (2017)," 1–15.

Littell, Jeremy S., Elaine E. Oneil, Donald McKenzie, Jeffrey A. Hicke, James A. Lutz, Robert A. Norheim, and Marketa M. Elsner. 2010. "Forest Ecosystems, Disturbance, and Climatic Change in Washington State, USA." *Climatic Change* 102 (1–2): 129–58. https://doi.org/10.1007/s10584-010-9858-x.

Liu, L., D. Shawki, Apostolos Voulgarakis, M. Kasoar, B. H. Samset, G. Myhre, P. M. Forster, et al. 2018. "A PDRMIP Multimodel Study on the Impacts of Regional Aerosol Forcings on Global and Regional Precipitation." *Journal of Climate* 31 (11): 4429–47. https://doi.org/10.1175/JCLI-D-17-0439.1.

Liu, Yongqiang. 2005. "Enhancement of the 1988 Northern U.S. Drought Due to Wildfires." *Geophysical Research Letters* 32 (10): 1–4. https://doi.org/10.1029/2005GL022411.

Liu, Yongqiang, Scott Goodrick, and Warren Heilman. 2014. "Wildland Fire Emissions, Carbon, and Climate: Wildfire-Climate Interactions." *Forest Ecology and Management* 317: 80–96. https://doi.org/10.1016/j.foreco.2013.02.020.

Loepfe, Lasse, Jordi Martinez-Vilalta, Jordi Oliveres, Josep Piñol, and Francisco Lloret. 2010. “Feedbacks between Fuel Reduction and Landscape Homogenisation Determine Fire Regimes in Three Mediterranean Areas.” *Forest Ecology and Management* 259 (12): 2366–74. https://doi.org/10.1016/j.foreco.2010.03.009.

M. G. Tosca, D. J. Diner, M.J.Garay, and O. V. Kalashnikova1. 2014. “JGR Atmospheres - 2014 - Tosca - Observational Evidence of Fire-driven Reduction of Cloud Fraction in Tropical Africa.”

Mangeon, Stéphane, Apostolos Voulgarakis, Richard Gilham, Anna Harper, Stephen Sitch, and Gerd Folberth. 2016. “INFERNO: A Fire and Emissions Scheme for the UK Met Office’s Unified Model.” *Geoscientific Model Development* 9 (8): 2685–2700. https://doi.org/10.5194/gmd-9-2685-2016.

Martins, Helena, and José G. Borges. 2007. “Addressing Collaborative Planning Methods and Tools in Forest Management.” *Forest Ecology and Management* 248 (1–2): 107–18. https://doi.org/10.1016/j.foreco.2007.02.039.

Maura, Kelly. 2021. “‘ Brutal ’ Weather Conditions Fan Flames of Deadly Fires in Greece.”

McKenzie, Donald, Uma Shankar, Robert E. Keane, E. Natasha Stavros, Warren E. Heilman, Douglas G. Fox, and Allen C. Riebau. 2014. “Smoke Consequences of New Wildfire Regimes Driven by Climate Change.” *Earth’s Future*, n/a-n/a. https://doi.org/10.1002/2014ef000019.

Michael, Yaron, Gilad Kozokaro, Steve Brenner, and Itamar M. Lensky. 2022. “Improving WRF-Fire Wildfire Simulation Accuracy Using SAR and Time Series of Satellite-Based Vegetation Indices.” *Remote Sensing* 14 (12): 1–14. https://doi.org/10.3390/rs14122941.

Mielonen, Tero, Anca Hienola, Thomas Kühn, Joonas Merikanto, Antti Lipponen, Tommi Bergman, Hannele Korhonen, et al. 2016. “Temperature-Dependence of Aerosol Optical Depth over the Southeastern US.” *Atmospheric Chemistry and Physics Discussions*, no. July: 1–28. https://doi.org/10.5194/acp-2016-625.

Millar, Constance I., Nathan L. Stephenson, and Scott L. Stephens. 2007. “Climate Change and Forests of the Future: Managing in the Face of Uncertainty.” *Ecological Applications* 17 (8): 2145–51. https://doi.org/10.1890/06-1715.1.

Moritz, Max A., Enric Batllori, Ross A. Bradstock, A. Malcolm Gill, John Handmer, Paul F. Hessburg, Justin Leonard, et al. 2014. “Learning to Coexist with Wildfire.” *Nature* 515 (7525): 58–66. https://doi.org/10.1038/nature13946.

Moritz, Max A., Marc-André Parisien, Enric Batllori, Meg A. Krawchuk, Jeff Van Dorn, David J. Ganz, and Katharine Hayhoe. 2012. “Climate Change and Disruptions to Global Fire Activity.” *Ecosphere* 3 (6): 1–22. https://doi.org/10.1890/es11-00345.1.

Morrison, Hugh, and Andrew Gettelman. 2008. “A New Two-Moment Bulk Stratiform Cloud Microphysics Scheme in the Community Atmosphere Model, Version 3 (CAM3). Part I: Description and Numerical Tests.” *Journal of Climate* 21 (15): 3642–59. https://doi.org/10.1175/2008JCLI2105.1.

Moss, Richard H., Jae A. Edmonds, Kathy A. Hibbard, Martin R. Manning, Steven K. Rose, Detlef P. van Vuuren, Timothy R. Carter, et al. 2010. "The next Generation of Scenarios for Climate Change Research and Assessment." *Nature* 463 (7282): 747–56. https://doi.org/10.1038/nature08823.

Navarro-Racines, Carlos, Jaime Tarapues, Philip Thornton, Andy Jarvis, and Julian Ramirez-Villegas. 2020. "High-Resolution and Bias-Corrected CMIP5 Projections for Climate Change Impact Assessments." *Scientific Data* 7 (1): 1–14. https://doi.org/10.1038/s41597-019-0343-8.

Neary, Daniel G., Karen A. Koestner, Ann Youberg, and Peter E. Koestner. 2012. "Post-Fire Rill and Gully Formation, Schultz Fire 2010, Arizona, USA." *Geoderma* 191: 97–104. https://doi.org/10.1016/j.geoderma.2012.01.016.

Nielsen-Pincus, Max, Cassandra Moseley, and Krista Gebert. 2014. "Job Growth and Loss across Sectors and Time in the Western US: The Impact of Large Wildfires." *Forest Policy and Economics* 38: 199–206. https://doi.org/10.1016/j.forpol.2013.08.010.

Noble, I. R., A. M. Gill, and G. A.V. Bary. 1980. "McArthur's Fire-danger Meters Expressed as Equations." *Australian Journal of Ecology* 5 (2): 201–3. https://doi.org/10.1111/j.1442-9993.1980.tb01243.x.

Novo, Ana, and Henrique Lorenzo. n.d. "Mapping Forest Fire Risk — A Case Study In."

O'Neill, Brian C., Elmar Kriegler, Keywan Riahi, Kristie L. Ebi, Stephane Hallegatte, Timothy R. Carter, Ritu Mathur, and Detlef P. van Vuuren. 2014. "A New Scenario Framework for Climate Change Research: The Concept of Shared Socioeconomic Pathways." *Climatic Change* 122 (3): 387–400. https://doi.org/10.1007/s10584-013-0905-2.

Okokpujie, Kennedy, Samuel Ndueso John, Etinosa Noma-Osaghae, Okokpujie P. Imhade Princess, and Okonigene Robert. 2019. "A Wireless Sensor Network Based Fire Protection System with SMS Alerts." *International Journal of Mechanical Engineering and Technology* 10 (2): 44–52.

Papadimas, C. D., N. Hatzianastassiou, C. Matsoukas, M. Kanakidou, N. Mihalopoulos, and I. Vardavas. 2012. "The Direct Effect of Aerosols on Solar Radiation over the Broader Mediterranean Basin." *Atmospheric Chemistry and Physics* 12 (15): 7165–85. https://doi.org/10.5194/acp-12-7165-2012.

Papagiannaki, K., T. M. Giannaros, S. Lykoudis, V. Kotroni, and K. Lagouvardos. 2020. "Weather-Related Thresholds for Wildfire Danger in a Mediterranean Region: The Case of Greece." *Agricultural and Forest Meteorology* 291 (June): 108076. https://doi.org/10.1016/j.agrformet.2020.108076.

Pausas, Juli G., and Santiago Fernández-Muñoz. 2012. "Fire Regime Changes in the Western Mediterranean Basin: From Fuel-Limited to Drought-Driven Fire Regime." *Climatic Change* 110 (1–2): 215–26. https://doi.org/10.1007/s10584-011-0060-6.

Pausas, Juli G., and Jon E. Keeley. 2009. "A Burning Story: The Role of Fire in the History of Life." *BioScience* 59 (7): 593–601. https://doi.org/10.1525/bio.2009.59.7.10.

Pausas, Juli G. 2004. “CHANGES IN FIRE AND CLIMATE IN THE EASTERN IBERIAN PENINSULA (MEDITERRANEAN BASIN).” *Climatic Change* 63: 337–50.

Paveglio, Travis B., Pamela J. Jakes, Matthew S. Carroll, and Daniel R. Williams. 2009. “Understanding Social Complexity within the Wildland-Urban Interface: A New Species of Human Habitation?” *Environmental Management* 43 (6): 1085–95. https://doi.org/10.1007/s00267-009-9282-z.

Paynter, D, and V Ramaswamy. 2014. “Investigating the Impact of the Shortwave Water Vapor Continuum upon Climate Simulations Using GFDL Global Models.” *Journal of Geophysical Research*, no. 119: 10,720–10,737. https://doi.org/10.1002/2013JD021040.

Peng, Zhen, Zhiquan Liu, Dan Chen, and Junmei Ban. 2017. “Improving PM2.5 Forecast over China by the Joint Adjustment of Initial Conditions and Source Emissions with an Ensemble Kalman Filter.” *Atmospheric Chemistry and Physics* 17 (7): 4837–55. https://doi.org/10.5194/acp-17-4837-2017.

Peterson, Garry D. 2002. “Contagious Disturbance, Ecological Memory, and the Emergence of Landscape Pattern.” *Ecosystems* 5 (4): 329–38. https://doi.org/10.1007/s10021-001-0077-1.

Peterson, W. David, and L. David Peterson. 2001. “MOUNTAIN HEMLOCK GROWTH RESPONDS TO CLIMATIC VARIABILITY AT ANNUAL AND DECADAL TIME SCALES.” *Ecology* 82 (12): 3330–45.

Pfister, G. G., C. Wiedinmyer, and L. K. Emmons. 2008. “Impacts of the Fall 2007 California Wildfires on Surface Ozone: Integrating Local Observations with Global Model Simulations.” *Geophysical Research Letters* 35 (19): 1–5. https://doi.org/10.1029/2008GL034747.

Pichon, A. Le, J. D. Assink, P. Heinrich, E. Blanc, A. Charlton-Perez, C. F. Lee, P. Keckhut, et al. 2015. “V.” *Journal of Geophysical Research*. https://doi.org/10.1002/2015JD023273.

Pielke, R. A., R. L. Walko, L. T. Steyaert, P. L. Vidale, G. E. Liston, W. A. Lyons, and T. N. Chase. 1999. “The Influence of Anthropogenic Landscape Changes on Weather in South Florida.” *Monthly Weather Review* 127 (7): 1663–72. https://doi.org/10.1175/1520-0493(1999)127<1663:tioalc>2.0.co;2.

Price, Colin, and David Rind. 1994. “The Impact of a 2xCO2 Climate on Lightning-Caused Fires.” *Lournal of Climate* 7.

Riahi, Keywan, Shilpa Rao, Volker Krey, Cheolhung Cho, Vadim Chirkov, Guenther Fischer, Georg Kindermann, Nebojsa Nakicenovic, and Peter Rafaj. 2011. “RCP 8.5—A Scenario of Comparatively High Greenhouse Gas Emissions.” *Climatic Change* 109 (1–2): 33–57. https://doi.org/10.1007/s10584-011-0149-y.

Richardson, Doug, Amanda S. Black, Didier P. Monselesan, James S. Risbey, Dougal T. Squire, Carly R. Tozer, and Josep G. Canadell. 2021. “Increased Extreme Fire Weather Occurrence in Southeast Australia and Related Atmospheric Drivers.” *Weather and Climate Extremes* 34 (February): 100397. https://doi.org/10.1016/j.wace.2021.100397.

Riva, Matteo Jucker, Hanspeter Liniger, Alejandro Valdecantos, and Gudrun Schwilch. 2016. “Impacts of Land Management on the Resilience of Mediterranean Dry Forests to Fire.” *Sustainability (Switzerland)* 8 (10). https://doi.org/10.3390/su8100981.

Rizza, Umberto, Mario Marcello Miglietta, Cristina Mangia, Pierina Ielpo, Mauro Morichetti, Chiara Iachini, Simone Virgili, and Giorgio Passerini. 2018. “Sensitivity of WRF-Chem Model to Land Surface Schemes: Assessment in a Severe Dust Outbreak Episode in the Central Mediterranean (Apulia Region).” *Atmospheric Research* 201 (October 2017): 168–80. https://doi.org/10.1016/j.atmosres.2017.10.022.

Rovithakis, Anastasios, Manolis G Grillakis, Konstantinos D Seiradakis, and Christos Giannakopoulos. 2022. “Future Climate Change Impact on Wildfire Danger over the Mediterranean : The Case of Greece OPEN ACCESS Future Climate Change Impact on Wildfire Danger over the Mediterranean : The Case of Greece.” *Environmental Research Letters* 17: 045022. https://doi.org/https://doi.org/10.1088/1748-9326/ac5f94.

Ruefenacht, B, MV Finco, R Czaplewski, Eileen Helmer, Ja Blackard, GR Holden, Aj Lister, D Salajanu, D Weyermann, and K Winterberger. 2008. “Mapping Using Forest Inventory and Analysis Data.” *Photogrammetric Engineering and Remote Sensing* 74 (11): 1379–88.

Ruffault, Julien, Thomas Curt, Vincent Moron, Ricardo M. Trigo, Florent Mouillot, Nikos Koutsias, François Pimont, et al. 2020. “Increased Likelihood of Heat-Induced Large Wildfires in the Mediterranean Basin.” *Scientific Reports* 10 (1): 1–9. https://doi.org/10.1038/s41598-020-70069-z.

Salis, Michele, Liliana Del Giudice, Roghayeh Jahdi, Fermin Alcasena-Urdiroz, Carla Scarpa, Grazia Pellizzaro, Valentina Bacciu, et al. 2022. “Spatial Patterns and Intensity of Land Abandonment Drive Wildfire Hazard and Likelihood in Mediterranean Agropastoral Areas.” *Land* 11 (11). https://doi.org/10.3390/land11111942.

Satir, O., S. Berberoglu, and A. Cilek. 2016. “Modelling Long Term Forest Fire Risk Using Fire Weather Index under Climate Change in Turkey.” *Applied Ecology and Environmental Research* 14 (4): 537–51. https://doi.org/10.15666/aeer/1404_537551.

Schoennagel, Tania, Thomas T. Veblen, and William H. Romme. 2004. “The Interaction of Fire, Fuels, and Climate across Rocky Mountain Forests.” *BioScience* 54 (7): 661–76. https://doi.org/10.1641/0006-3568(2004)054[0661:TIOFFA]2.0.CO;2.

Scott, C. E., A. Rap, D. V. Spracklen, P. M. Forster, K. S. Carslaw, G. W. Mann, K. J. Pringle, et al. 2014. “The Direct and Indirect Radiative Effects of Biogenic Secondary Organic Aerosol.” *Atmospheric Chemistry and Physics* 14 (1): 447–70. https://doi.org/10.5194/acp-14-447-2014.

Senande-Rivera, Martín, Damián Insua-Costa, and Gonzalo Miguez-Macho. 2022. “Spatial and Temporal Expansion of Global Wildland Fire Activity in Response to Climate Change.” *Nature Communications* 13 (1): 1–9.

https://doi.org/10.1038/s41467-022-28835-2.

Sharples, J. J., R. H.D. McRae, R. O. Weber, and A. M. Gill. 2009. "A Simple Index for Assessing Fire Danger Rating." *Environmental Modelling and Software* 24 (6): 764–74. https://doi.org/10.1016/j.envsoft.2008.11.004.

Sharples, Jason J. 2009. "An Overview of Mountain Meteorological Effects Relevant to Fire Behaviour and Bushfire Risk." *International Journal of Wildland Fire* 18 (7): 737–54. https://doi.org/10.1071/WF08041.

Shi, Hanyu, Zhiqiang Xiao, Xuchen Zhan, Han Ma, and Xiaodan Tian. 2019. "Evaluation of MODIS and Two Reanalysis Aerosol Optical Depth Products over AERONET Sites." *Atmospheric Research* 220 (November 2018): 75–80. https://doi.org/10.1016/j.atmosres.2019.01.009.

Silveira, Carlos, Ana Martins, Sónia Gouveia, Manuel Scotto, Ana I. Miranda, and Alexandra Monteiro. 2021. "The Role of the Atmospheric Aerosol in Weather Forecasts for the Iberian Peninsula: Investigating the Direct Effects Using the WRF-Chem Model." *Atmosphere* 12 (2). https://doi.org/10.3390/atmos12020288.

Simoneit, Bernd R.T. 2002. *Biomass Burning - A Review of Organic Tracers for Smoke from Incomplete Combustion*. *Applied Geochemistry*. Vol. 17. https://doi.org/10.1016/S0883-2927(01)00061-0.

Smirnov, A., B. N. Holben, T. F. Eck, O. Dubovik, and I. Slutsker. 2003. "Effect of Wind Speed on Columnar Aerosol Optical Properties at Midway Island." *Journal of Geophysical Research: Atmospheres* 108 (24): 1–8. https://doi.org/10.1029/2003jd003879.

Sokolik, I. N., A. J. Soja, P. J. DeMott, and D. Winker. 2019. "Progress and Challenges in Quantifying Wildfire Smoke Emissions, Their Properties, Transport, and Atmospheric Impacts." *Journal of Geophysical Research: Atmospheres* 124 (23): 13005–25. https://doi.org/10.1029/2018JD029878.

Stafoggia, Massimo, Tom Bellander, Simone Bucci, Marina Davoli, Kees de Hoogh, Francesca de' Donato, Claudio Gariazzo, et al. 2019. "Estimation of Daily PM10 and PM2.5 Concentrations in Italy, 2013–2015, Using a Spatiotemporal Land-Use Random-Forest Model." *Environment International* 124 (January): 170–79. https://doi.org/10.1016/j.envint.2019.01.016.

Stavros, E. Natasha, Donald Mckenzie, and Narasimhan Larkin. 2014. "The Climate-Wildfire-Air Quality System: Interactions and Feedbacks across Spatial and Temporal Scales." *Wiley Interdisciplinary Reviews: Climate Change* 5 (6): 719–33. https://doi.org/10.1002/wcc.303.

Stein, Ariel F., Glenn D. Rolph, Roland R. Draxler, Barbara Stunder, and Mark Ruminski. 2009. "Verification of the NOAA Smoke Forecasting System: Model Sensitivity to the Injection Height." *Weather and Forecasting* 24 (2): 379–94. https://doi.org/10.1175/2008WAF2222166.1.

Stocks, B. J. 1993. "Global Warming and Forest Fires in Canada." *Forestry Chronicle* 69 (3): 290–93. https://doi.org/10.5558/tfc69290-3.

Stocks, BJ, ME Alexander, CE Van Wagner, RS McAlpine, TJ Lynham, DE Dube, X Wang, et al. 1989. *Weather Guide Canadian Forest Fire Danger Rating System*. *The Forestry Chronicle*. Vol. 65.

Swann, Abigail L., Inez Y. Fung, Samuel Levis, Gordon B. Bonan, and Scott C. Doney. 2010. "Changes in Arctic Vegetation Amplify High-Latitude Warming through the Greenhouse Effect." *Proceedings of the National Academy of Sciences of the United States of America* 107 (4): 1295–1300. https://doi.org/10.1073/pnas.0913846107.

Tang, Aohan, Guoshun Zhuang, Ying Wang, Hui Yuan, and Yele Sun. 2005. "The Chemistry of Precipitation and Its Relation to Aerosol in Beijing." *Atmospheric Environment* 39 (19): 3397–3406. https://doi.org/10.1016/j.atmosenv.2005.02.001.

Tang, Tao, Drew Shindell, Yuqiang Zhang, Apostolos Voulgarakis, Jean Francois Lamarque, Gunnar Myhre, Camilla W. Stjern, Gregory Faluvegi, and Bjørn H. Samset. 2020. "Response of Surface Shortwave Cloud Radiative Effect to Greenhouse Gases and Aerosols and Its Impact on Summer Maximum Temperature." *Atmospheric Chemistry and Physics* 20 (13): 8251–66. https://doi.org/10.5194/acp-20-8251-2020.

Tedim, Fantina, Vittorio Leone, Malik Amraoui, Christophe Bouillon, Michael R. Coughlan, Giuseppe M. Delogu, Paulo M. Fernandes, et al. 2018. "Defining Extreme Wildfire Events: Difficulties, Challenges, and Impacts." *Fire* 1 (1): 1–28. https://doi.org/10.3390/fire1010009.

Tomašević, Ivana Čavlina, Kevin K.W. Cheung, Višnjica Vučetić, Paul Fox-Hughes, Kristian Horvath, Maja Telišman Prtenjak, Paul J. Beggs, Barbara Malečić, and Velimir Milić. 2022. "The 2017 Split Wildfire in Croatia: Evolution and the Role of Meteorological Conditions." *Natural Hazards and Earth System Sciences* 22 (10): 3143–65. https://doi.org/10.5194/nhess-22-3143-2022.

Torma, Csaba, Filippo Giorgi, and Erika Coppola. 2015. "Added Value of Regional Climate Modeling over Areas Characterized by Complex Terrain-Precipitation over the Alps." *Journal of Geophysical Research*. https://doi.org/10.1002/2014JD022781.

Tosca, M. G., J. T. Randerson, and C. S. Zender. 2013. "Global Impact of Smoke Aerosols from Landscape Fires on Climate and the Hadley Circulation." *Atmospheric Chemistry and Physics* 13 (10): 5227–41. https://doi.org/10.5194/acp-13-5227-2013.

Tramblay, Yves, Aristeidis Koutroulis, Luis Samaniego, Sergio M. Vicente-Serrano, Florence Volaire, Aaron Boone, Michel Le Page, et al. 2020. "Challenges for Drought Assessment in the Mediterranean Region under Future Climate Scenarios." *Earth-Science Reviews*. Elsevier B.V. https://doi.org/10.1016/j.earscirev.2020.103348.

TRIGO, RICARDO M., JOSE M. C. PEREIRA, MARIO G. PEREIRA, BERNARDO MOTA, TERESA J. CALADO, CARLOS C. DACAMARA, and FATIMA E. SANTO. 2006. "ATMOSPHERIC CONDITIONS ASSOCIATED WITH THE EXCEPTIONAL FIRE SEASON

OF 2003 IN PORTUGAL." *International Journal of Climatology* 26: 1741–1757. https://doi.org/10.1002/joc.1333.

Tsibart, A. S., N. S. Gamova, T. S. Koshovskii, and A. N. Gennadiev. 2015. "Wildfires in Russia: Features, Regimes and Consequences." *Wildland Fires: A Worldwide Reality*, no. May 2016: 199–210.

Tsiros, Ioannis X., Panagiotis Nastos, Nikolaos D. Proutsos, and Alexandros Tsaousidis. 2020. "Variability of the Aridity Index and Related Drought Parameters in Greece Using Climatological Data over the Last Century (1900–1997)." *Atmospheric Research* 240 (July 2019): 104914. https://doi.org/10.1016/j.atmosres.2020.104914.

Tuladhar, Avalokita, Palistha Manandhar, and Kundan Lal Shrestha. 2021. "Assessment of Health Impact of PM2.5 Exposure by Using WRF-Chem Model in Kathmandu Valley, Nepal." *Frontiers in Sustainable Cities* 3 (June): 1–9. https://doi.org/10.3389/frsc.2021.672428.

Turco, Marco, Juan José Rosa-Cánovas, Joaquín Bedia, Sonia Jerez, Juan Pedro Montávez, Maria Carmen Llasat, and Antonello Provenzale. 2018. "Exacerbated Fires in Mediterranean Europe Due to Anthropogenic Warming Projected with Non-Stationary Climate-Fire Models." *Nature Communications* 9 (1): 1–9. https://doi.org/10.1038/s41467-018-06358-z.

Turquety, S., D. Hurtmans, J. Hadji-Lazaro, P. F. Coheur, C. Clerbaux, D. Josset, and C. Tsamalis. 2009. "Tracking the Emission and Transport of Pollution from Wildfires Using the IASI CO Retrievals: Analysis of the Summer 2007 Greek Fires." *Atmospheric Chemistry and Physics* 9 (14): 4897–4913. https://doi.org/10.5194/acp-9-4897-2009.

Ukhov, Alexander, Suleiman Mostamandi, Arlindo Da Silva, Johannes Flemming, Yasser Alshehri, Illia Shevchenko, and Georgiy Stenchikov. 2020. "Assessment of Natural and Anthropogenic Aerosol Air Pollution in the Middle East Using MERRA-2, CAMS Data Assimilation Products, and High-Resolution WRF-Chem Model Simulations." *Atmospheric Chemistry and Physics* 20 (15): 9281–9310. https://doi.org/10.5194/acp-20-9281-2020.

Valente, S, C Coelho, C Ribeiro, and J Soares. 2013. "Forest Intervention Areas (ZIF): A New Approach for Forest Management in Portugal." *Silva Lusitana* 21 (2): 137–61. https://ui.adsabs.harvard.edu/abs/2012EGUGA..14..894V/abstract.

Velikou, Kondylia, Georgia Lazoglou, Konstantia Tolika, and Christina Anagnostopoulou. 2022. "Reliability of the ERA5 in Replicating Mean and Extreme Temperatures across Europe." *Water (Switzerland)* 14 (4). https://doi.org/10.3390/w14040543.

Vilén, Terhi, and Paulo M. Fernandes. 2011. "Forest Fires in Mediterranean Countries: CO 2 Emissions and Mitigation Possibilities through Prescribed Burning." *Environmental Management*. https://doi.org/10.1007/s00267-011-9681-9.

Vitolo, Claudia, Francesca Di Giuseppe, Christopher Barnard, Ruth Coughlan, Jesus San-Miguel-Ayanz, Giorgio Libertá, and Blazej Krzeminski. 2020. "ERA5-Based Global Meteorological Wildfire Danger Maps." *Scientific Data* 7 (1): 1–11.

https://doi.org/10.1038/s41597-020-0554-z.

Voulgarakis, Apostolos, and Robert D. Field. 2015. “Fire Influences on Atmospheric Composition, Air Quality and Climate.” *Current Pollution Reports* 1 (2): 70–81. https://doi.org/10.1007/s40726-015-0007-z.

Vuuren, Detlef P. van, Elke Stehfest, Michel G.J. den Elzen, Tom Kram, Jasper van Vliet, Sebastiaan Deetman, Morna Isaac, et al. 2011. “RCP2.6: Exploring the Possibility to Keep Global Mean Temperature Increase below 2°C.” *Climatic Change* 109 (1): 95–116. https://doi.org/10.1007/s10584-011-0152-3.

Wagner, C. E. Van. 1987. *Development and Structure of the Canadian Forest Fire Weather Index System*. *Forestry*. http://scholar.google.com/scholar?hl=en&btnG=Search&q=intitle:Development+and+Structure+of+the+Canadian+Forest+Fire+Weather+Index+System#0.

Wang, Jun, Yun Yue, Yi Wang, Charles Ichoku, Luke Ellison, and Jing Zeng. 2018. “Mitigating Satellite-Based Fire Sampling Limitations in Deriving Biomass Burning Emission Rates: Application to WRF-Chem Model Over the Northern Sub-Saharan African Region.” *Journal of Geophysical Research: Atmospheres*. https://doi.org/10.1002/2017JD026840.

Wang, Sally S.C., Yun Qian, L. Ruby Leung, and Yang Zhang. 2022. “Interpreting Machine Learning Prediction of Fire Emissions and Comparison with FireMIP Process-Based Models.” *Atmospheric Chemistry and Physics* 22 (5): 3445–68. https://doi.org/10.5194/acp-22-3445-2022.

Wang, Xianli, Dan K. Thompson, Ginny A. Marshall, Cordy Tymstra, Richard Carr, and Mike D. Flannigan. 2015. “Increasing Frequency of Extreme Fire Weather in Canada with Climate Change.” *Climatic Change* 130 (4): 573–86. https://doi.org/10.1007/s10584-015-1375-5.

Ward, D S, S Kloster, N M Mahowald, B M Rogers, J T Randerson, and P G Hess. 2012. “The Changing Radiative Forcing of Fires Atmospheric Chemistry and Physics Discussions The Changing Radiative Forcing of Fires: Global Model Estimates for Past, Present and Future The Changing Radiative Forcing of Fires The Changing Radiative Forcing of Fi.” *Atmos. Chem. Phys. Discuss* 12: 10535–621. https://doi.org/10.5194/acpd-12-10535-2012.

Ward, Darold E., and Colin C. Hardy. 1991. “Smoke Emissions from Wildland Fires.” *Environment International* 17 (2–3): 117–34. https://doi.org/10.1016/0160-4120(91)90095-8.

Wegesser, Teresa C., Kent E. Pinkerton, and Jerold A. Last. 2009. “California Wildfires of 2008: Coarse and Fine Particulate Matter Toxicity.” *Environmental Health Perspectives* 117 (6): 893–97. https://doi.org/10.1289/ehp.0800166.

Werf, G. R. Van Der, J. T. Randerson, L. Giglio, G. J. Collatz, P. S. Kasibhatla, and A. F. Arellano. 2006. “Interannual Variability in Global Biomass Burning Emissions from 1997 to 2004.” *Atmospheric Chemistry and Physics* 6 (11): 3423–41. https://doi.org/10.5194/acp-6-3423-2006.

Wise, Marshall, Katherine Calvin, Allison Thomson, Leon Clarke, Benjamin Bond-

Lamberty, Ronald Sands, Steven J Smith, Anthony Janetos, and James Edmonds. 2009. “Implications of Limiting CO2 Concentrations for Land Use and Energy.” *Science (New York, N.Y.)* 324 (5931): 1183–86. https://doi.org/10.1126/science.1168475.

Wotton, B. M., and M. D. Flannigan. 1993. “Length of the Fire Season in a Changing Climate.” *Forestry Chronicle* 69 (2): 187–92. https://doi.org/10.5558/tfc69187-2.

Wu, Zhongfang, Xueling Wu, Ying Wang, and Siyuan He. 2020. “PM2.5ĝ•PM10 Ratio Prediction Based on a Long Short-Term Memory Neural Network in Wuhan, China.” *Geoscientific Model Development* 13 (3): 1499–1511. https://doi.org/10.5194/gmd-13-1499-2020.

Xie, Peng, Xiaoyun Liu, Zhaorong Liu, Tiantian Li, Liujv Zhong, and Yunrong Xiang. 2011. “Human Health Impact of Exposure to Airborne Particulate Matter in Pearl River Delta, China.” *Water, Air, and Soil Pollution* 215 (1–4): 349–63. https://doi.org/10.1007/s11270-010-0483-0.

Yokelson, R. J., J. D. Crounse, P. F. DeCarlo, T. Karl, S. Urbanski, E. Atlas, T. Campos, et al. 2009. “Emissions from Biomass Burning in the Yucatan.” *Atmospheric Chemistry and Physics* 9 (15): 5785–5812. https://doi.org/10.5194/acp-9-5785-2009.

Yu, Huizhen, Hongli Wang, Zhiyong Meng, Mu Mu, Xiang Yu Huang, and Xin Zhang. 2017. “A WRF-Based Tool for Forecast Sensitivity to the Initial Perturbation: The Conditional Nonlinear Optimal Perturbations versus the First Singular Vector Method and Comparison to MM5.” *Journal of Atmospheric and Oceanic Technology* 34 (1): 187–206. https://doi.org/10.1175/JTECH-D-15-0183.1.

Zang, Lin, Zemin Wang, Bo Zhu, and Yu Zhang. 2019. “Roles of Relative Humidity in Aerosol Pollution Aggravation over Central China during Wintertime.” *International Journal of Environmental Research and Public Health*. https://doi.org/10.3390/ijerph16224422.

Zeydan, Özgür, and Yuhang Wang. 2019. “Using MODIS Derived Aerosol Optical Depth to Estimate Ground-Level PM2.5 Concentrations over Turkey.” *Atmospheric Pollution Research* 10 (5): 1565–76. https://doi.org/10.1016/j.apr.2019.05.005.

Zhang, L., W. Lau, W. Tao, and Z. Li. 2020. “Large Wildfires in the Western United States Exacerbated by Tropospheric Drying Linked to a Multi-Decadal Trend in the Expansion of the Hadley Circulation.” *Geophysical Research Letters* 47 (16): 1–11. https://doi.org/10.1029/2020GL087911.

Zhang, Tian Hang, and Hong Liao. 2016. “Aerosol Absorption Optical Depth of Fine-Mode Mineral Dust in Eastern China.” *Atmospheric and Oceanic Science Letters* 9 (1): 7–14. https://doi.org/10.1080/16742834.2015.1126154.

Zhong, Shiyuan, Ting Wang, Pietro Sciusco, Meicheng Shen, Lisi Pei, Jovanka Nikolic, Kevin McKeehan, et al. 2021. “Will Land Use Land Cover Change Drive Atmospheric Conditions to Become More Conducive to Wildfires in the United States?” *International Journal of Climatology* 41 (6): 3578–97. https://doi.org/10.1002/joc.7036.

Zittis, George, Panos Hadjinicolaou, Marina Klangidou, Yiannis Proestos, and Jos

Lelieveld. 2019. “A Multi-Model, Multi-Scenario, and Multi-Domain Analysis of Regional Climate Projections for the Mediterranean.” *Regional Environmental Change* 19 (8): 2621–35. https://doi.org/10.1007/s10113-019-01565-w.

Zohdi, T. I. 2021. “A Digital Twin Framework for Machine Learning Optimization of Aerial Fire Fighting and Pilot Safety.” *Computer Methods in Applied Mechanics and Engineering* 373: 113446. https://doi.org/10.1016/j.cma.2020.113446.